In Situ Measurements of Acoustic Properties of Surfaces

by

Scott W. Mallais

A thesis
presented to the University of Waterloo
in fulfillment of the
thesis requirement for the degree of
Master of Science
in
Physics

Waterloo, Ontario, Canada, 2009

I hereby declare that I am the sole author of this thesis. This is a true copy of the thesis, including any required final revisions, as accepted by my examiners.

I understand that my thesis may be made electronically available to the public.

Abstract

The primary goal of this work is to measure the acoustic properties of a surface *in situ*. This generally involves sound pressure measurements and a calculation of the acoustic reflection factor of a surface, which may then be used to calculate the acoustic impedance or the acoustic absorption coefficient. These quantities are of use in acoustic simulations, architectural design, room acoustics and problems in noise control. It is of great interest to determine the performance of a particular surface where it is used, as opposed to measurements conducted in a laboratory. *In situ* measurements are not trivial, caution must be taken to ensure that high signal-to-noise levels are achieved and that the reflections of sound from the measurement environment are taken into consideration. This study presents five measurement methods that may be applied *in situ*. The acoustic absorption coefficient is calculated for each method on various surfaces spanning the whole range of absorption. Emphasis is placed on frequency resolution, in order to determine absorption characteristics in the bass region (50 Hz to 200 Hz). Advantages and disadvantages of each method are demonstrated and discussed. Finally, the *in situ* implementation of the surface pressure method is presented and measurements are made in order to test the limitations of this approach.

Acknowledgements

First and foremost, I would like to thank Professor John Vanderkooy for giving me the opportunity to study with the Audio Research Group and for his contributions to my research. Professor Stanley Lipshitz had also helped significantly with this research project. Their knowledge of Physics, Acoustics, Electronics and Digital Signal Processing were of great help during my studies at the University of Waterloo. I feel very fortunate to have had the opportunity to learn from such wonderful Professors.

I am grateful for Professor Susan Tighe's interest in my research and her help with the portable reverberation chamber. Discussions with Ryan Matheson have aided my understanding of Physics and Acoustics.

Robert Stevens has kindly guided me in the early development of this project by referring me to some of his previous work and clarifying the results of measurements in buildings.

I would also like to thank my close friends: Serge Cormier, Justin Levangie, Chretien Bourque, Chris Lynar, Dapeng Zhou, Zi Jian Long and Brett Tayles for their interest in my research, with the transportation of measurement equipment and many useful discussions.

This work would not have been possible without the help of Elaine Bourgoin, whose knowledge, patience and love greatly contributed to the completion of this thesis.

Dedication

This is dedicated to my father,
who encouraged me to ask questions,
and made me realize that there are no boundaries.

Contents

List of Tables

List of Figures

Nomenclature

α	Absorption coefficient of a surface. This is the ratio of absorbed to incident sound intensity.
α_k	Absorption coefficient per unit area of a given surface denoted by k.
δ	Acoustic centre of a loudspeaker.
$\delta(q)$	Dirac delta, equal to infinity when $q = 0$ and zero elsewhere.
ϵ	Material strain.
η	Material damping coefficient.
λ	Wavelength of sound wave.
λ_p	Wavelength of vibrations in a panel.
ω	Angular frequency, equal to $2\pi f$.
ϕ	Angle of incidence of floor pressure wave reflected from surface.
ρ	Reflection coefficient of a surface. This is the ratio of reflected to incident sound intensity.
ρ_m	Density of a medium/material [kg/m^3].
ρ_o	Density of air at standard temperature and pressure, equal to approximately 1.18 kg/m^3.
σ	Mass per unit area of a sheet or plate.
τ	Transmission coefficient of a surface. This is the ratio of transmitted to incident sound intensity.
τ_m	Transmission coefficient of wall in the mass controlled region.
τ_s	Transmission coefficient of wall in the stiffness region.
θ^*	Coincidence angle.
$\tilde{t}$	Transmission factor, given by the ratio of transmitted to incident pressure.

$\vec{k}$ Wave vector, its magnitude is given by $2\pi/\lambda$. The direction of this vector is the same as the direction of the wavefronts of a wave.

$\vec{n}_{in}$ Inward normal vector to the surface.

$\vec{q}$ Displacement of sound wave.

A Total absorption of a room, given by the product of absorption coefficients per unit area and the area of the room surfaces.

a Absorption factor of a surface. This is the ratio of absorbed to incident acoustic pressure.

B Bending modulus.

b Acoutics source radius.

B_ω Amplitude of pressure component p_ω.

c Speed of sound in a medium, for air at 20℃ this is equal to approximately 344 m/s.

C_s Mechanical compliance of a panel, equal to the reciprocal of the spring constant of the panel.

E Elastic modulus.

F Force.

f_c Corner frequency.

f_{amn} Resonance frequencies of an aluminium sheet.

f_{smn} Resonance frequencies of a steel sheet.

FFT Fast Fourier Transform.

FR Frequency Response, the Fourier transform of the impulse response.

h Thickness of a sheet/plate.

I_a Absorbed intensity by a surface.

I_i Incident intensity on a surface.

I_r Reflected intensity from a surface.

j Imaginary unit equal to $\sqrt{-1}$.

k Wave number, equal to $2\pi/\lambda$.

l_x Length of plate.

l_y Width of plate.

M_x Bending moment of a plate, x-component.

M_y Bending moment of a plate, y-component.

MLS Maximum length sequence.

p Acoustic pressure.

p^* Complex conjugate of the acoustic pressure.

p_ω One frequency component of the total pressure p.

P_a Absorbed sound power by a surface.

p_a Absorbed pressure by a surface.

P_i Incident sound power on a surface.

p_i Incident pressure.

p_o Pressure wave amplitude.

P_r Reflected sound power from a surface.

p_R Acoustic pressure at the rigid surface (steel sheet).

p_r Reflected pressure by surface under study.

$p_{\tilde{t}}$ Transmitted pressure.

p_{ir} Incident and Reflected sound waves from a surface under study using subtraction technique.

p_{ref} Reference pressure, equal to 20 μPa.

p_{Rm} Pressure waves reflected off room surfaces.

p_{rRm} Reflection of the room reflections by the surface.

p_{rsl} Reflection of the scattered wave by the surface.

p_{sl} Scattered wave by the loudspeaker.

p_s Acoustic pressure at the surface under study.

q Distance variable.

q_h Microphone height with respect to floor.

q_l Half the distance for the propagation path from loudspeaker to floor to microphone.

q_o Loudspeaker-microphone distance.

q_{ref} Reference distance in metres, used to normalize units when writing spherical waves.

q_s Distance from loudspeaker to surface under study.

r Reflection factor of a surface under study. This is the ratio of reflected to incident acoustic pressure.

$r_\perp$ Reflection factor at normal incidence.

S Material stress.

s Poisson's ratio.

S_k Area of a room surface.

t Time.

T_{60} Reverberation time.

U Volume velocity.

V Volume of a room.

v_i Incident particle velocity of sound wave.

v_r Reflected particle velocity of sound wave.

$v_{\tilde{t}}$ Transmitted particle velocity of sound wave.

v_{iz} z-component of the incident particle velocity.

v_{rz} z-component of the reflected particle velocity.

v_s Particle velocity at the surface under study.

x_o Position on x-axis.

y Distance variable.

y_o Position on y-axis.

z Distance variable.

Z_c Characteristic acoustic impedance. This is the ratio of acoustic pressure to the particle velocity of a plane wave, which is the product of the density of the medium times the wave speed.

Z_m Mechanical impedance of a plate, given by the ratio of force to velocity at the plate.

Z_s Specific acoustic impedance. This is the ratio of acoustic pressure to the particle velocity.

ASTM American society for testing and materials.

BD2 Back door 2nd floor location for surface pressure method.

BD3 Back door 3rd floor location for surface pressure method.

dB Decibel, a unit of measurement for sound pressure level, defined as $20 \log_{10}(p/p_{ref})$.

FD2 Front door 2nd floor location for surface pressure method.

IR Impulse response.

SPL Sound pressure level.

Chapter 1

Introduction

It seems appropriate to begin the discussion of absorption characteristics of surfaces with a mention of its usefulness in acoustics. Two of the main types of treatments used in rooms are diffusers and absorbers [6]. Diffusers attempt to scatter sound spatially and temporally in order to prevent coherent reflections from arriving at a nearby listener, which provides an audience with a similar listening environment. Absorbers on the other hand reduce the sound pressure or sound energy that is reflected from a surface by means of some loss mechanism or transmission through the surface. A combination of these strategies is generally needed in order to solve acoustics problems in listening spaces.

Absorption of sound is required in numerous contexts, such as: listening rooms, classrooms, studios, theatres, concert halls and manufacturing facilities. Of course, absorptive materials may be of use in every type of building, be it residential, commercial or industrial. The configuration and type of materials may vary in each case; however, the recurring theme is the reduction in the reflected sound wave (and energy) returning from a surface. Special materials are therefore chosen in order to reduce reflections from surfaces in rooms. This reduction usually depends on the frequency and the angle of incidence of the incident acoustic wave.

In general, the interaction between an acoustic wave and an absorptive surface will result in a change in the amplitude and the phase of the reflected wave. The relationship between the reflected portion and the absorbed portion of the acoustic pressure will be discussed further in this study. Reflections, as well as transmission through surfaces separating adjacent rooms, may create unwanted noise in enclosed spaces. Absorptive materials are therefore used to decrease the level of the reflected and transmitted sound waves. This is useful in many situations, for example:

1. Speech intelligibility
2. Speech privacy
3. Sound reproduction

4. Machine noise

Reflections in enclosed spaces add to the acoustic pressure from a source (i.e. loudspeaker, person, instrument). This addition to the environment can reduce speech intelligibility and privacy. In sound reproduction, there are issues in relaying the original information from a recording. The original sound is generally modified by the reproduction system itself and the listening environment. The listening space is a key factor here, since it has a bias on which frequencies it accentuates and which it does not. One example of this is found at low frequencies, where room resonances occur. These resonances are distinct and significantly audible. Machine noise is easily noticed with all of the technology that we use today: cars on highways and roads, manufacturing buildings, shops and heavy equipment are a few examples. These have to be assessed on an individual basis with the ultimate goal of reducing the sound levels at particular locations. This is where absorptive materials are needed.

In the following chapters we will focus on determining the absorption factor or absorption coefficient. This may introduce some confusion when talking about transmission factors or coefficients. The transmission of sound describes how much sound actually passes through a given surface. A portion of the sound is lost when the wave travels through the surface, this may sometimes be referred to as absorption. In addition, part of the incident sound on the surface is reflected. In this study, we restrict ourselves to the acoustic properties of the room in which we are situated, and therefore do not verify how much sound is transmitted. Our approach is solely to see how much sound is reflected from a surface, which allows the absorption characteristics of the surface to be calculated. The term absorption here, describes the fraction of the incident wave amplitude (or energy) that is no longer in front of the surface, which encompasses losses in a structure and the transmission of sound through it.

1.1 Survey of Current Literature

The measurement of absorption characteristics of surfaces has been carried out for quite some time. Only a few of the many scientific articles will be mentioned here, and others throughout the text. Several methods have been used and summarized by Stevens [35] and Dutilleux [8] in their respective theses.

1.1.1 Standard Methods

Acoustic absorption characteristics of a surface may be measured in many different ways. Acoustics standards pertaining to the absorption characteristics of surfaces may be found in technical standards by ASTM international (American Society for Testing and Materials). Two measurement approaches are widely used, the first is

by use of the impedance tube [15], and the second by using a reverberation chamber [16].

The impedance tube method [15] may be used to calculate the acoustic absorption coefficient of a sample at normal incidence. A loudspeaker and a sample are placed inside of a rigid tube, at the tube extremities. Partial standing waves are formed in the tube when sending sinusoidal signals to the loudspeaker. These may be detected by moving a microphone inside the tube and recording measurements [20]. Alternatively, a maximum length sequence (MLS) may be used with one or two microphones fixed at positions inside the impedance tube [35]. The impulse response may be found at these positions and subsequently, their ratio taken or, the incident and reflected signals from the sample separated. This then allows one to calculate the absorption coefficient of the surface. It has been discussed [15], and shown [8], that errors may occur if the sample is not properly mounted in this method.

The reverberation room method [16] may be used to calculate the acoustic absorption coefficient of a sample at random incidence. In this case sound is incident from all directions on the sample. A special room is used in order to create this environment, which requires the sound field to be diffuse. Noise band exciation signals may be used to measure decay times of the sound in the chamber with and without the surface under study present. Alternatively a MLS may be used, and the reverberation time may be calculated from the measured impulse response [34]. Once again, a measurement with and without the sample in the room is required. The random incidence absorption coefficient is determined from these measurements. Unfortunately, round robin tests of this method have shown significant differences in absorption coefficients for identical samples [16] [20] [8].

These ASTM international standards may only be used in controlled environments. Samples either have to be cut from a surface or constructed precisely to fit in an impedance tube. A reverberation chamber is built specifically for acoustics measurements. A sample has to be placed in the reverberation chamber in order to conduct measurements. These methods would have to be modified in order to implement them in a normal room. One such case will be described in section 3.6. *In situ* measurements are possible using alternative approaches, described in the following section.

1.1.2 *In Situ* Methods

The reflection method, discussed by Garai in [24] [11] has a simple arrangement, requiring only a loudspeaker and one microphone to calculate the acoustic absorption coefficient of a surface. A loudspeaker is oriented towards a surface under study and placed a distance q_s away. A microphone is then placed halfway in between the loudspeaker and the surface ($q_s/2$). The impulse response is determined by use of a MLS excitation signal. The sound waves are separated into incident and reflected

components from the surface and the absorption coefficient is calculated. The measurement configuration greatly affects this method. Reflections of sound from the other surfaces in this room may create measurement errors. These reflections must therefore be excluded from the incident and reflected signals. This separation requires time windowing and generally results in poor frequency resolution [25]. This will result in a smoothed version of the actual data at low frequencies.

Several other reflection-based methods have been implemented. A similar arrangement to the reflection method was presented which improved frequency resolution. This is discussed by Mommertz [27]. The method utilizes two measurements, one at the surface under study, and a second away from all room surfaces. This first measurement includes the incident and reflected waves from the surface under study. The second measurement contains only the incident sound wave from the loudspeaker. The difference between these measurements is the reflected wave, which may be recovered by subtracting one measurement from the other. The absorption characteristics of the surface may then be calculated from the incident and reflected sound waves. This principle is used in [23] and the Adrienne method [2], which has resulted in a European standard [1].

Once again, this approach is limited by the reflections of sound from the other surfaces in the room. There is also the reflection or scattering of sound from the loudspeaker itself. Windowing in the time domain must then be used to separate the wanted data from the room and loudspeaker scattered contributions. In addition, the loudspeaker-microphone distance must be kept fixed for both of the measurements mentioned above. Errors may arise when there is an incomplete subtraction between measurements [27]. Better frequency resolution is obtained in this method, however it is still difficult to be certain of results at low frequencies. Note that one measurement is taken as far as possible from the surfaces of a room and the second is taken at the surface under study. There is always the possibility that different spectral characteristics exist at each location, especially at low frequencies where room resonances occur. Note that the noise spectrum in a room generally increases as frequency decreases.

Many measurement approaches discuss the use of transfer functions. Some configurations implement one microphone at one location [30], one microphone at two locations [21], two microphones at two locations [9] [37] or even a microphone array [7]. The use of several microphones has the disadvantage that these must be properly calibrated in order to reduce measurement errors. All of these methods may be utilized *in situ*, however each method has its respective limitations, primarily at low frequencies. In particular Li and Hodgson [21] use one microphone at two locations near a surface with a MLS excitation signal fed to a loudspeaker. The sound waves are modelled as plane waves in one calculation and spherical waves in another in order to verify which assumption is appropriate. Results were improved using a spherical wave assumption [21]. Both Nocke [30] and Dutilleux *et al.* [9] have used transfer function techniques with microphones positioned near the surface under study at oblique incidence. In Nocke's case, results down to 80 Hz were possible, however this is not the case when measurements are performed *in*

situ. Dutilleux has proposed several measurement methods in his PhD thesis [8], however difficulties such as those discussed previously, and long computation times, have limited the accuracy of his results at low frequencies.

Frequency resolution limitations have sparked the interest in the shortening of the impulse response [10] [42]. This is done by high-pass filtering a flattened frequency response (flattened meaning that the frequency response has equal amplitude at all frequencies), which in turn causes a quick decay of the impulse response. Such techniques are designed for loudspeaker measurements, though we are interested in combining this principle with acoustic absorption measurements. The approach would involve the filtering of the entire frequency response, resulting in a quick decay of the impulse response in the time domain. The incident and reflected impulse responses would then be safely windowed with reduced error than if no filtering was used. Mommertz had also discussed a similar method by pre-filtering of the impulse response in order to create an acoustic pulse of short duration which could be separated from nearby room reflections [27] [28]. The frequency response of this system resembles a first order high-pass with a frequency corner at 100 Hz.

It is very important to mention that many of the methods listed above have been tested using absorptive materials, meaning that most of the incident sound on the surface under study is absorbed. The reflection of sound from this type of surface has a very small amplitude. The results that authors have obtained for such materials are reasonable. This is not necessarily the case for the measurement of rigid surfaces that reflect most, or all of the incident sound. In this case, experimental values may exceed the theoretical range of the measurement variables [27]. It is not always clear why this happens. Diffraction may be one cause, while the assumption of the wave form, plane or spherical, may be another. The reverberation room method has also shown absorption coefficients that exceed one for absorptive materials [16]. This has been attributed to diffraction effects at the edges of a measurement sample.

Diffraction is a difficult problem to assess and correct for these measurement methods. Even worse, it is often neglected. As we stated previously, diffraction from a measurement sample may be significant. Studies such as [19] have considered the minimum sample size required in order to perform *in situ* measurements, based on the time it takes for the diffracted waves to arrive at the microphone position. In addition, typical loudspeakers will have diffraction effects from the edges of their rectangular enclosures [38]. We therefore have incident/reflected waves, room reflections and diffracted waves at the microphone position. The detailed effects of diffraction have not been included in this thesis due parlty to their complexity.

An interesting measurement method was proposed and validated by Ingård and Bolt in the 1950's [14]. Two measurements were made in an anechoic chamber, one at a rigid surface and another at a surface under study at the same location. By taking both measurements at the same location in the room, the noise and reverberation should be similar in both cases. These measurements were used to determine the absorption characteristics of a surface. Samples were constructed in

order to verify the accuracy of this method. The results of this study were in good agreement with the presented theory. To our knowledge, this method has not been attempted *in situ*. Applying this approach *in situ* would require a rigid surface to be placed in the same location as the surface under study. This challenge will be discussed further in Chapter 4.

1.2 Objective of Research

An idea presented by Stevens [36] sparked the interest for this study, related to the *in situ* characterization of plane outdoor surfaces [17] (for example, road noise barriers). Road noise was used as a sound source in his measurements. Two microphones recorded the sound pressure levels at two locations, one at the surface under study and another 2 metres from the surface. The sound waves are assumed to be plane. At the surface under study the incident and reflective waves will add coherently. At the 2 metre position, the incident and reflected waves will add incoherently (on a power basis). It is shown that the difference between the measurements at these two locations is between 0 and 3 dB, 0 dB if the surface is fully absorbing (no reflected wave) and 3 dB if the surface is fully reflective. These facts were used in order to determine the absorption coefficient of the surface under study. This approach did not work *in situ* in its present form. We cannot assume plane wave propagation between the loudspeaker and the microphone position. In addition, room reflections and diffraction will add to the response at the microphone position, which are not taken into consideration in this method.

The difficulties in applying measurement approaches as described by Garai, Mommertz and Stevens (as well as many others) have shown that work is needed in this area. The primary goal of this research is to measure the absorption characteristics of a surface *in situ*. Methods already exist to partially achieve this goal. As you may have noticed throughout this discussion, one of the greatest challenges for *in situ* measurements exists at low frequencies. This will therefore be emphasized throughout the study. In addition, the acoustical characteristics of surfaces should not only be determined for absorptive materials, but reflective materials as well. We therefore require a method that is applicable over the entire range of absorption or reflection characteristics.

It was decided that five measurement methods will be introduced, implemented and compared. Comparison criteria will include frequency resolution, applicability, configuration and accuracy. Practical and theoretical limitations will be investigated in each case. In particular, we would like the method to give results between 50 Hz and 4 kHz, which is an extension towards lower frequencies than conventional methods. It should be applicable for surfaces regularly found in rooms and buildings, independent of the reflection or absorption characteristics of the surface. The measurement configuration should be relatively simple and portable. Finally, we would like this method to be accurate.

1.3 Outline

Chapter 2 covers the theory related to the calculation of the acoustic absorption coefficient from pressure measurements. Definitions of reflection and absorption factors and coefficients are given, in addition to the relationship between them. Acoustic impedance is also defined and related to the reflection factor, which may be deduced from pressure measurements. Finally, a discussion illustrates the different characteristics which govern the transmission of sound through a wall or panel.

Chapter 3 begins by summarizing the difficulties with *in situ* measurements and introducing the measurement system. All five measurement methods are discussed and implemented in Chapter 3: the reflection method introduced by Garai [24], the subtraction technique introduced by Mommertz [27], impulse response shortening and gating as discussed by Fincham [10], Vanderkooy and Lipshitz [42], the *in situ* application of the reverberation chamber, and the surface pressure method as discussed by [14].

Poor frequency resolution will be demonstrated for the reflection method and the subtraction technique. The impulse response shortening and gating method will implement frequency response filtering in order to attempt to recover low-frequency information. A portable reverberation chamber, consisting of a wooden box with slanted sides and a loudspeaker and microphone holder will be used to measure floors, pavement and fibreglass panels. This chamber will be compared with the recommendations of the ASTM international standard for the reverberation room method of measuring acoustic absorption coefficients [16].

The last section of Chapter 3 introduces the preferred method for *in situ* absorption measurements, the "Surface Pressure Method" [14]. This is initially carried out using a small metal sheet on the surface under study in order to create a rigid boundary. This sheet is of relatively small dimension. In addition, the absorption coefficient of the surface under study was calculated without any consideration of room reflections, sound scattered by the loudspeaker or diffraction from the edges of the sheet.

Chapter 4 develops this idea further and clarifies the approximations made in order to implement this approach in a regular room. A support system was constructed in order to hold a 1.2 by 1.2 metre sheet up to a surface under study. Different mounting conditions may be used with this setup, including variable sheet height and variable contact between the sheet and the surface under study. This has been tested on rigid surfaces, a resonant surface and an absorptive surface. Chapter 5 concludes the thesis, discusses measurements in rooms, absorption coefficients, and future work in a broad context.

Chapter 2

Reflection, Absorption and Impedance

2.1 Principles

2.1.1 Reflection and Absorption

The principle behind acoustic reflection and absorption is shown in Figure 2.1. Sound waves that are incident on a surface are either reflected or absorbed. The term absorption here refers to the amount of sound leaving the room. In general, the term transmission is used for the pressure wave on the other side of the wall and absorption refers to the pressure wave that is "absorbed" in the material. Our measurements of surfaces in rooms will only consider the amount of pressure returning from the surface (reflected), therefore, whether the sound is transmitted or absorbed is not important to us. We will consider absorption and transmission phenomena to be the same for measurement purposes. The following theory will employ both the terms absorption and transmission in order to maintain consistency with other literature. In general, the amount of absorption is dependent on the frequency (or wavelength) and the angle of incidence of the incident sound wave.

This phenomenon also depends on the media which we are considering. A wall or sample surface is a change in medium for the sound wave. It is the difference in acoustic impedance of this medium which results in reflection and absorption. We will typically consider sound propagation in air which interfaces with a surface under study. Several layers of media may be found behind this surface, each of which will affect the sound absorption and reflection.

Reflection and absorption of pressure from a surface is generally described by factors or coefficients. These represent the fraction of pressure or intensity that is reflected or absorbed by a surface under study. For simplicity, we will consider plane waves in order to define the factors and coefficients. The phase of the reflected and absorbed waves are generally not identical to the incident wave phase. This

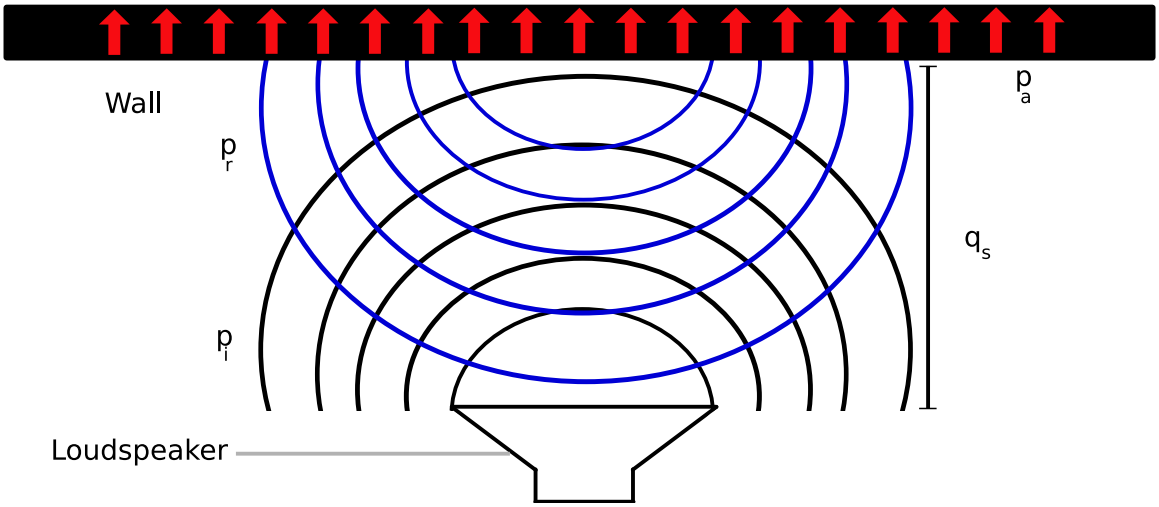

Figure 2.1: Reflection and absorption of sound incident on a wall. The incident portion of the acoustic pressure wave is in black, the reflection of this wave by the surface is shown in blue and the absorbed sound wave is symbolized by the red arrows.

phase change is included in the pressure factors, which we will now define. The reflection factor is the ratio of reflected pressure to the incident pressure at the surface ($q = q_s$)

$$r = \frac{p_r(q)}{p_i(q)}\Big|_{q=q_s} \tag{2.1}$$

where r is the reflection factor, p_i is the incident pressure, p_r is the reflected pressure, q is a distance variable and q_s is the distance from the origin to the surface under study (see Figure 2.1), signifying that the pressure waves are evaluated at the surface in (2.1). The reflection factor will describe the reflection of the incident sound wave from the surface in magnitude and in phase.

The intensity reflection coefficient is similarly the ratio of reflected sound intensity to the incident sound intensity at the surface ($q = q_s$)

$$\rho = \frac{I_r(q_s)}{I_i(q_s)} = \left|\frac{p_r(q_s)}{p_i(q_s)}\right|^2 = |r|^2. \tag{2.2}$$

For plane waves at normal incidence, $I = |p|^2/\rho_o c$ [12], where ρ_o is the density and c the sound speed in air (ρ with a subscript refers to the mass density of a medium, ρ without a subscript will always refer to the reflection coefficient). Note that p is generally a complex quantity, described by a magnitude and a phase. We may then write $|p|^2 = pp^*$, where p^* is the complex conjugate of p. In the same fashion, the absorption factor is defined as the ratio of absorbed pressure to the incident pressure at the surface,

$$a = \frac{p_a(q)}{p_i(q)}\Big|_{q=q_s} \tag{2.3}$$

and for the absorption coefficient

$$\alpha = \left|\frac{p_a(q_s)}{p_i(q_s)}\right|^2 = |a|^2. \tag{2.4}$$

We must have conservation of energy at the boundary surface, or the conservation of power, requiring that

$$P_i = P_r + P_a \tag{2.5}$$

where P_i is the incident sound power, P_r the reflected sound power and P_a the absorbed sound power. Therefore, the same should be true for the sound intensities, which signify the flow of energy through a given area. In other words, we would look at how much power is going through (or being reflected from) a given area of the surface. This gives

$$I_i = I_r + I_a \tag{2.6}$$

where $I_i = |p_i|^2/\rho_o c$ is the incident sound intensity, $I_r = |p_r|^2/\rho_o c$ is the reflected sound intensity and $I_a = |p_a|^2/\rho_o c$ is the absorbed sound intensity. Using this in (2.6),

$$|p_i|^2 = |p_r|^2 + |p_a|^2. \tag{2.7}$$

If we divide (2.7) by $|p_i|^2$, and use the definitions of the reflection and absorption coefficients (2.2), (2.4), we get the following relationship

$$\alpha + \rho = 1. \tag{2.8}$$

Substituting (2.2) into (2.8), we obtain

$$\alpha = 1 - \rho = 1 - |r|^2 \tag{2.9}$$

for the absorption coefficient. This equation indicates that knowledge of the reflection factor is sufficient to determine the absorption coefficient of a surface. We can not determine the reflection factor from the absorption coefficient since the latter has no phase information.

2.1.2 Impedance

Acoustic impedance is analogous to electrical and mechanical impedance in their respective systems. It relates the acoustic pressure to the particle velocity,

$$Z_s = \frac{p}{v} \tag{2.10}$$

where p is the acoustic pressure (the pressure fluctuations above and below atmospheric pressure) and v is the particle velocity. This relationship is important in acoustical simulations and active noise control systems. Since the pressure in a plane wave is $\rho_m c v$ [5], the specific acoustic impedance becomes

$$Z_c = \rho_m c \tag{2.11}$$

where Z_c is the characteristic acoustic impedance of the medium, ρ_m is the density [kg/m^3] of the medium and c is the speed of sound in the medium. If the medium is air at approximately 20℃ and atmospheric pressure, the ambient density is about 1.18 kg/m^3 (which we will call ρ_o) while the speed of sound is 344 m/s. This results in a characteristic impedance of 406 mks rayls (1 mks rayl = 1 Ns/m^3) [5].

The acoustic impedance, reflection factor and absorption (or transmission) factor are all related. A surface may be characterized by its acoustic impedance or its reflection factor. Having this information, one can go from the reflection factor to the acoustic impedance or *vice versa*. The relationship between the reflection and absorption factors are determined by boundary conditions which require assumptions to be made about the surface. This may be difficult *in situ*, since we may not necessarily have boundary conditions and construction information about the surface. However, the relationship given by (2.9) is generally true, since this comes from the conservation of energy and the definitions of the intensity coefficients. We will see in the following section that the reflection factor and the specific acoustic impedance present the same information, however in a different form, for a given surface.

2.1.3 Relationship Between the Acoustic Impedance and the Reflection Factor

Consider a plane pressure wave incident on an infinite surface as depicted in Figure 2.2. We will assume that the surface is locally reacting, in this case, the normal air velocity at a given point only depends on the pressure at that same point. The acoustic impedance would then be independent of the angle of incidence of the pressure wave [31]. With this assumption we may determine the relationship between the acoustic impedance and the reflection factor. A similar treatment is given in Morse and Ingård [29], where the pressure and the particle velocity are written as a function of the scalar potential. We begin by writing the incident and

reflected pressure waves as plane waves, which do not attenuate since there is no spreading of the sound wave (we are ignoring any attenuation in air as well). A plane wave is a complex exponential, with an argument that depends on frequency, time, the wave speed in the medium and the displacement of the wave:

$$p_i = p_o e^{j(\omega t - \vec{k}\cdot\vec{q})} = p_o e^{j(\omega t - ky\sin\theta + kz\cos\theta)} \tag{2.12}$$

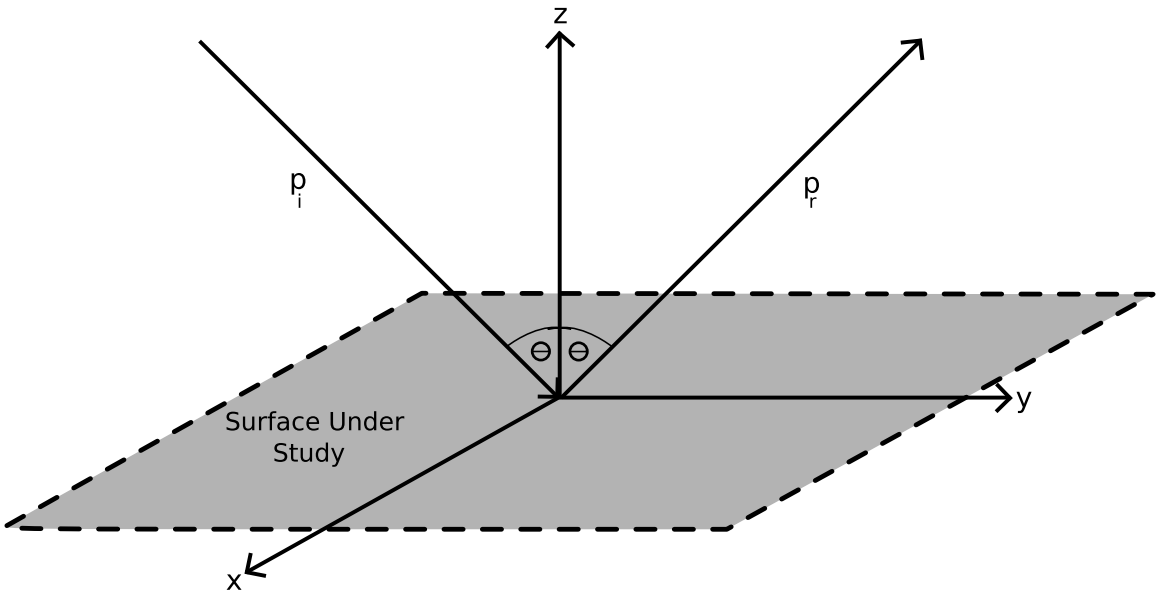

Figure 2.2: Reflection of plane waves by an infinite surface. The angle of incidence of p_i is θ, which is also the angle of reflection of p_r.

where p_o is the pressure amplitude, j the imaginary unit, t the time, $\vec{q} = x\hat{\imath} + y\hat{\jmath} + z\hat{k}$ is the displacement of the plane wave and $\vec{k} = k_x\hat{\imath} + k_y\hat{\jmath} + k_z\hat{k}$ is the wave vector. For the incident wave $\vec{k} = k\sin\theta\hat{\imath} - k\cos\theta\hat{k}$, where $k = |\vec{k}|$. The wave vector is in the direction of propagation of the acoustic wave, and equal in magnitude to

$$k = \frac{\omega}{c} = \frac{2\pi}{\lambda}. \tag{2.13}$$

We represent the angular velocity by $\omega = 2\pi f$, with f being the frequency of the wave. The wavelength is given by λ, which satisfies the following equation

$$c = \lambda f. \tag{2.14}$$

In the same fashion, the reflected wave has a modified amplitude compared to the incident wave, given by the product of the reflection factor and the incident pressure amplitude: rp_o (from (2.1), $p_r = rp_i$). The argument of the reflected pressure has also changed, due to the direction of propagation of the wave ($\vec{k}\cdot\vec{q}$), resulting in

$$p_r = rp_o e^{j(\omega t - ky\sin\theta - kz\cos\theta)}. \tag{2.15}$$

The particle velocity and the pressure of a sound wave are related by the Newtonian equation of motion. This may be used to determine the particle velocity from the plane pressure waves. The Newtonian equation of motion is

$$\vec{\nabla} p = -\rho_o \frac{\partial \vec{v}}{\partial t}. \tag{2.16}$$

Substitution of the incident pressure, (2.12) into (2.16) and solving for the z-component of the particle velocity yields

$$v_{iz} = -\frac{p_o \cos\theta}{\rho_o c} e^{j(\omega t - ky\sin\theta + kz\cos\theta)} \tag{2.17}$$

and likewise for the reflected z-component of the particle velocity,

$$v_{rz} = r\frac{p_o \cos\theta}{\rho_o c} e^{j(\omega t - ky\sin\theta - kz\cos\theta)}. \tag{2.18}$$

We would like to take the ratio of the pressure to the particle velocity into the surface, which would give us the specific acoustic impedance of the boundary. The acoustic pressure at the surface is given by the sum of (2.12) and (2.15),

$$p_s = (p_i + p_r)_{z=0} = (1+r)p_o e^{j(\omega t - ky\sin\theta)}. \tag{2.19}$$

The z-component of the particle velocity is the normal component needed at the surface, this is given by the sum of (2.17) and (2.18),

$$v_s = (v_{iz} + v_{rz})_{z=0} = (r-1)\frac{p_o \cos\theta}{\rho_o c} e^{j(\omega t - ky\sin\theta)}. \tag{2.20}$$

Finally, the specific acoustic impedance of the surface is given by the ratio of p_s to $\vec{v}_s \cdot \vec{n}_{in} = -v_s$, where $\vec{n}_{in}$ is the inward normal to the surface

$$Z_s = \frac{Z_c}{\cos\theta}\frac{1+r}{1-r} \tag{2.21}$$

or by rearranging

$$r = \frac{Z_s\cos\theta - \rho_o c}{Z_s\cos\theta + \rho_o c} = \frac{Z_s\cos\theta - Z_c}{Z_s\cos\theta + Z_c} \tag{2.22}$$

and at normal incidence

$$r_\perp = \frac{Z_s - Z_c}{Z_s + Z_c}. \tag{2.23}$$

This is a very important result. We see that the reflection factor or the impedance characterizes the surface. If we determine the reflection factor, we may determine the specific acoustic impedance and *vice versa*. This is the basis for many measurement techniques in use today. Some methods determine the impedance, and thus the reflection factor and absorption coefficient by use of (2.22) and (2.9). Others determine the reflection factor and therefrom, the absorption coefficient and specific acoustic impedance.

We may deduce a bit of intuition from (2.23). If the wall is rigid, meaning that the surface velocity tends to zero, the impedance tends to infinity. In the limiting case where $Z_s \to \infty$ we obtain $r_\perp = 1$. On the other hand, if the specific acoustic impedance of the surface is equal to $\rho_o c$, $r_\perp = 0$ and the absorption coefficient becomes unity in (2.9). This demonstrates the principle of impedance matching in order to maximize the transmission of a signal. In the following we will use r and not $r_\perp$ as the reflection factor. Normal incidence should be assumed unless we explicitly indicate non-normal incidence.

2.2 Reflection and Transmission of Sound for Sheets and Plates

2.2.1 Case of a Thin Sheet

We will now discuss the reflection and transmission of acoustic waves for a thin sheet. Instead of speaking of absorption, we will use the term transmission, since the wave travels through the sheet and continues to propagate on the opposite side. The relationship between the reflection factor and the transmission factor[1] depends on the boundary conditions at the surface. For now, we will consider only the reflection and transmission of sound at a thin sheet, neglecting any absorption or losses in the material. This means that we may effectively treat the transmission factor as the absorption factor. In this case, the "absorbed" pressure is transmitted to the medium on the other side of the sheet.

We begin by assuming plane wave propagation at normal incidence to a sheet that is infinite in extent in the xy plane, as in Figure 2.3. There are two boundary conditions at the sheet that must be satisfied. The first, is the continuity of velocity normal to the sheet

$$(\vec{v}_i + \vec{v}_r)_{z=0} = \vec{v}_{\tilde{t}}|_{z=0} \tag{2.24}$$

where $\vec{v}_i$, $\vec{v}_r$, $\vec{v}_{\tilde{t}}$ are the incident, reflected and transmitted particle velocities. The second, is that the acceleration of the sheet is caused by the difference in pressure at its two sides,

[1]The transmission factor's definition is analogous to that for reflection or absorption: $\tilde{t} = p_{\tilde{t}}/p_i$ where $p_{\tilde{t}}$ is the transmitted pressure.

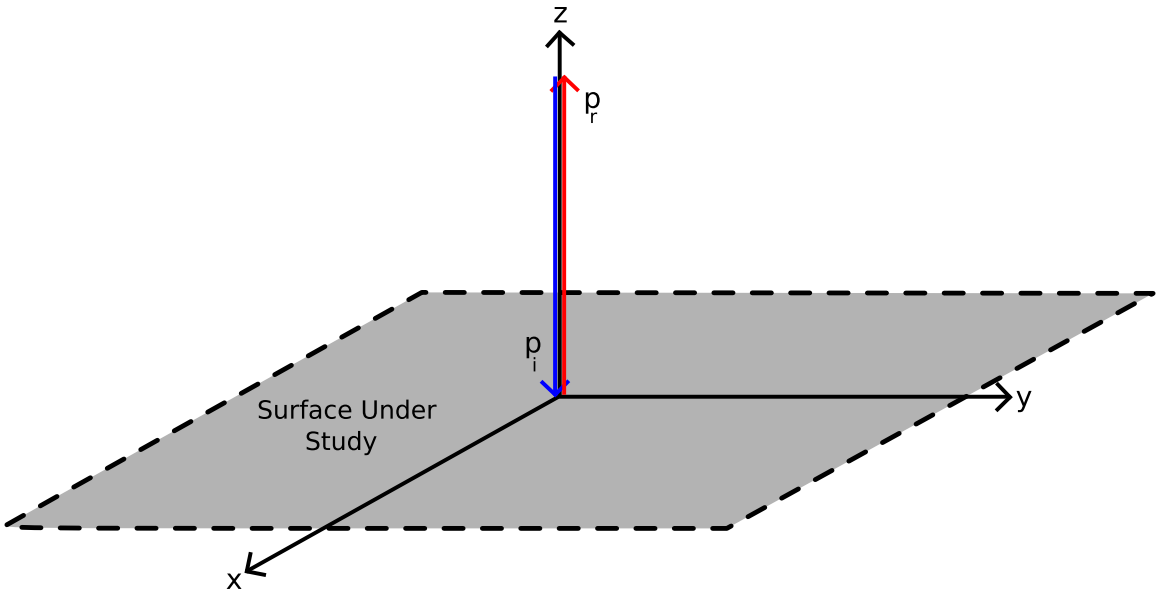

Figure 2.3: Reflection of plane sound waves at normal incidence. The incident and reflected waves are respectively shown in blue and red.

$$(p_i + p_r - p_{\tilde{t}})_{z=0} = \sigma \frac{d^2 z}{dt^2}|_{z=0} \tag{2.25}$$

where p is pressure, σ is the mass per unit area of the sheet and d^2z/dt^2 is the second derivative of the z-component of the displacement with respect to time (acceleration). Following the form of the pressures presented in section 2.1.3, we have

$$p_i = p_o e^{j(\omega t - kz)} \tag{2.26}$$

$$p_r = r p_o e^{j(\omega t + kz)} \tag{2.27}$$

and

$$p_{\tilde{t}} = \tilde{t} p_o e^{j(\omega t - kz)}. \tag{2.28}$$

Likewise, the velocities may be expressed in terms of the pressures, noting that the ratio of pressure to velocity for a plane wave is the characteristic impedance of the medium in which the wave is travelling (see (2.16)) and note that $\cos\theta = 1$),

$$v_i = -\frac{p_o}{\rho_o c} e^{j(\omega t + kz)} \tag{2.29}$$

$$v_r = \frac{r p_o}{\rho_o c} e^{j(\omega t - kz)} \tag{2.30}$$

$$v_{\tilde{t}} = -\frac{\tilde{t}p_o}{\rho_o c}e^{j(\omega t+kz)}. \tag{2.31}$$

We may now write the boundary conditions using (2.26)-(2.31), for the particle velocity at the sheet:

$$\left[-\frac{p_o}{\rho_o c}e^{j(\omega t+kz)} + \frac{rp_o}{\rho_o c}e^{j(\omega t-kz)}\right]_{z=0} = -\frac{\tilde{t}p_o}{\rho_o c}e^{j(\omega t+kz)}|_{z=0} \tag{2.32}$$

which gives

$$r + \tilde{t} = 1. \tag{2.33}$$

The second boundary condition, this time for the pressure becomes

$$\left[p_o e^{j(\omega t+kz)} + rp_o e^{j(\omega t-kz)} + \tilde{t}p_o e^{j(\omega t+kz)}\right]_{z=0} = \sigma\frac{d^2z}{dt^2}|_{z=0}. \tag{2.34}$$

At this point we use $d^2z/dt^2 = j\omega dz/dt = j\omega v_t$, since we have an $e^{j\omega t}$ time dependence. This results in

$$1 + r = \left(\frac{j\omega\sigma}{\rho_o c} + 1\right)\tilde{t}. \tag{2.35}$$

Substitution of (2.33) into (2.35) results in the expression for the reflection factor [32],

$$r = \frac{j\omega\sigma/\rho_o c}{2 + j\omega\sigma/\rho_o c} \tag{2.36}$$

and the transmission factor [32],

$$\tilde{t} = \frac{2}{2 + j\omega\sigma/\rho_o c}. \tag{2.37}$$

Both of these results represent first order filters. The reflection factor is described by a high-pass filter and the transmission factor is described by a low-pass filter. The corner frequency of this system, f_c, is given by

$$f_c = \frac{1}{\pi}\frac{\rho_o c}{\sigma} = \frac{1}{\pi}\frac{\rho_o c}{\rho_m h} \tag{2.38}$$

where ρ_m and h are the density and the thickness of the sheet, and its mass per unit area is $\sigma = \rho_m h$. Let us now calculate the corner frequency for a thin sheet of steel, which will be of use in Chapter 4. The volume density of steel is $\rho_m \simeq 7.8 \cdot 10^3$

kg/m^3. If the sheet were $1/16^{th}$ of an inch, or $1.59 \cdot 10^{-3}$ m thick, then the corner frequency would be about 10 Hz. The reflection and transmission factors for a $1/16^{th}$ of an inch steel and aluminium sheet are shown in Figure 2.4. This indicates that a steel sheet is more reflective than an aluminium sheet of the same thickness[2].

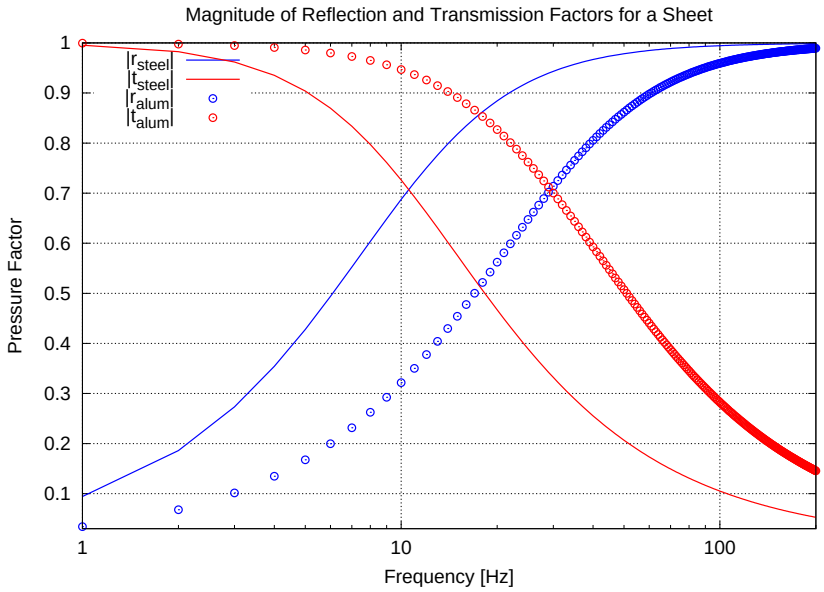

Figure 2.4: Reflection and transmission factors for a 1/16 inch sheet. We see that the aluminium sheet has a higher corner frequency and therefore more transmission of sound at low frequencies.

It is also useful to show this data in terms of decibels (dB) by taking $20\log_{10}(g)$, where g is the magnitude of the reflection or transmission factor. This will indicate how many dB lower the reflected and transmitted signals are relative to the incident sound wave. This is shown in Figure 2.5, and indicates that the transmission is 20 dB down relative to the incident signal at about 100 Hz and continues to drop at approximately 6 dB per octave. The aluminium sheet transmission data is only about 11 dB down relative to the incident signal at 100 Hz.

These results apply when the motion of a sheet or a plate is dominated by its mass. Bending stiffness effects will now be taken into consideration. The theory in the present section, as well as the following section 2.3, is presented to identify the causes of reflection and transmission (which we will call absorption if the plate/sheet is a wall in a room) phenomena through plates and walls. This will not necessarily be used in later chapters in order to compare with measurements quantitatively, but will, however, build comprehension to how a wall reacts to a wave of a given frequency. Recall that it is our goal to determine the absorption characteristics of a surface *in situ* by use of experimental methods.

[2]We are not considering the effect of sheet stiffness, which will be covered in the following section.

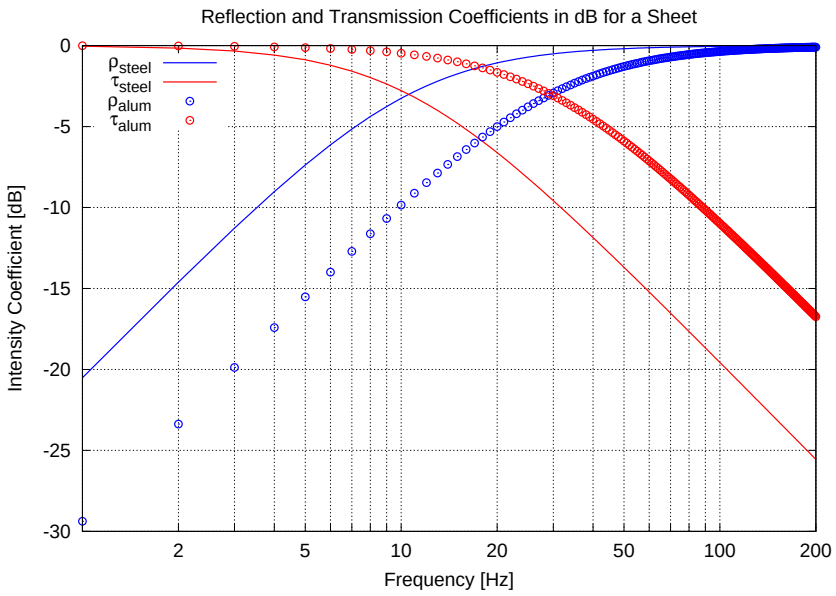

Figure 2.5: Reflection and transmission coefficients in dB for a 1/16 inch sheet. We may note that the transmitted intensity is 20 dB down for steel and 11 dB down for aluminium relative to the incident intensity at about 100 Hz.

2.3 Reflection and Transmission Through Walls

One of the applications of *in situ* measurements is in determining the acoustic impedance of a particular wall in a room. There are many methods used to achieve this, however here we will discuss the theory for plane sound waves having normal incidence on a wall. Walls come in many different forms, such as concrete, brick or drywall for example. There may also be airspaces, studs or insulation behind the wall. In general, a combination of materials is used. Due to the configuration and properties of such a wall, different transmission effects are observed. This depends whether the wall motion is dominated by its stiffness, mass, the wave coincidence effect or damping [4] (see Figure 2.6). Note that the loss increases in the positive direction of the vertical axis.

We are particularly interested in the behaviour of a solid wall (one material) when it is stiffness controlled or mass controlled. Effects due to coincidence and damping are generally above the frequency range of interest (4 kHz). Each phenomenon has dominance in different frequency regions. The following sections will present the results for a stiffness controlled wall and a mass controlled wall, which are developed in [4]. In addition, we will discuss the resonance caused by an airspace between two panels [32].

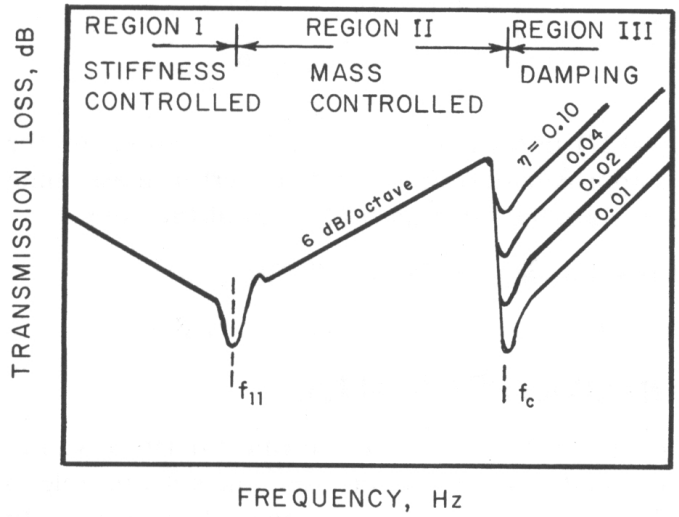

General variation of the transmission loss with frequency for a homogeneous wall or panel.

Figure 2.6: Transmission regions, as per [4].

2.3.1 Stiffness Controlled Region

In the stiffness controlled region, the stiffness of the sheet, panel or wall is the dominant factor in the transmission of sound. The full development for this case will not be carried out, only the results from [4] will be shown here. We proceed in a fashion similar to the approach in Section 2.2.1; however in this case the motion of the wall is dominated by the influence of restoring forces which are similar to that of a spring:

$$(p_i + p_r - p_t)_{z=0} = -\frac{p_o e^{j\omega t}}{j\omega c \rho_o C_s}. \tag{2.39}$$

This may be compared with (2.25). The factor C_s is the mechanical compliance of the panel. If we restrict our analysis to rectangular panels, the mechanical compliance is given by

$$C_s = \frac{64}{B\pi^8(1/l_x^2 + 1/l_y^2)^2} \tag{2.40}$$

where B is the bending modulus (see A.1), l_x the length and l_y the width of the panel. The transmission factor for this system is given by combining the particle velocity and pressure equations at the boundary, as in (2.32) and (2.34). We then isolate the transmission factor and square its magnitude as in (2.4), to obtain the transmission coefficient, τ_s

$$\tau_s = \frac{1}{1 + (1/2\omega\rho_o c C_s)^2} \tag{2.41}$$

where the subscript s denotes stiffness for the importance of stiffness in this region. This behaviour is dominant up to the first resonance of the panel, corresponding to $m = n = 1$ in (A.9),

$$\omega_{11} = \pi^2 \sqrt{\frac{B}{\rho_s h}} \left[\left(\frac{1}{l_x}\right)^2 + \left(\frac{1}{l_y}\right)^2 \right] \tag{2.42}$$

or

$$f_{11} = \frac{\pi}{2} \sqrt{\frac{B}{\rho_s h}} \left[\left(\frac{1}{l_x}\right)^2 + \left(\frac{1}{l_y}\right)^2 \right]. \tag{2.43}$$

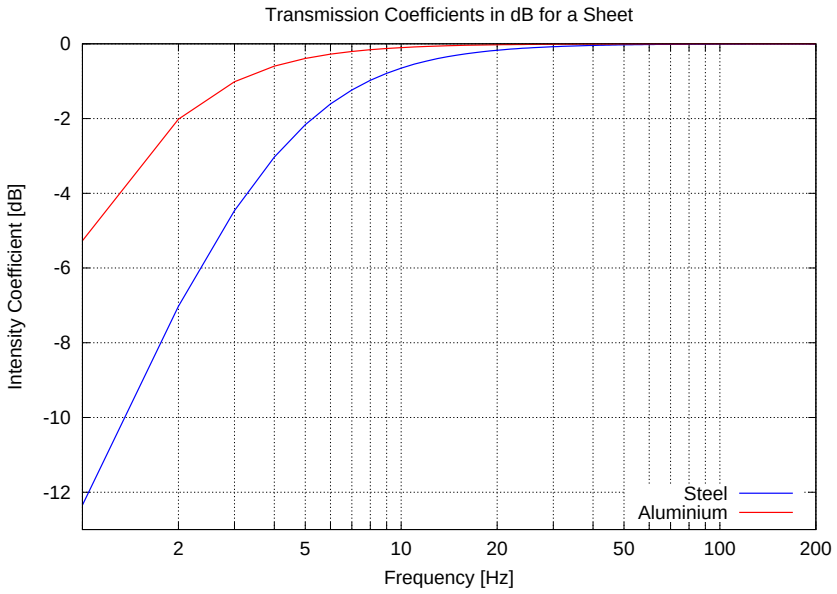

Figure 2.7: Transmission coefficients in dB for a 1.6 mm sheet in the stiffness region. We see that the only differences between a steel and an aluminium sheet are below 30 Hz. If the sheet were controlled solely by its stiffness perfect transmission would occur above 30 Hz. Note that we are neglecting the effects of mass.

There exist many more resonance frequencies (see A.9), however, the first resonance is most important for the low frequency behaviour of the panel [4] (high-frequency resonances fall into the coincidence region). The first resonance is at 5.3-5.4 Hz for both an aluminium or a steel sheet that is 1.6 mm thick with $l_x = l_y = 1.2$ m (see A.1). The logarithm of the transmission coefficient is shown for an aluminium and a steel sheet in Figure 2.7. If we neglect the sheet mass, all of the incident

sound intensity would be transmitted above 30 Hz for both of these sheets. The sheet mass becomes important above the first resonance [4] (5.3-5.4 Hz), which will reduce the transmission of sound as the frequency is increased. This is shown in Figure 2.5 and the rising (increased loss) central portion of Figure 2.6. In addition, we are interested in the transmission of sound above 50 Hz, which falls in the mass controlled region.

2.3.2 Mass Controlled Region

The mass controlled region was described in Section 2.2 where we neglect the bending stiffness and damping effects of the panel. This resulted in (2.37), yielding a transmission coefficient of

$$\tau_m = \frac{1}{1 + (\omega m / 2\rho_o c)^2} \tag{2.44}$$

which governs the transmission effects of the panel up to the critical frequency, given by [4]

$$f_c = \frac{c^2}{2\pi}\sqrt{\frac{\rho_m h}{B}}. \tag{2.45}$$

For our 1/16th of an inch steel sheet, $f_c \simeq 7.7$ kHz. A wooden panel of the same thickness made out of pine, $\rho_m = 640$ kg/m^3, has a critical frequency of about 7.9 kHz. These are both above our frequency range of interest (4 kHz).

2.3.3 Transmission Through a Wall With an Airspace

It is also important to consider a composite wall formed of two panels with an airspace in between them. This is a very common design in homes and buildings, sometimes with insulation filling the space. We will consider the effect without any insulation. We then have a situation as depicted in Figure 2.8. This is a mass-spring-mass system which has a natural frequency given by [32]

$$f_{mam} = \frac{1}{2\pi}\sqrt{\frac{\rho_o}{d}}\sqrt{\frac{M_1 + M_2}{M_1 M_2}} \simeq 60\sqrt{\frac{M_1 + M_2}{M_1 M_2 d}} \tag{2.46}$$

where the subscript mam, signifies "mass-air-mass", since the compression and expansion of air in the cavity acts as a spring. This configuration can be seen as two springs connected in series, each holding a different mass.

We will now present an example which will be of use later in this study: A wall consists of a 3 mm wooden panel backed by an 9 cm airspace and a 10 cm rigid concrete or brick wall. We will use approximate values of the mass per unit area of each surface, $M_{wood} = 1.8$ and $M_{brick} = 180$ kg/m^3. With a depth of $d = 9$ cm, this gives a resonance frequency of 150 Hz.

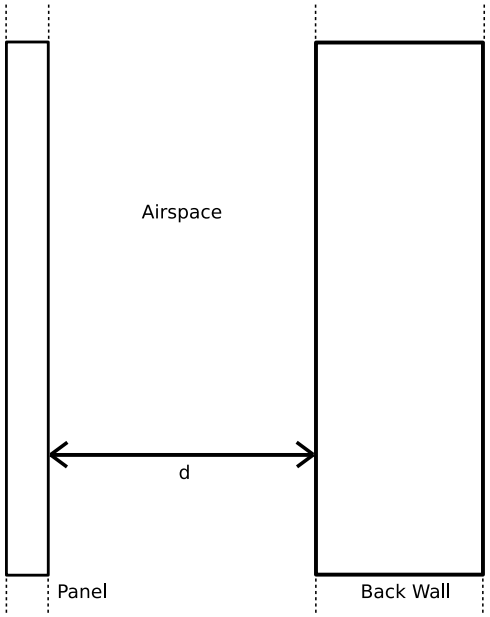

Figure 2.8: Mass air mass resonance. Each wall plays the role of a mass, separated by an airspace which acts as a spring for this system. The incident sound wave would come in on the left, incident on a panel. The sound then vibrates the panel, air and back wall forming a resonance.

Chapter 3

In Situ Measurement Methods

3.1 The Challenge of In Situ Measurements

The environment in which measurements are performed is of key importance in acoustics. There are many interactions happening around an experiment that will contribute noise or unwanted reflections to the sound field. In buildings we have heating and air conditioning units, coworkers, water pipes and various machines. Some of these may be controlled, however some others have to be tolerated. Also, objects in a room will modify the passing of sound by creating reflections, absorption, scattering or diffraction. On the other hand, one may go outside to perform a measurement. In this case, there may be sound contributions from vehicle traffic, wind interacting with structures and of course, people. In the following we will assume that measurements are carried out in a room.

Rooms come in various sizes and are constructed using different materials. Floors are generally rigid and reflect much of the incident sound besides perhaps at lower frequencies. Walls can be solid, hollow or partitioned, and may be constructed using a combination of materials. Some have airspaces, wood or metal studs and perhaps insulation. Our goal is to determine the acoustic absorption characteristics of such a surface independent of its structure[1].

When performing measurements, multiple reflections arrive at the microphone position. Some of these are required for a measurement (such as the incident and reflected sound waves from the surface under study), however others, from the floor and other walls are unwanted and create error in the recorded data.

In addition, multiple sources of noise exist in a typical room, some of which are periodic. These range from heating units, air conditioning units, fans and sound from external environments. In some situations these disturbances may be controlled, however this is not always the case. A high signal-to-noise ratio is therefore required, such that the incident and reflected signals from the surface

[1]The surface under study is generally required to be flat for our measurements. This is an assumption that is used throughout the thesis.

under study have a greater level than the reflections from neighbouring surfaces in the room. Windowing of the impulse response is used if this cannot be achieved. It is also important to mention that ambient noise may always be apparent, and therefore, contribute to the acoustic pressure recorded at a microphone position.

Problems exist at low frequencies in rooms. In this case, the wavelength of the acoustic waves is comparable to the dimensions of the room, allowing the formation of standing waves as the sound reflects back and forth between the room surfaces. This will create an uneven distribution of acoustic pressure in the room, which will depend on the measurement location. All of the above problems have to be considered when taking a measurement in such an environment. Discussion of the challenges with *in situ* measurements will continue throughout this study.

3.2 Measurement Configuration

The measurement configuration typically used in this study is shown in Figure 3.1. An excitation signal is created by a computer program, converted into analog form, amplified and sent to a loudspeaker. The excitation signal is called a maximum length sequence (MLS), which is broad-band and pseudo-random. The properties of MLS systems are well known and have been shown to result in high noise immunity. More information on MLS is given in [33]. A cross-correlation is performed between the input signal to the loudspeaker and the recorded response at the microphone position. The result of this is the impulse response of the system[2](loudspeaker, microphone and room). An impulse response represents the response of a linear, time invariant system to a Dirac delta function excitation (see Figure 3.2). In other words this is the output of a system when the input is of infinitesimal duration and infinite amplitude. In the frequency domain, the Dirac delta function has a flat spectrum, which is unity amplitude at all frequencies. Understanding the response of a system to a Dirac delta input will therefore allow one to understand the response of a system for any input, or at any frequency. This is why we use the impulse response as a measurement tool. We may then take its Fourier transform to go to the frequency domain in order to obtain the frequency response of the system. Mathematically, this is written as [45]

$$H(\omega) = \int_{-\infty}^{\infty} h(t) e^{-j\omega t} dt \tag{3.1}$$

where $H(\omega)$ is the frequency response of a system and $h(t)$ its impulse response. For more details on linear time invariant systems and Dirac delta functions, see [45]. There are some considerations when discrete time sampling is used, but usually the sampling rate is chosen high enough that the system closely approximates a continuous time system.

[2]The periodic impulse response is actually obtained, which is equal to the impulse response if the period of the MLS is longer than or equal to the duration impulse response of the system being measured.

Figure 3.1: Signal chain of measurement system.

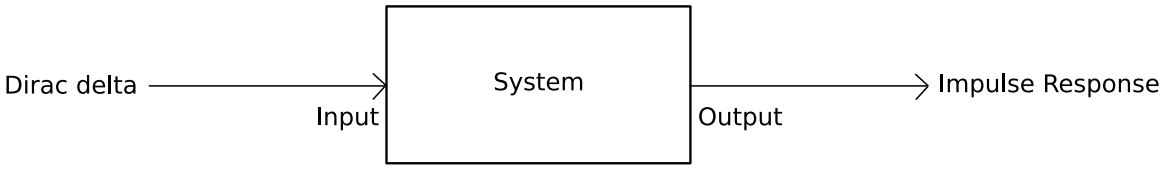

Figure 3.2: Relationship between the impulse response and the Dirac delta. This holds for a linear time invariant system.

Pressure data is collected from a microphone in this configuration. The impulse response therefore represents the response of a system to pressure signals. We will often present the impulse and frequency responses at a given measurement position. The frequency response is used to calculate the reflection factor, and thus the absorption coefficient or acoustic impedance. This is because the frequency response is simply the acoustic pressure amplitude as a function of frequency at the measurement position. In addition the phase of the frequency components in the measured signal may be determined. The relationship between the amplitude (magnitude of the frequency response) and the phase of pressure waves is used to determine the effect of a surface in a particular environment. The following sections present the measurement approaches used in practice to determine acoustic reflection and absorption properties of surfaces *in situ*.

3.3 Reflection Method

3.3.1 Theory

The reflection method exploits the difference in position of the source, microphone and the surface under study in order to separate the incident and reflected impulse responses in the time domain. The time it takes a sound wave to travel a distance q is given by

$$t = \frac{q}{c} \tag{3.2}$$

where t is the time between the creation of the sound wave and the arrival at the position q. The speed of sound is c. A common loudspeaker-microphone-sample configuration is found in Figure 3.3. In the given setup, the incident wave would travel a distance q_o, while the reflected wave would travel a distance $3q_o$. We

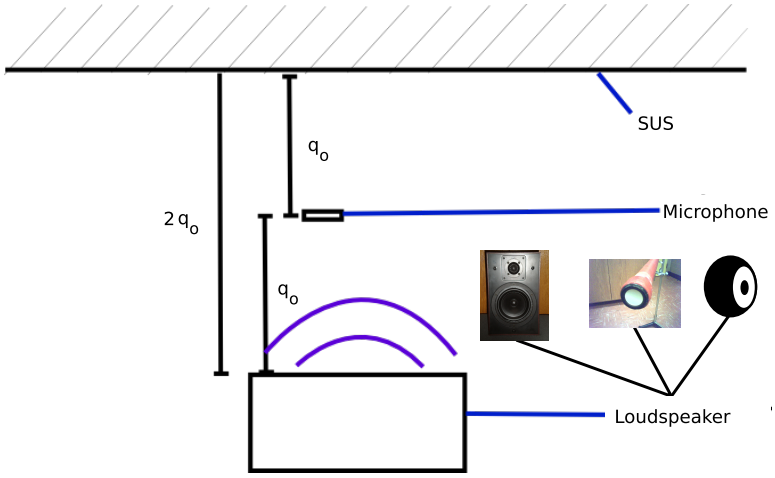

Figure 3.3: Experimental setup of absorption coefficient measurement. Geometrically, the reflected wave path is three times the incident wave path.

may therefore determine the arrival time of the incident and reflected signals using (3.2). The incident and reflected pressure waves would respectively arrive at q_o/c and $3q_o/c$. However here, we assume that the centre of radiation of the loudspeaker is at the loudspeaker itself. This is what is assumed in the papers by Garai [24] as well as Li and Hodgson [21], which is not necessarily the case. We will nevertheless proceed with this assumption for the moment (we will then use the concept of the acoustic centre).

We begin by identifying a form for the pressure waves, p. This of course depends on the acoustical source that we are using in our measurements. However, in general we use the compact source approximation, which is valid when the source is much smaller than the wavelength of its radiation ($2\pi b \ll \lambda$) [29]:

$$p\left(t - \frac{q}{c}\right) = \frac{\rho_o}{4\pi q} U'\left(t - \frac{q}{c}\right) \tag{3.3}$$

where b is the source radius. The derivative of the volume velocity U is with respect to its argument, the retarded time $(t - r/c)$. In this case, this is an approximation stating that the source loudspeaker is producing spherical waves, depending on the acceleration of its diaphragm. Each frequency component of the acoustic pressure will be of the form

$$p_\omega(q,t) = \frac{q_{ref}}{q} B_\omega e^{j(\omega t - kq)} \tag{3.4}$$

where p_ω represents one frequency component of the total pressure. Since the pressure amplitude generally varies with frequency we denote it as B_ω. The factor q_{ref} is included to adjust units, and allows B_ω to represent the pressure amplitude at a distance q_{ref}. Each frequency component of a pressure signal should satisfy

(3.4) as long as the compact source approximation is valid. The total pressure would therefore be

$$p(q,t) = \sum_{\omega} p_{\omega}(q,t) = \frac{q_{ref}}{q} \sum_{\omega} B_{\omega} e^{j(\omega t - kq)}. \tag{3.5}$$

This is a Fourier series representation of the pressure wave. We may look at a single pressure component, p_{ω} without loss of generality, knowing that the following will apply to each frequency component and therefore the entire pressure, p. The time dependence in (3.4) is often omitted since it is present in all of the acoustic waves, this gives

$$p_{\omega}(q) = \frac{q_{ref}}{q} B_{\omega} e^{-jkq}. \tag{3.6}$$

The incident and reflected acoustical pressures adopt this form. These are respectively

$$p_{i\omega}(q_i) = \frac{q_{ref}}{q_i} B_{i\omega} e^{-jkq_i} \tag{3.7}$$

and

$$p_{r\omega}(q_r) = \frac{q_{ref}}{q_r} B_{r\omega} e^{-jkq_r}. \tag{3.8}$$

Here q_i and q_r represent the different propagation distances travelled by the respective sound waves. The pressure amplitudes are not necessarily the same. In the special case where $p_{i\omega} = p_{r\omega}$ at the surface, the boundary is said to be rigid, having a reflection coefficient of unity.

The ratio of the reflected pressure to the incident pressure at the surface gives the reflection factor r, as in (2.1). In this case we obtain

$$r_{\omega} = \frac{p_{r\omega}(q)}{p_{i\omega}(q)}\Big|_{q=q_s} = \frac{B_{r\omega}}{B_{i\omega}} \tag{3.9}$$

which is the ratio of wave amplitudes (remember the units of B_{ω} are $\mathrm{N/m^2}$). Suppose we now were to measure the pressure at a distance q_o from a surface as in Figure 3.3. The incident and reflected pressure waves no longer have the same propagation distance, $q_s = 2q_o$. The incident wave will travel a distance q_o and the reflected wave $3q_o$. This then gives

$$p_{i\omega}(q_o) = \frac{q_{ref}}{q_o} B_{i\omega} e^{-jkq_o} \tag{3.10}$$

and

$$p_{r\omega}(3q_o) = \frac{q_{ref}}{3q_o} B_{r\omega} e^{-jk(3q_o)}. \tag{3.11}$$

By taking the ratio of (3.11) to (3.10) and isolating r_ω by use of (3.9), one obtains

$$r_\omega = 3\frac{p_{r\omega}(3q_o)}{p_{i\omega}(q_o)} e^{jk2q_o}. \tag{3.12}$$

Therefore a measurement of the incident and reflected pressure waves at the microphone position, q_o will allow us to determine the reflection factor. Introducing this result into (2.9), the absorption coefficient becomes

$$\alpha_\omega = 1 - |r_\omega|^2 = 1 - 9\left|\frac{p_{r\omega}(3q_o)}{p_{i\omega}(q_o)}\right|^2. \tag{3.13}$$

Once again, the subscript ω indicates that we have only to evaluate (3.13) at the frequency of interest to obtain the acoustic absorption coefficient at the same frequency. This notation is cumbersome, and the index ω will often be omitted.

Acoustic Centre

If we are to use the compact source approximation, we must prescribe the proper $1/q$ factors describing the spherical spreading of the acoustic pressure waves. We will call the origin of these spherical waves δ, the acoustic centre. At low frequencies, it has been shown that the acoustic centre of a piston in a sealed enclosure is approximately a cabinet half-width away from the baffle [39].

The acoustic centre may be found from a series of pressure measurements at multiple distances from a loudspeaker. Since the pressure should vary as $1/q$ in the far field, a plot of the magnitude of $1/p$ versus q should be linear. Referring to the acoustic pressure in (3.6), we have

$$\frac{1}{|p(q)|} = \frac{q}{q_{ref}|B_\omega|}, \qquad q > 0. \tag{3.14}$$

Now if we consider that the acoustic centre is at a point away from the origin (taken as the baffle of the loudspeaker in Figure 3.3), we replace q with $q - \delta$ in (3.14) to obtain

$$\frac{1}{|p(q-\delta)|} = \frac{q-\delta}{q_{ref}|B_\omega|}, \qquad q - \delta > 0. \tag{3.15}$$

This equation has a q-intercept at $q = \delta$, the acoustic centre. We may thus plot (3.15) as a function of q in order to obtain the acoustic centre of the loudspeaker.

The factor δ is required as a correction to the propagation distance at low frequencies. At high frequencies, the acoustic centre has approximately the same position as the baffle of the loudspeaker.

We must now determine the reflection factor using the appropriate $1/q$ factors. The incident and reflected pressures are

$$p_{i\omega}(q_o - \delta) = \frac{q_{ref}}{q_o - \delta} B_{i\omega} e^{-jk(q_o - \delta)} \tag{3.16}$$

and

$$p_{r\omega}(3q_o - \delta) = \frac{q_{ref}}{3q_o - \delta} B_{r\omega} e^{-jk(3q_o - \delta)} \tag{3.17}$$

yielding a reflection factor of

$$r_\omega = \frac{3q_o - \delta}{q_o - \delta} \frac{p_{r\omega}(3q_o - \delta)}{p_{i\omega}(q_o - \delta)} e^{jk2q_o} \tag{3.18}$$

and by substitution of (3.18) in (2.9), the absorption coefficient is

$$\alpha = 1 - \left(\frac{3q_o - \delta}{q_o - \delta} \right)^2 \left| \frac{p_r(3q_o - \delta)}{p_i(q_o - \delta)} \right|^2 \tag{3.19}$$

where we have omitted the subscript ω. It may be seen that (3.18) becomes (3.12) and (3.19) becomes (3.13) when $\delta = 0$, as it should be.

Loudspeakers

A KEF loudspeaker was used as a source in the first experiment. This loudspeaker is composed of two drivers in a closed box enclosure (Figure 3.4). A significant amount of diffraction is assumed for this speaker, due to the edges of its rectangular enclosure [38]. The pressure received at the microphone position is thus the sum of the direct and diffracted pressures.

The loudspeaker enclosure has the dimensions of 21 cm by 25 cm by 34 cm (width, depth, height), with a 3 cm tweeter and a 13 cm woofer (diameters). The enclosure in which these units are mounted affects the acoustic centre. The acoustic centre of this loudspeaker should be about a cabinet half-width away from the loudspeaker baffle [40].

In addition, a loudspeaker was constructed using a plastic pipe 1.3 m in length, with outer diameter of 4.5 cm and inner diameter of 4 cm. The pipe has a 3 cm diameter driver in one end and a plug in the other (Figure 3.5). In addition, this pipe is filled with a fibrous filler material. This loudspeaker will act as a compact source up to higher frequencies than the KEF. In terms of diffraction, it is useful

Figure 3.4: KEF two-way loudspeaker. Grill was removed to show the tweeter (3 cm diameter) and woofer (13 cm diameter) units.

to note that this enclosure is fairly smooth and does not have long edges like those from a rectangular box. This loudspeaker should create less diffraction at the microphone position than the KEF loudspeaker. In the following, this loudspeaker will be referred to as the tube loudspeaker.

Figure 3.5: Small driver loudspeaker. a) 3 cm diameter loudspeaker driver. b) End of tube showing plug and connectors. c) 1.3 m tube loudspeaker.

3.3.2 Experiments

Measurements were performed in a rectangular room with various surfaces (Figure 3.6). The first experiment was performed using a wood panelled wall as a sample with the KEF loudspeaker. In the second, the same wall was measured using the tube loudspeaker. This room is shown in Figure 3.7.

The wall is assumed to be rigid at high frequencies, however absorption is expected at the mass-air-mass resonance of this wall. This resonance frequency was predicted to be approximately 150 Hz in section 2.3.3. The actual wall parameters are not known which is often the case when performing *in situ* measurements. Approximate values for the mass per unit area of the panels and the airspace were used to obtain the resonance frequency.

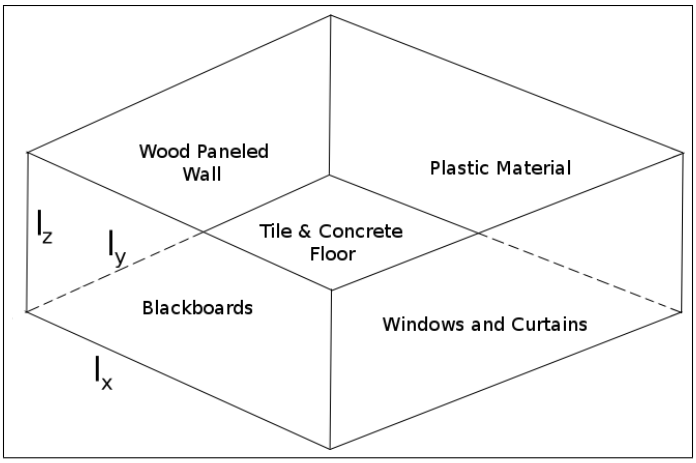

Figure 3.6: Rectangular room of dimensions $l_x = 5.5$, $l_y = 7.5$ and $l_z = 2.8$ metres. Measurements were performed on the wood panelled wall shown in Figure 3.7.

Figure 3.7: Physics lounge showing wood panelled wall on the left.

Choice of $\mathbf{q_o}$

The choice of q_o depends on the geometry and the layout of objects in the measurement environment. Rooms are typically compromised of six plane surfaces that partially absorb and reflect sound. It is therefore important to identify the unwanted reflections from these surfaces before a measurement is performed. This is done by measuring the distance between the loudspeaker, room surface and the microphone. For the floor reflection in the given configuration, this is $q_l + q_l = 2q_l$, as shown in Figure 3.8. Using the geometry shown, we find that

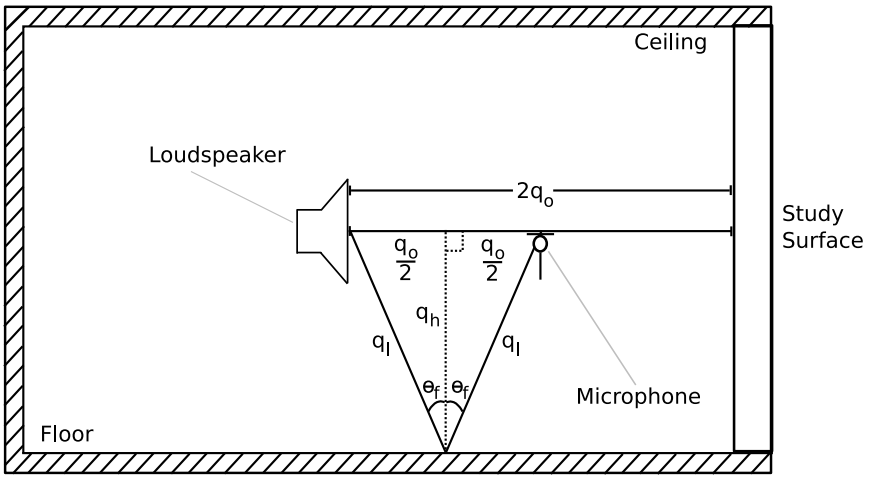

Figure 3.8: Reflections from other surfaces in a room. Here we assume that the closest surface is the floor, which is usually the case.

$$q_l = \sqrt{\frac{q_o^2}{4} + q_h^2}. \tag{3.20}$$

Twice this distance divided by the speed of sound will then yield the time it will take for this reflection to arrive at the microphone position,

$$t_{floor} = \frac{2q_l}{c} = \frac{1}{c}\sqrt{q_o^2 + 4q_h^2}. \tag{3.21}$$

We also have to consider the time it takes for the incident and reflected sound components to arrive at the microphone, which are

$$t_{inc} = \frac{q_o}{c} \tag{3.22}$$

and

$$t_{ref} = \frac{3q_o}{c}. \tag{3.23}$$

Note also that the loudspeaker itself may reflect sound. The time it would take for this reflection to reach the microphone position is

$$t_{spk} = \frac{5q_o}{c}. \tag{3.24}$$

The impulse response will show these reflections, allowing for the separation of signals in the time domain. However, in principle we cannot fully separate the impulse response of the incident and reflected components since the low frequency

tails of these are still oscillating when other reflections arrive. We therefore get an overlap of signals.

Ultimately, the closest reflection will dictate the time window used in gating the incident and reflected signals. A time window is used to separate a portion of the incident and reflected components from each other. As the name indicates, a window will only allow a particular portion of the signal to pass unobstructed. The portion of the signal which lies outside the time window is attenuated, reducing the amplitude of the signal in this time region. This also is used to remove the parasitic reflections from other surfaces. It is important to position the loudspeaker, microphone and sample as far as possible from the surfaces which are not being measured. This is often difficult, especially in small rooms.

We may now consider the relationship between the window length and the frequency resolution obtained. The time window length Δt is related to the frequency resolution Δf by the reciprocal relationship

$$\Delta f \simeq \frac{1}{\Delta t}. \tag{3.25}$$

As we stated before, the time window length depends on the proximity of room surfaces that contribute unwanted reflections of sound at the microphone position. We see that a frequency resolution on the order of ten hertz requires a time window of one tenth of a second, corresponding to a nearest surface of about seventeen metres away. This is half the distance that the reflected sound wave travels. On the other hand, a frequency resolution on the order of one hundred hertz is achieved with a nearest surface of almost two metres. It is therefore clear that the frequency resolution of a measurement is limited by the geometry of the experimental setup. The first unwanted reflection arriving at the microphone will dictate the time window length used (in order to prevent or minimize the overlap of signals). The length of the time window will be the smallest of:

1. The difference between the arrival time of the reflected wave and the arrival time of the incident wave: $\Delta t_{ri} = t_{ref} - t_{inc}$.
2. The difference between the arrival time of the floor reflection and the arrival time of the reflected wave: $\Delta t_{fr} = t_{floor} - t_{ref}$.
3. The difference between the arrival time of the speaker reflection and the arrival time of the reflected wave: $\Delta t_{sr} = t_{spk} - t_{ref}$.

In other words, we would not like any reflections, from the surface under study or other surfaces, to overlap the incident sound wave or the reflected sound wave. Note that for the given configuration $\Delta t_{ri} = \Delta t_{sr} = t_{spk} - t_{ref}$ (see (3.22) to (3.24)). The previous conditions can be written mathematically as

$$\Delta t = min\{t_{ref} - t_{inc}, t_{floor} - t_{ref}, t_{spk} - t_{ref}\} \tag{3.26}$$

where *min* is simply the lowest value of the evaluated arguments. This ensures that we exclude the unwanted reflections from the measurement, and, that the window length is constant for both the gated incident and reflected waves. In practice, the window length is chosen to be slightly smaller than the value of Δt to ensure the prevention of overlapping signals. It is important to mention that the smaller the time window, Δt, the larger the frequency spacing Δf in the frequency domain. A reflection from an unwanted surface may be excluded by employing a time window, however a portion of the signal of interest is lost as well. This results in the loss of low frequency data.

3.3.3 Results

Using the KEF Loudspeaker on a Wood Panelled Wall

A loudspeaker-wall distance ($2q_o$) of about 100 cm was used, making $q_o = 50$ cm. The loudspeaker height, q_h was approximately 160 cm. Using (3.21) to (3.24), this gives: $t_{inc} = 1.46$ ms, $t_{ref} = 4.37$ ms, $t_{floor} = 9.44$ ms and $t_{spk} = 7.29$ ms. We then obtain $\Delta t_{ri} = \Delta t_{sr} = 2.91$ ms and $\Delta t_{fr} = 5.07$ ms. The upper bound of the time window length is $\Delta t = \Delta t_{ri} = 2.91$ ms, which prevents an overlap between the incident and reflected sound waves. As we stated before, we will use a value slightly smaller than this, in this case $\Delta t = 2.8$ ms. Substitution of this value in (3.25) gives a frequency resolution of 357 Hz. This means that all data will be a smoothed representation of the actual data. This causes problems at low frequencies due to the small frequency spacing.

The impulse response of this configuration is shown in Figure 3.9. The first pulse represents the incident pressure wave on the wall. The second pulse is the reflection of the incident wave from the wood panelled wall. The third pulse is the reflection of sound from the loudspeaker itself. It is important to stress however that the impulse response of the incident acoustic wave is still oscillating well into the arrival of the reflected wave. High-frequency components of this signal have decayed significantly; however the low-frequency response of the loudspeaker has not. There is therefore an overlap of signals. In this case we can no longer discern what is the incident wave and what is the reflected wave. The only way to remedy this problem is to increase the distance between the loudspeaker, microphone and the surface under study. However this strategy has a limiting case, if $q_o \gg 2q_h$ in (3.21), we see that $t_{floor} \to q_o/c$. This is the same amount of time it takes for the incident acoustic wave to arrive at the microphone, which would indicate that both waves would arrive at the same time.

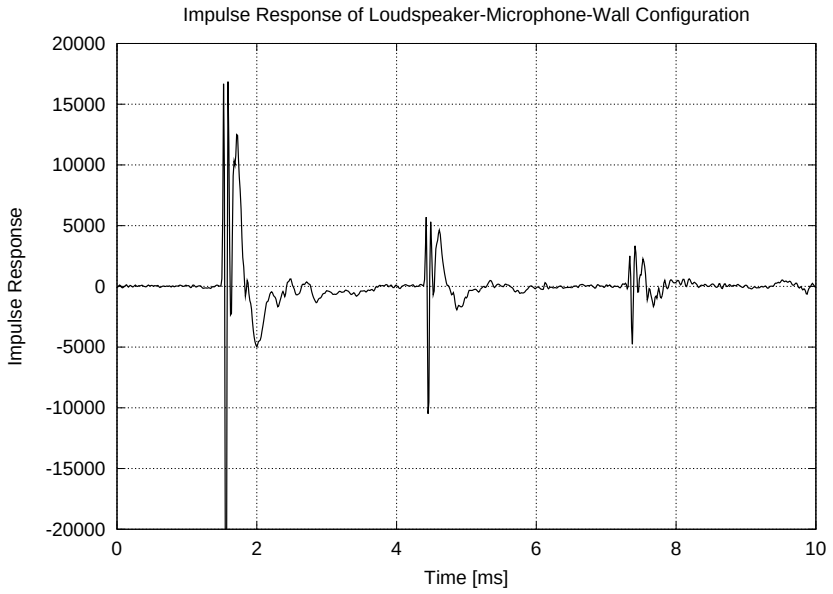

Figure 3.9: Impulse response of loudspeaker-microphone-wood panelled wall configuration. The incident signal begins at 1.5 ms, the wall reflection at 4.4 ms and the reflection off of the loudspeaker itself at 7.3 ms. There is an overlapping of the signal tails here as well.

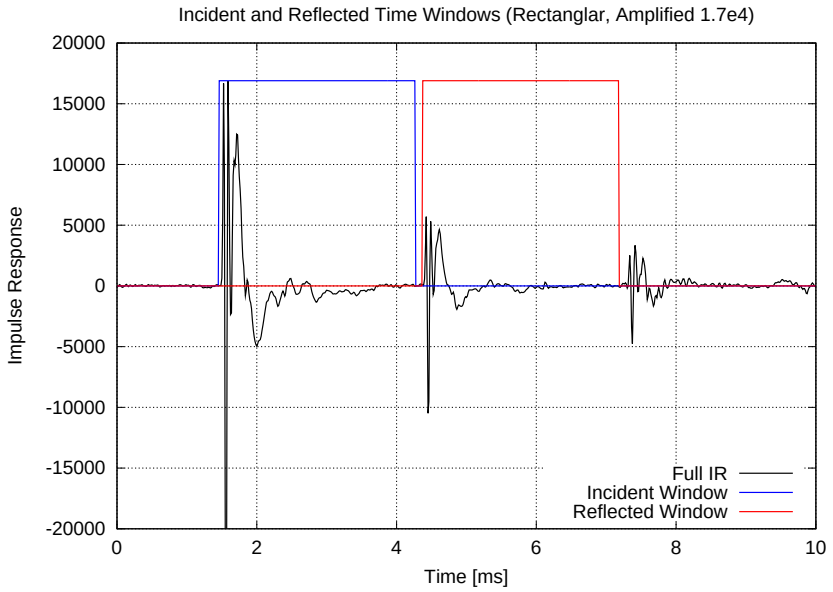

Figure 3.10: Impulse response of loudspeaker-microphone-wood panelled wall configuration, shown with rectangular windows on incident and reflected pressure components.

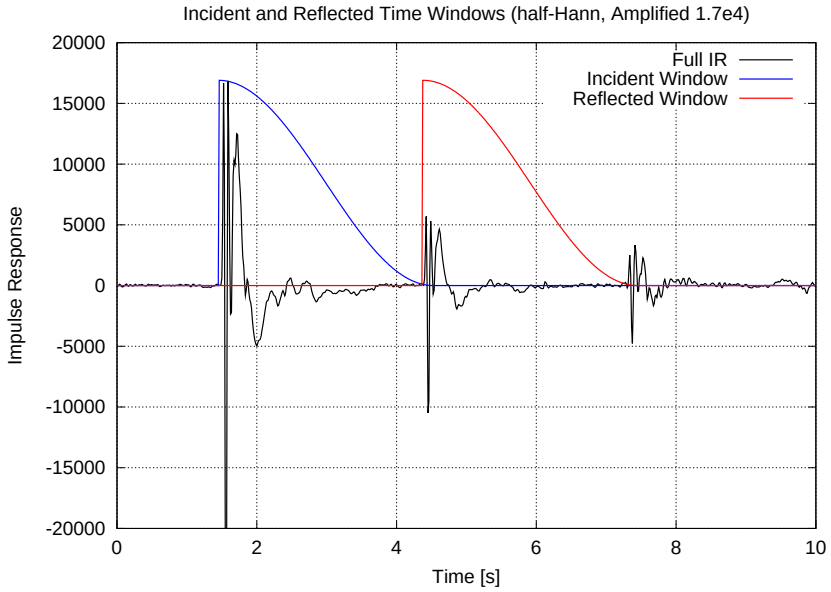

Figure 3.11: Impulse response of loudspeaker-microphone-wood panelled wall configuration, shown with half-Hann windows on incident and reflected pressure components.

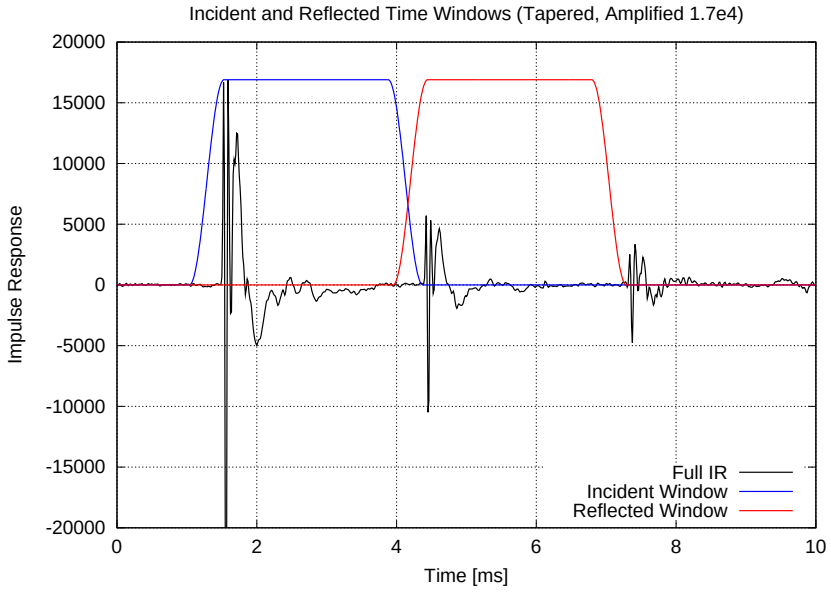

Figure 3.12: Impulse response of loudspeaker-microphone-wood panelled wall configuration, shown with tapered windows on incident and reflected pressure components.

We have already established that there is overlap of signals in this method. It is still possible to separate the incident and reflected waves in order to calculate the reflection (or absorption) characteristics at high frequencies. Different windows may be used to separate the acoustic wave components. The impulse response is shown with three choices of windows: a rectangular window, a half-Hann window and a hybrid of the two which we will call the tapered window (a rectangular window with half-Hann portions on either side). These windows are shown with the original impulse response in Figures 3.10 to 3.12. Note that the windows are shown with expanded vertical scales in every figure in this document. This shows which portion of the impulse response lies inside and outside the window.

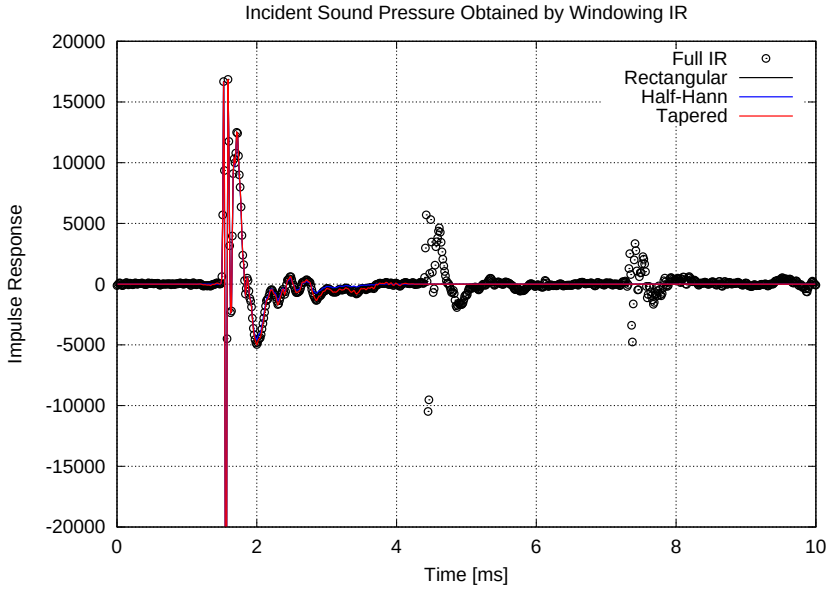

Figure 3.13: Incident pressure wave obtained from the windowing of the impulse response.

Figure 3.13 shows the incident wave with each applied window. Likewise, Figure 3.15 shows the reflected wave with each window applied. Figures 3.14 and 3.16 show a magnified version of the impulse responses for the incident and reflected waves. We see that the rectangular and tapered window data follow very well. However the half-Hann windowed data steers away from the other responses as time progresses. This is due to the fact that this window increasingly attenuates the data with time. The half-Hann window also starts abruptly with a zero-to-one transition. The data to the left of this window are set to zero. After these windows are applied, a Fast Fourier Transform (FFT) is taken of each incident and reflected pressure wave, which is then smoothed 1/3 of an octave. This is shown in Figure 3.17 for the incident portion and in Figure 3.18 for the reflected portion.

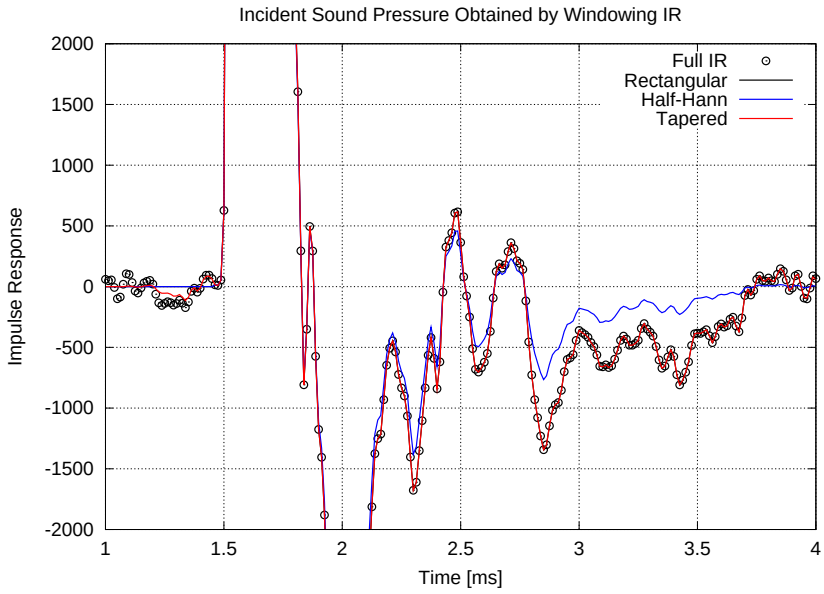

Figure 3.14: Incident sound pressure obtained from the windowing of the impulse response. This is magnified to show the separation of the half-Hann windowed data relative to the rectangular and tapered windowed data.

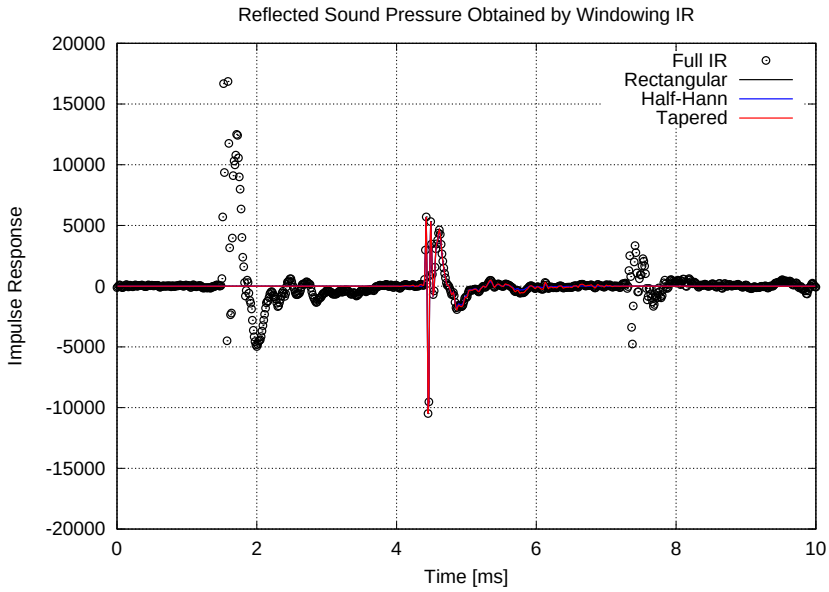

Figure 3.15: Reflected sound pressure obtained from the windowing of the impulse response.

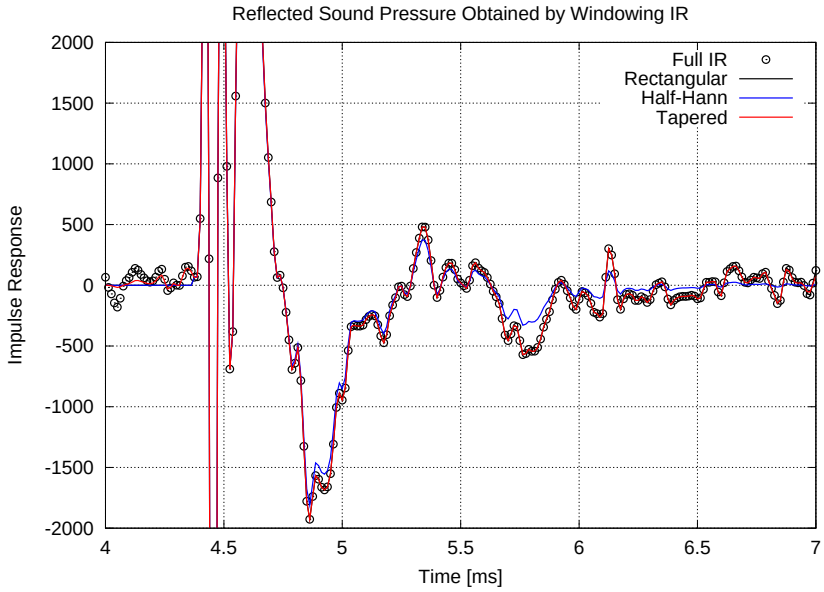

Figure 3.16: Reflected sound pressure obtained from the windowing of the impulse response. This is magnified to show the separation of the half-Hann windowed data relative to the rectangular and tapered windowed data.

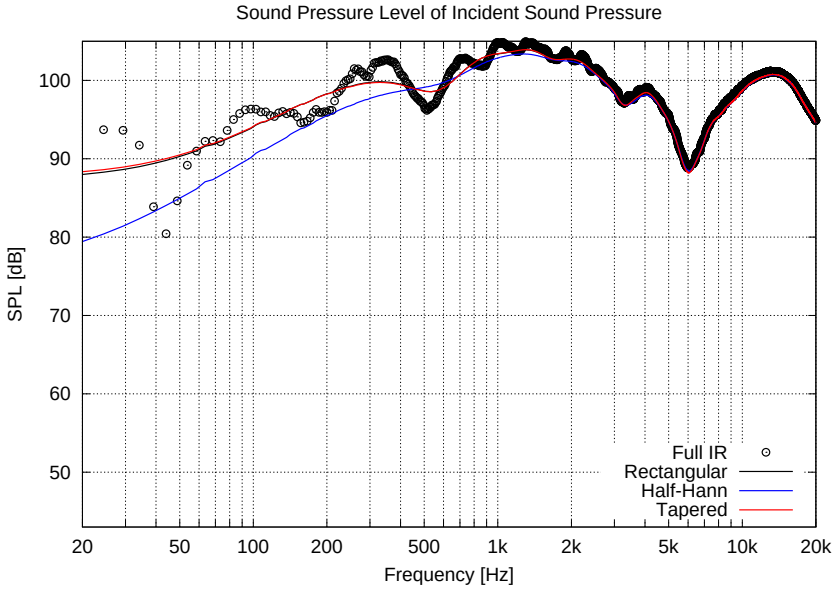

Figure 3.17: 1/3-Octave smoothed sound pressure levels of incident wave for different windows. Notice that the rectangular and tapered windowed data follow closely. In this instance, the half-Hann windowed data features a drop in level towards the low frequencies. This could also rise depending on where the impulse response is truncated.

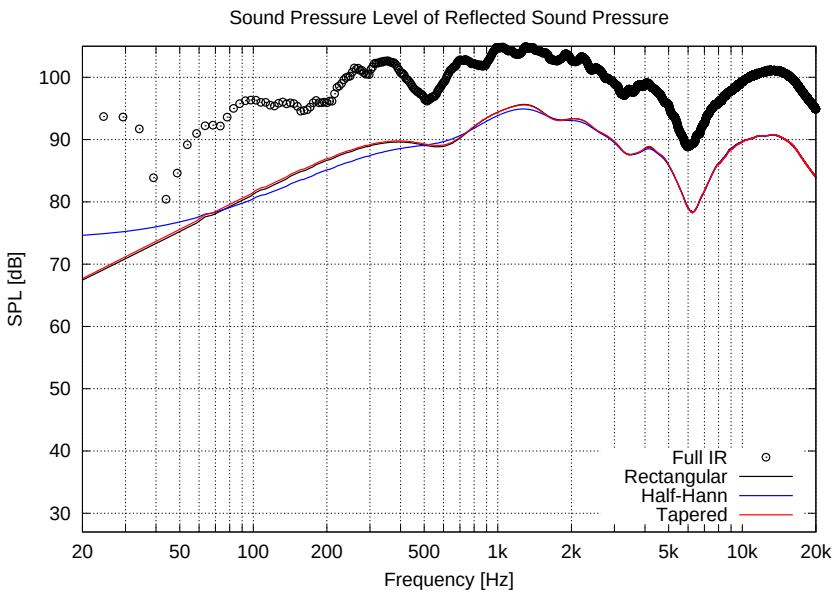

Figure 3.18: 1/3-Octave smoothed sound pressure levels of reflected wave for different windows. Notice that the rectangular and tapered windowed data follow closely. The half-Hann windowed data features a rise in level towards the low frequencies. This data is much lower than the sound pressure level of the whole impulse response.

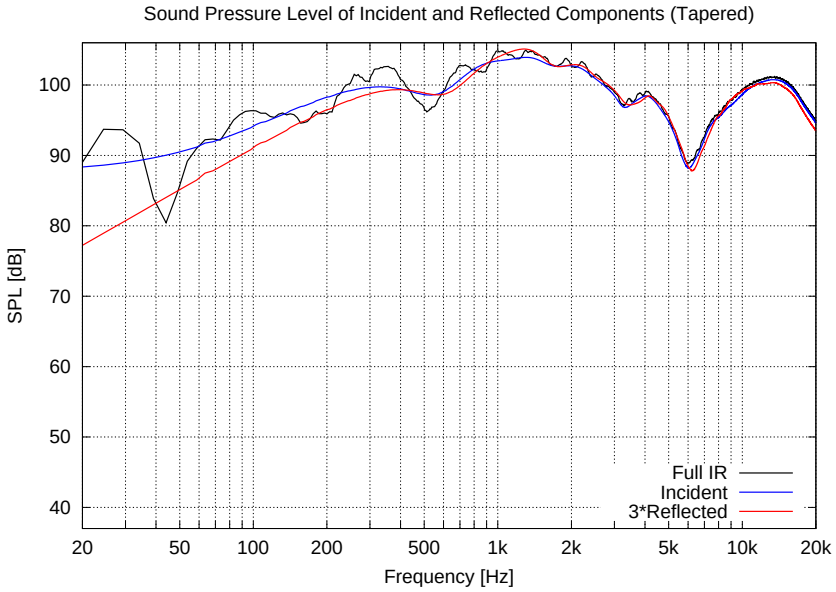

Figure 3.19: 1/3-Octave smoothed sound pressure levels of reflected and incident waves using a tapered window. The reflected pressure amplitude is multiplied by three in order to account for the spherical spreading of the waves. We notice that the reflected pressure is sometimes greater than the incident pressure.

Again we see that the tapered and rectangular windowed data are almost identical over the whole frequency range, while the half-Hann windowed data drops below or rises above the former results. For the incident wave, the half-Hann windowed data drops towards low frequencies since it reduces the long-time behaviour of the impulse response. The reflected wave features a rise at low frequencies. We should note that the reflected portion of the impulse response includes the oscillating tail of the incident wave. We may not trust this data over the whole frequency range. By using only 2.8 ms of data for each pressure wave, we may only be able to have confidence in data which is above 357 Hz (perhaps even higher than this value). Results below 357 Hz are a smoothed representation of the actual sound pressure levels.

For the moment we will not consider the effect of the acoustic centre on our calculations. We assume that the reflections from the surface under study are specular, and that the spherical nature of the sound wave is preserved. In order to compensate for the spherical spreading of the sound waves, the reflected wave should be multiplied by a factor of three (it has travelled $3q_o$ whereas the incident wave has travelled a distance of q_o (see (3.10) and (3.11)). This is shown in Figure 3.19. The incident and reflected sound pressure levels follow closely above 500 Hz, however we see that the reflected pressure amplitude often rises higher than the incident pressure amplitude. This indicates that there is one of two problems occurring: 1) There is more reflected acoustic pressure from the wall than there is incident (wall is producing energy) or 2) We are not fully characterizing the incident sound field. We speculate that the cause is of the latter nature, due to diffraction effects occurring at the loudspeaker. The effect of the acoustic centre has been considered, however this would result in an increase in the multiplication factor ($3p_{r\omega}/p_{i\omega}$ would become $3.22p_{r\omega}/p_{i\omega}$ for an acoustic centre of 10 cm), and therefore worsen our situation. In addition, we should only consider using the acoustic centre at low frequencies (below 200 Hz for example).

The reflection coefficient is calculated using (2.2) and shown smoothed 1/3 of an octave in Figure 3.20, and smoothed 1 octave in Figure 3.21. The 1-octave smoothing increasingly suppresses the peaks and dips as expected; however both sets of data have reflection coefficients exceeding unity. This again is due to the fact that the reflected pressure amplitude rises above the incident pressure amplitude at many frequencies. On the other hand, this measurement has indicated that the wood panelled wall is highly reflective above 500 Hz. A sudden rise of the half-Hann windowed data is seen at low frequencies. This is somewhat arbitrary, since the low frequency response will depend on where the impulse response is truncated. We should note however that the tail of the incident wave is oscillating into the reflected wave.

In addition, we see that the tapered windowed data results in increased reflection towards low frequencies. This may be explained by the fact that the beginning of the window is a half-Hann that includes more of the incident signal (which is overlapping the reflected signal) than the rectangular window would allow.

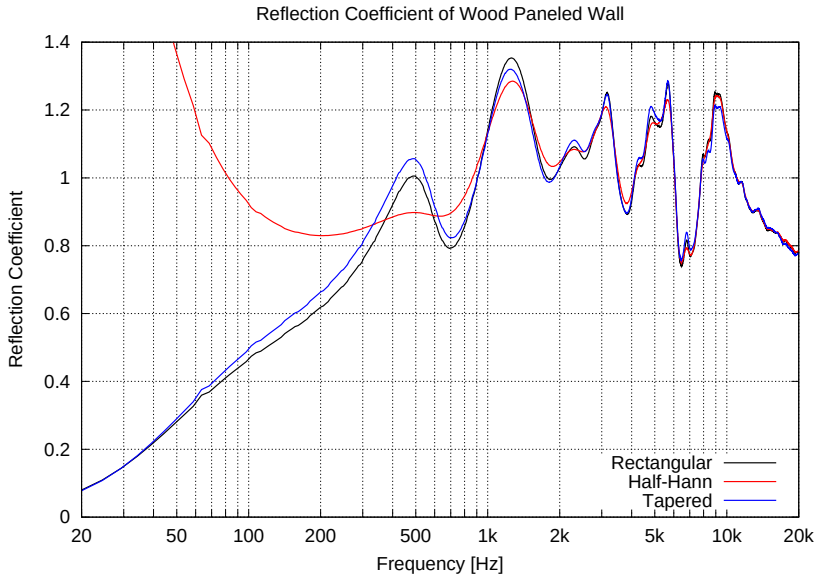

Figure 3.20: 1/3-Octave smoothed reflection coefficient of wood panelled wall. Values rising above unity indicate that the reflected pressure is greater than the incident pressure. The sudden rise of the reflection coefficient at low frequencies compared to the rectangular window data supports the fact that the overlapping tail of the incident pressure wave is present in the windowed reflected pressure.

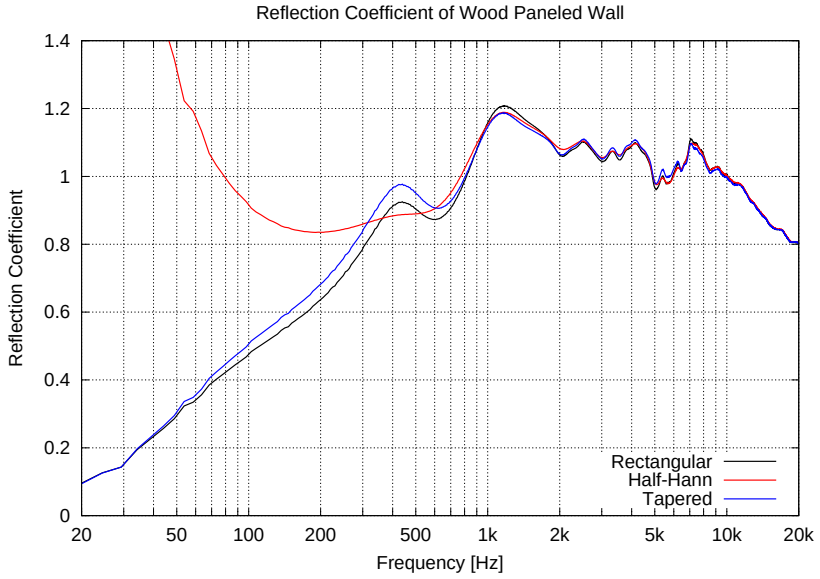

Figure 3.21: 1-Octave smoothed reflection coefficient of wood panelled wall. Values rising above unity indicate that the reflected pressure is greater than the incident pressure. The sudden rise of the reflection coefficient at low frequencies compared to the rectangular window data supports the fact that the overlapping tail of the incident pressure wave is present in the windowed reflected pressure.

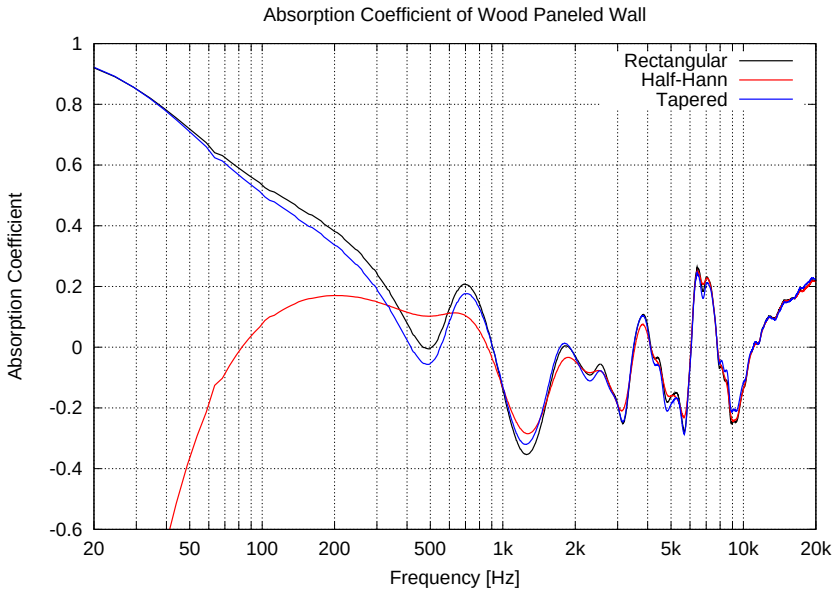

Figure 3.22: 1/3-Octave smoothed absorption coefficient of wood panelled wall. Values below zero indicate that the reflected pressure is greater than the incident pressure. The drop in absorption at low frequencies for the half-Hann data relative to the rectangular windowed data supports the fact that the reflected wave has an overlapping incident pressure contribution.

The absorption coefficient is presented in Figure 3.22. No new information is given here, this is simply $1 - \rho = 1 - |r|^2$. Our discussion of the results for the reflection coefficient apply to the absorption coefficient as well; however we have to flip our reasoning (if the reflection coefficient is large then the absorption coefficient is small for example). It is seen that the absorption coefficient drops below zero at the locations where the reflection coefficient is greater than one. This indicates that we are not fully characterizing the incident sound wave. We will continue to present the absorption coefficient as our key result in the remainder of this study. The tapered window will continue to be applied on the incident and reflected portions of the measured impulse response.

Using the Tube Loudspeaker on a Wood Panelled Wall

The KEF loudspeaker is a 2-way system having both woofer and tweeter units. Therefore the resulting sound wave from such a device has two centres of radiation. Ideally we would have loudspeakers that are able to operate over the entire audible frequency range. For this reason, we have constructed a low diffraction, compact loudspeaker with a large throw (large motion of the cone). This was earlier shown in Figure 3.5. The front of the loudspeaker is 3-4 cm in diameter which indicates that it will follow the compact source approximation to higher frequencies than an 8-10 cm driver loudspeaker.

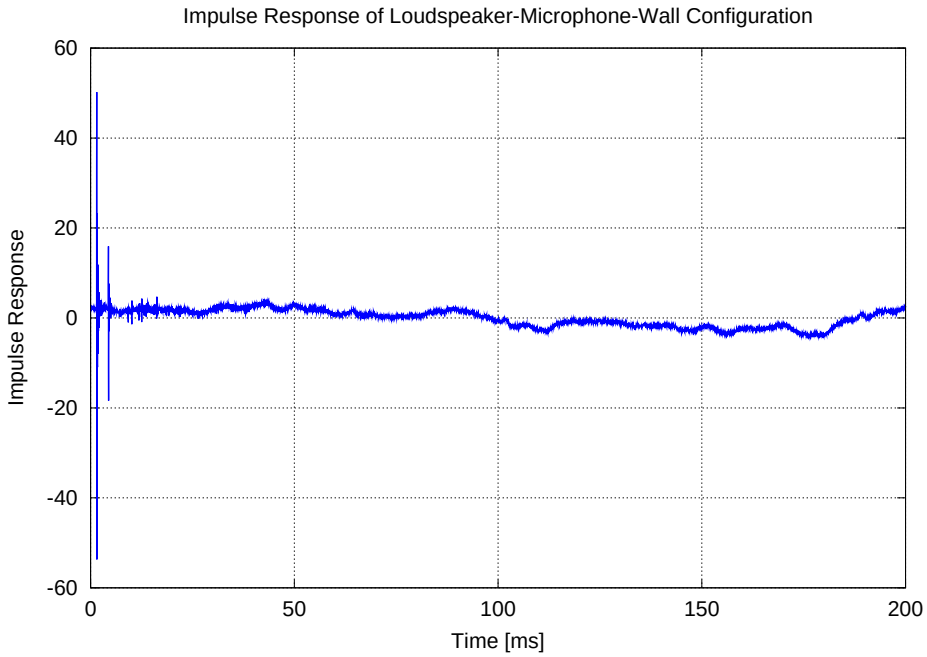

Figure 3.23: Impulse response of loudspeaker-microphone-wood panelled wall configuration using the tube loudspeaker. Low frequency oscillations from ambient room noise are clearly seen. This indicates that this measurement does not have a high signal-to-noise ratio at low frequencies.

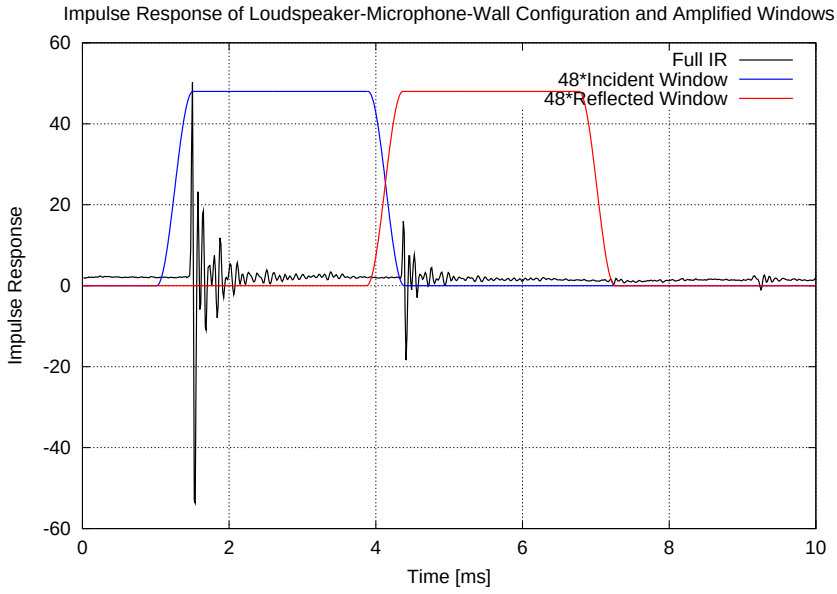

Figure 3.24: Impulse response of loudspeaker-microphone-wood panelled wall configuration with windows using the tube loudspeaker. Low frequency oscillations from ambient room noise create an offset of the impulse response.

The wood panelled wall from the previous section was tested using this loudspeaker. We can see that this measurement suffers from a low signal-to-noise ratio in Figure 3.23. Large low frequency oscillations are seen which indicate that the loudspeaker is not radiating enough energy in this region. This will create an offset and truncation error if a rectangular window is used. We will therefore use the tapered window. Figure 3.24 displays the overlapping windows on the incident and reflected pressure components (recall that windows are amplified for display purposes). We see an offset of the impulse response due to the low frequency noise in the room. This data would benefit from high-pass filtering. Figure 3.25 shows the incident and reflected sound waves.

In the frequency domain (see Figure 3.26), we notice that the reflected sound pressure level rises above the incident sound pressure level below 3 kHz. This should not be due to the low signal level coming from the loudspeaker: this is a high frequency. In addition, this loudspeaker should contribute less diffraction at the microphone position. We speculate that diffraction could not account for a 10 dB difference in level. We do see however that the incident and reflected components are about equal above 3 kHz. The absorption coefficient is therefore approximately zero in this frequency range (see Figure 3.27). It is difficult to make any conclusions below 3 kHz. As we discussed before, it is also apparent that this loudspeaker should not be used in the current configuration due to poor output level. Note that high-pass filtering could be used to reduce the low frequency oscillations seen in the impulse response.

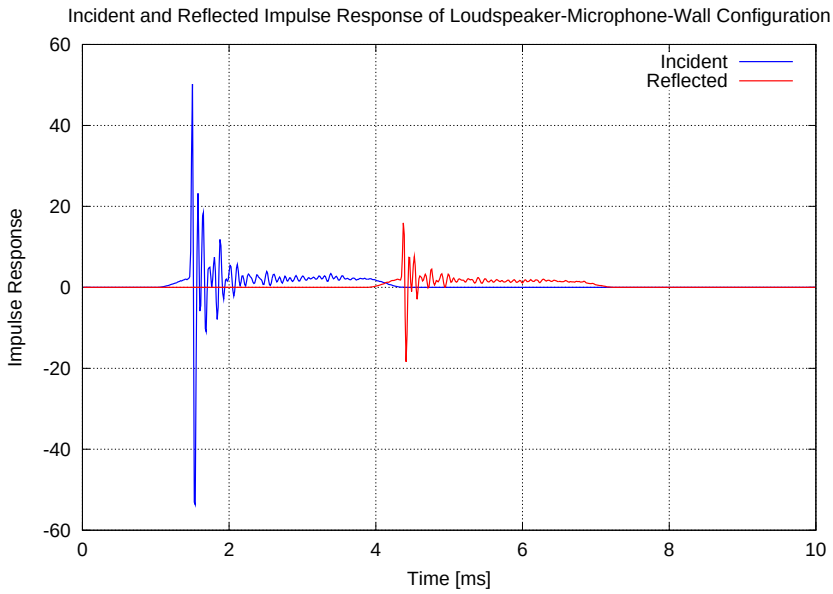

Figure 3.25: Incident and reflected components of impulse response for wood panelled wall (Tube). These have a slight offset which has been attenuated partially by the tapered window.

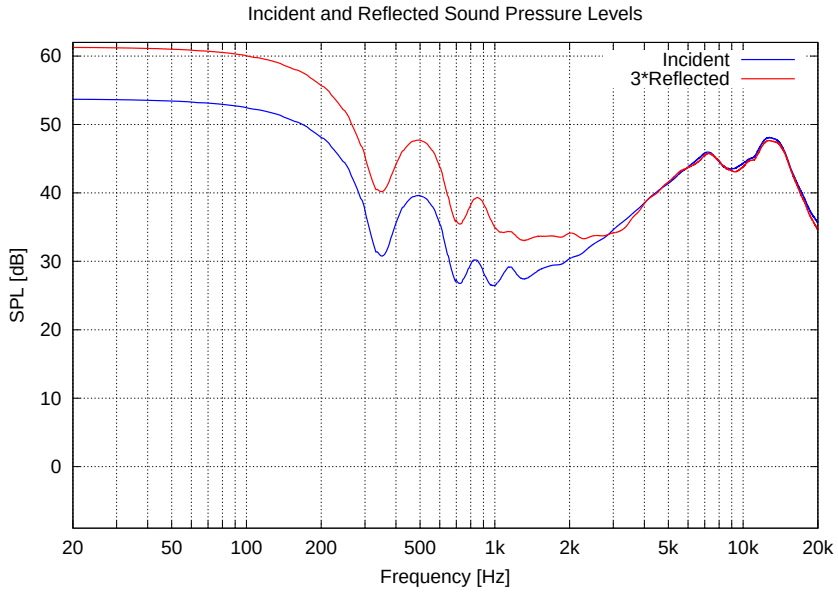

Figure 3.26: 1/3-Octave smoothed incident and reflected sound pressure levels for wood panelled wall (Tube). The reflected pressure amplitude is multiplied by a factor of three in order to account for spherical spreading of the acoustic waves. We see the reflected sound pressure level rise above the incident below 3 kHz.

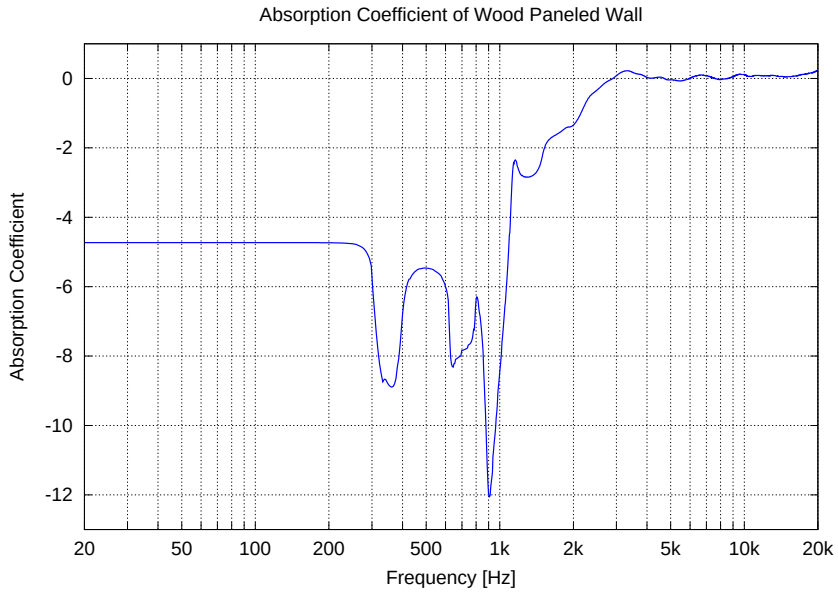

Figure 3.27: 1/3-Octave smoothed absorption coefficient of wood panelled wall using the tube loudspeaker. It is difficult to make any conclusions below 3 kHz. This data suffers from a poor signal-to-noise ratio. At high frequencies the absorption oscillates about zero.

3.3.4 Discussion

The reflection method is simple, fast and intuitive. However, we have also shown that it has several drawbacks.The fact that this technique depends on the separation of reflections in the time domain is advantageous and disadvantageous. It allows the onset of incident and reflected acoustic pressure waves to be seen, however, we cannot specify where these signals end. That is, each pressure wave picked up at the microphone is still oscillating into the onset of the next reflection. For the results given previously, we have stated that this overemphasizes the reflection coefficient at low frequencies when using a half-Hann window.

The frequency resolution obtained from our measurement setup is coarse, approximately 350 Hz. This resolution results in the smoothing of data at all frequencies, but this effect is significant at low frequencies. The loudspeaker-microphone (q_o) distance may be increased, however the height of the loudspeaker is generally fixed. We have shown that the arrival time of the incident pressure wave and the reflection from the floor become closer in time as q_o is increased.

The concept of the acoustic centre was presented in order to stress the difficulty in prescribing the proper $1/q$ factors due to spherical spreading. If our source is truly spherical, where is its centre of radiation? At low frequencies this is typically half a box width in front of the loudspeaker baffle [41]. For high frequencies this centre reduces in distance to approximately the baffle of the loudspeaker. The KEF loudspeaker is a 2-way unit and therefore the distances are even more difficult to specify, since in general we measure the distance q_o from the midpoint of the two drivers to the microphone. Attempts to measure the acoustic centre were made for the loudspeakers used in this study; however no results were conclusive. The measurements were performed in a normal room and therefore have the same resolution problems mentioned above.

Diffraction effects are not taken into account in this theory, and in general they are difficult to model. The KEF loudspeaker has a box-like enclosure which exhibits sharp transitions (edge of the box to air transition for example). This will contribute diffraction at the microphone position and it would be an added complication to account for this.

The tube loudspeaker was used since the driver diameter and front of the loudspeaker are compact, enabling the compact source approximation to be valid up to higher frequencies than the KEF unit. In addition, its construction is smooth and of small dimension[3]. This loudspeaker should have lower diffraction effects than the KEF loudspeaker. This loudspeaker featured poor signal-to-noise ratio, the worst being at low frequencies. This has introduced low frequency fluctuations in the impulse response, causing an offset in the incident and reflected signals.

The problems we are discussing are not necessarily unique to this measurement method. In general we should be aware of these effects when performing measure-

[3]The tube or pipe of this loudspeaker is 1.3 metres long, however the diameter of the pipe is about 4.5 cm.

ments. The method presented in the next section can improve frequency resolution slightly. Another loudspeaker will be used, which will have satisfactory output at low frequencies and less diffraction than a box-like enclosure. In addition, the measurement method will not require any specification of the wave form, or correction for spherical wave spreading.

3.4 Subtraction Technique

3.4.1 Theory

The subtraction technique [27] is an experimental approach that is used in conjunction with some aspects of the reflection method described in Section 3.3. This may be used in the determination of *in situ* reflection or absorption coefficients. First, a measurement is taken, p_i, with a test loudspeaker positioned as far as possible from any nearby surface (see Figure 3.28a). This is a pseudo-free field response which would require truncation at the onset of unwanted reflections. Secondly, keeping the loudspeaker-microphone distance fixed, a measurement is taken with the microphone positioned very close to (ideally at) the surface under study, p_{ir} (see Figure 3.28b). This measurement includes the incident sound wave from the loudspeaker and the reflected sound wave from the surface.

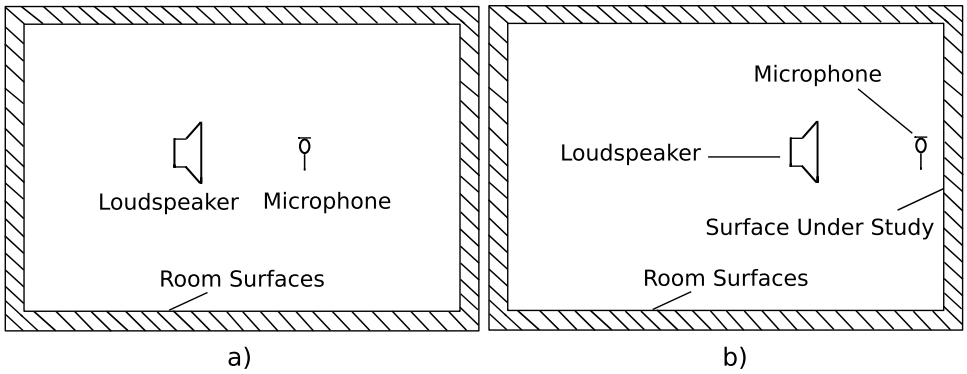

Figure 3.28: a) Pseudo-free field measurement. b) Surface proximity measurement.

Placing the microphone very close to the test surface increases the amount of time between the arrival of wanted and unwanted reflections. This allows for a longer time window when gating the reflected signal, improving the frequency resolution of the measurement (this was discussed in Section 3.3.2). It is of key importance to keep the loudspeaker-microphone distance fixed in these two measurements. After performing these measurements, the reflected sound wave from the test surface is obtained by subtracting the pseudo-free field pressure from the flush pressure:

$$p_r = p_{ir} - p_i. \tag{3.27}$$

The reflection factor is then readily calculated by taking the ratio of (3.27) to the incident pressure,

$$r = \frac{p_r}{p_i} = \frac{p_{ir} - p_i}{p_i}. \tag{3.28}$$

No form (plane or spherical) for the pressures in (3.28) is prescribed. The task of describing the nature of the source is not required, since the distance from the loudspeaker to the microphone is fixed in both measurements. This requirement on the loudspeaker-microphone distance is also the difficulty of this method, in addition to other conditions affecting the propagation of sound waves in the room. Small variations in temperature, or the distance between the loudspeaker and microphone, will result in the misalignment of samples when performing the subtraction [27]. However, this difficulty could perhaps be overcome if the two measurement data were interpolated and aligned in the time domain. We would expect errors regardless of this strategy when there are large variations in the loudspeaker-microphone distance between measurements. In this case, the spreading of the pressure waves would no longer be similar and the subtraction would not recover the reflected wave.

3.4.2 Results

Wood Panelled Wall

A spherical enclosure loudspeaker with a driver diameter of 15 cm is used for this method (Figure 3.29). This method is shown in Figures 3.30 to 3.32. In this case, a source loudspeaker is positioned 50 centimetres away from a microphone. Figure 3.30 shows the arrival of an incident and overlapped reflected pulse (1.5 ms) and the reflections from the room surfaces at the microphone position. The reflection at 4.5 ms is from the loudspeaker itself. The red curve represents a pseudo-free field impulse response which is the first measurement in the subtraction method (see Figure 3.28a).

The second measurement is at the surface, using the same loudspeaker-microphone distance (see Figure 3.28b). This is the flush measurement in Figure 3.30. A tapered window is shown with the impulse response data which truncates the response before the arrival of a reflection from the loudspeaker itself (4.5 ms). Since both measurements were carried out using the same loudspeaker-microphone distance, we may then simply subtract the pseudo free field measurement from the flush measurement, as in (3.27). This effectively removes the incident pressure response from the data, leaving the reflected response behind.

Figure 3.29: Spherical enclosure loudspeaker. A 15 cm diameter driver in a spherical enclosure.

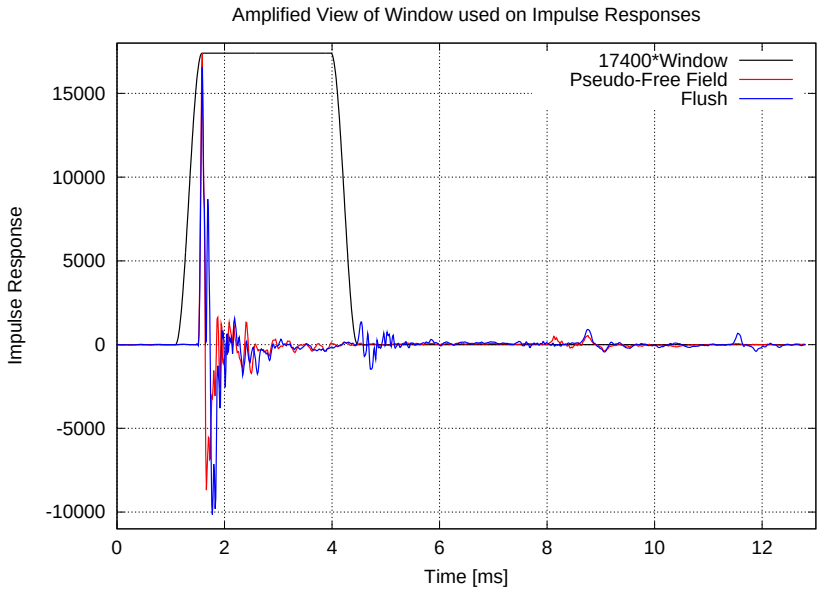

Figure 3.30: Impulse response of pseudo-free field and flush measurement at wood panelled wall. The incident and reflected sound waves overlap starting at 1.5 ms. The reflection off the loudspeaker is seen just after 4 ms.

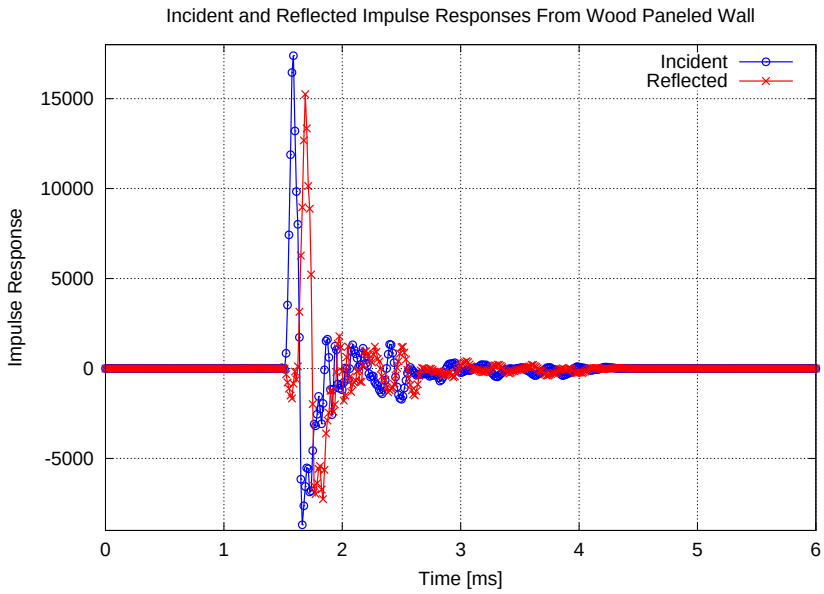

Figure 3.31: Incident and reflected pressure waves at wood panelled wall. We notice a slight time delay between the two waves of about 0.1 ms. This could be due to improper cancellation of the incident wave or a non-zero microphone-surface distance.

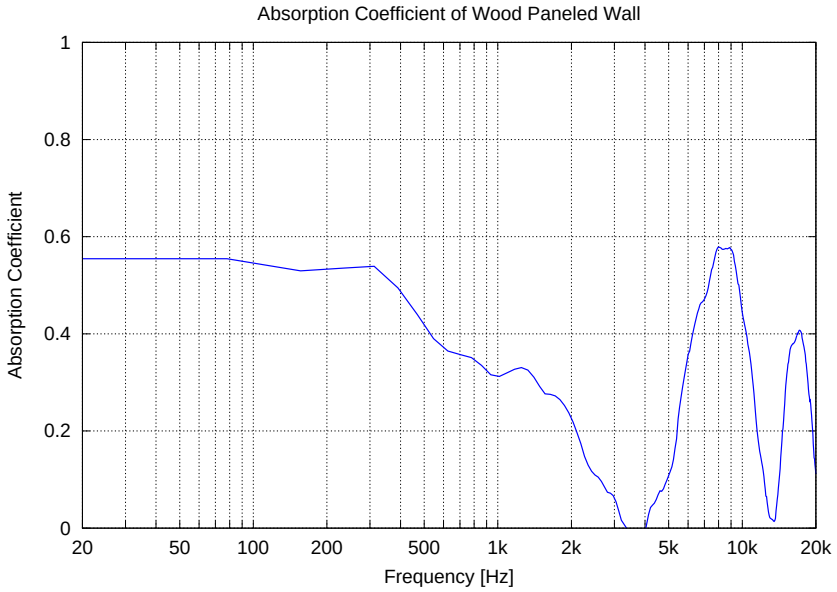

Figure 3.32: Absorption coefficient of wood panelled wall. This wall should absorb very little sound at high frequencies.

The incident and reflected sound waves are shown in Figure 3.31. We notice a slight time delay between the incident and reflected sound waves. This may be caused by an incomplete subtraction of the incident wave from the flush measurement. In practice this is possible since the loudspeaker and microphone were moved together up to the surface, allowing for changes in position of the order of a centimetre. The other possibility would be the fact that the microphone is not exactly at the surface under study. It is a finite distance away, however, this is generally less than a centimetre. The reflection coefficient is then calculated by taking the ratio of the reflected response to the incident response (3.28).

The absorption coefficient is calculated using $1 - \rho$, which is in Figure 3.32. Our window has only allowed us a resolution of about 400 Hz, which is not an improvement over the reflection method. In this case, the reflection or scattering of sound by the loudspeaker is much closer. In general, the loudspeaker may be placed further from the surface in order to improve the frequency resolution. We should only therefore look at the higher frequencies for information about the surface. Actually, the results for this wall look nothing like what we had expected. It is not clear why there are peaks and dips ranging from zero to half absorption. This surface should have very little absorption at high frequencies. We speculate that diffraction, or some form of reverberation may be the cause. Mommertz has reported some difficulty with this method when the loudspeaker-microphone distance or the temperature has changed between measurements [27].

Office Divider

The subtraction method was also used on an absorptive surface: an office divider. We would expect that the absorption coefficient would be close to unity for high frequencies. At low frequencies the absorption decreases due to the thickness of absorbent necessary to attenuate sound at large wavelengths. Here we have used a one metre loudspeaker-microphone spacing. The impulse responses of the two measurements are presented in Figure 3.33. Reflections from the loudspeaker and the floor arrive from 8.5 to 9.1 ms.

This surface has significant absorption towards the higher frequencies, as displayed in Figure 3.34. The window we have chosen results in a frequency resolution of 200 Hz. This limitation causes a smoothing of data, which will not resolve fluctuations in absorption at low frequencies. Note that the values of the absorption coefficient do not exceed one.

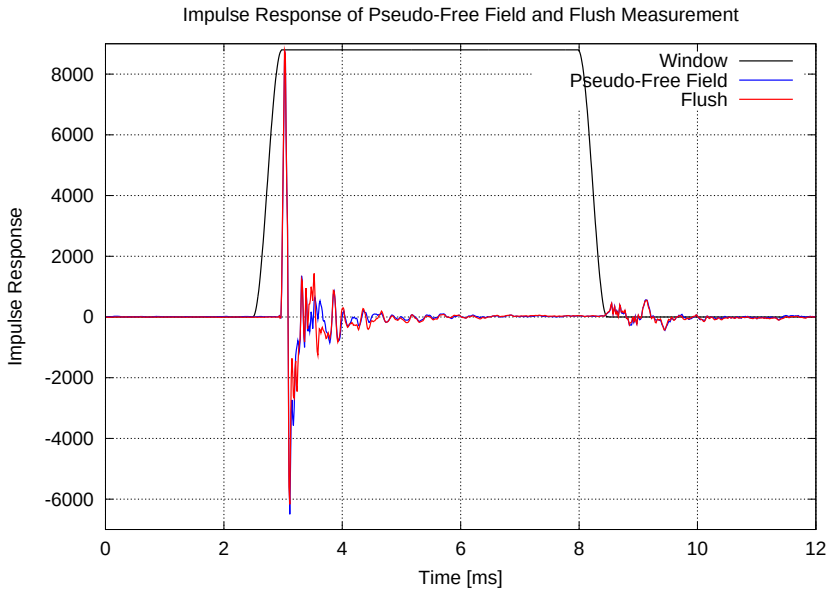

Figure 3.33: Impulse response of pseudo-free field and flush measurement at office divider. The incident and reflected sound waves overlap starting at 2.96 ms. Unwanted reflections begin to arrive at 8.5 ms.

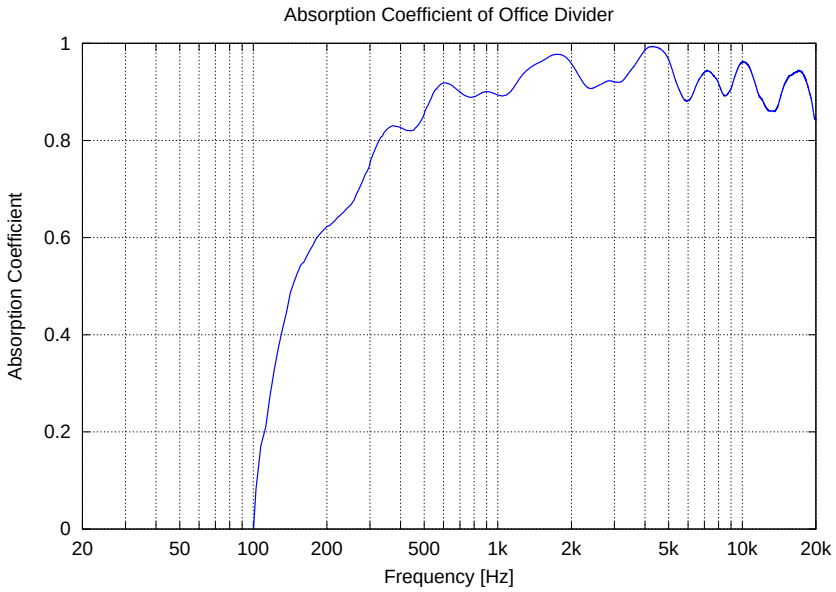

Figure 3.34: Absorption coefficient of office divider. This surface should absorb most of the incident sound at high frequencies.

3.4.3 Discussion

The subtraction technique requires a reference measurement (pseudo-free field) in order to remove the incident sound wave from a measurement at the surface under study. It is possible that the room reflections differ between the two measurements. In certain cases, the pseudo-free field response is taken in the middle of the room, as far away from surfaces as possible. The loudspeaker and microphone may then be positioned in front of the study surface, always maintaining the loudspeaker-microphone distance fixed, in order to perform the flush measurement. In this scenario, reflections from the room surfaces may arrive prior to the reflections in the initial measurement. Care must then be taken when windowing data to consider this fact.

Alternatively, the loudspeaker and microphone may be left in the same position for both measurements: 1) The pseudo-free field response would be recorded in the absence of a sample surface and 2) A sample would then be positioned close to the microphone in order to perform the flush measurement. The choice of the method would depend primarily of the size and mobility of the sample surface. If we required the measurement of a room wall, the former approach would be used since the surface cannot be removed from its current position.

A problem arises if the incident sound wave is not completely subtracted from the flush measurement. Mommertz has shown that small variations in temperature can result in errors when calculating the reflection coefficient [27]. These post-processing errors are due to the incomplete subtraction of the incident sound wave, which occurs when there are changes in the time delay of the arriving signals at the microphone position. This could also be caused by slight variations in the position of the loudspeaker relative to the microphone. In the method suggested above, the flush measurement is taken after moving the loudspeaker-microphone apparatus up to the surface under study. Keeping the loudspeaker-microphone distance fixed during the repositioning of the apparatus may be difficult with the available mounting hardware, and thus result in small changes in time delay.

In addition, the recorded data are discrete. There is therefore a possibility that the time samples in multiple measurements differ by a fraction of a sample. This poses a problem when subtracting one measurement from the other, even when the temperature in the environment or the loudspeaker-microphone distance is kept fixed. One possible solution is to re-sample both the pseudo-free field and flush measurements in order reduce the separation of the data samples. This was not attempted in the present situation since we are searching for a method that yields results down to low frequencies. The resolution obtained here is above the bass region (> 200 Hz) and therefore will not satisfy our requirement.

3.5 Impulse Response Shortening and Gating

3.5.1 Theory and Application

In all of the proposed methods, we are plagued with the additional complications caused by the surfaces of the room. This information comes in the form of reflections (disregarding noise for the moment) which arrive at the measurement position before the end of the impulse response of the loudspeaker and the surface under study. We thus obtain an overlap of wanted and unwanted information. Now suppose that the onset of reflections in the room commences at $t = t_o$. If the impulse response of the loudspeaker and the surface under study were to decay before the onset of room reflections, then the impulse response could safely be truncated without truncation error or overlap of information. In addition, a quick decay of the impulse response could avoid the overlapping of incident and reflected pressures at the microphone position.

It has occurred to several authors[42, 10, 3] that modifications to the impulse response, by use of specific filters, may solve the problem. Two methods exist, the first [3] approach flattens the frequency response to DC which increases the duration of the impulse response (in principle infinite) and lowers the amplitude of the tail of the impulse response to zero [42]. The second method is essentially the application of the flattening filter followed by a high-pass filter used to yield a quick decay of the impulse response. This is achieved by attenuating low-frequency data (see [10]). This will be the method we employ since it results in a quick decay of the impulse response and no problem at DC (zero frequency).

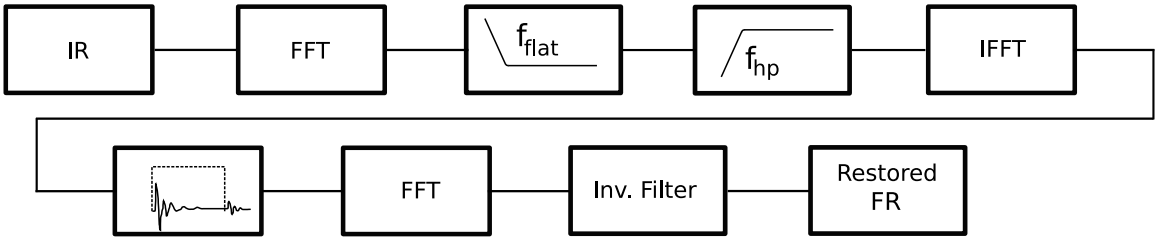

Figure 3.35: Signal chain used in impulse shortening method. IR: Impulse Response. FR: Frequency Response. FFT: Fast Fourier Transform. IFFT: Inverse Fast Fourier Transform. f_{flat} and f_{hp} are the corner frequencies of the flattening and high-pass filters, respectively. The inverse filter is the inverse of the flattening filter times the high-pass filter.

After an impulse response is recorded, it is fed into the block diagram of the post processing technique shown in Figure 3.35. A fast Fourier transform (FFT) is performed on the impulse response (IR), yielding the frequency response (FR). This is subsequently multiplied by a flattening filter and a high-pass filter having different corner frequencies. The flattening filter corner frequency is chosen as the corner frequency of the loudspeaker. The high-pass filter used is of first order. Its

frequency corner is generally taken to be high enough to attenuate the low frequency region of the frequency response (300 or 400 Hz), resulting in a quick decay of the impulse response. This modified frequency response is then inverse transformed back to the time domain. The filtering operations could also be carried out in the time domain, without the need of the FFT and IFFT blocks. The impulse response will now decay very quickly due to the attenuation of low frequencies and thus can be windowed with reduced truncation error. A rectangular window is therefore safe to use here. The flattened/truncated response is then brought to the frequency domain where the inverse filter is applied (this removes the effect of the previous filters). This yields the final shortened/flattened frequency response, which goes to very low frequencies. The details of this technique are described by Vanderkooy and Lipshitz [42].

For our purposes, this processing algorithm would have to be utilized in the same fashion on each data set used to determine the reflection factor: (1) In the case of the reflection method, this would have to be applied to the incident and reflected waves. (2) In the case of the subtraction method, this would have to be applied to both the pseudo-free field and flush responses.

We must now specify the form of the filters used in this procedure. We generally are using sealed box loudspeakers, such as the tube or sphere we have presented. These have a second order high-pass character, described by

$$H_{spk}(s) = \frac{As^2}{s^2 + \frac{s\omega_o}{Q} + \omega_o^2} \tag{3.29}$$

where $s = \sigma + j\omega$, A is the gain of the filter in the high-pass region, ω_o its corner frequency and Q its quality factor. In the case where $\sigma = 0$ we are in Fourier space, which gives

$$H_{spk}(\omega) = \frac{-A\omega^2}{-\omega^2 + \frac{j\omega\omega_o}{Q} + \omega_o^2}. \tag{3.30}$$

This transfer function has three parameters that we must determine. This is done by fitting H_{spk} to the measured near field response of the loudspeaker. For the spherical loudspeaker, we obtained $A = 1470$, $\omega = 660$ rad/s and $Q = 0.82$. Figure 3.36 shows the near field and fitted responses in terms of sound pressure levels. The amplitude will not actually be used in the impulse shortening algorithm, however it was used here to determine if the fit was appropriate. We may then use the inverse of H_{spk} as the flattening filter, which satisfies

$$H_{flat}(\omega)H_{spk}(\omega) = 1 \tag{3.31}$$

for all angular frequencies ω in our range of interest. The flattening filter is therefore $H_{spk}^{-1}(\omega)$. The frequency response of the measurement is multiplied by $H_{flat}(\omega) =$

$H_{spk}^{-1}(\omega)$ and the first order high-pass filter (frequency corner of 400 Hz), resulting in attenuation at the low frequencies. The procedure depicted in Figure 3.35 is then continued until the restored frequency response is obtained.

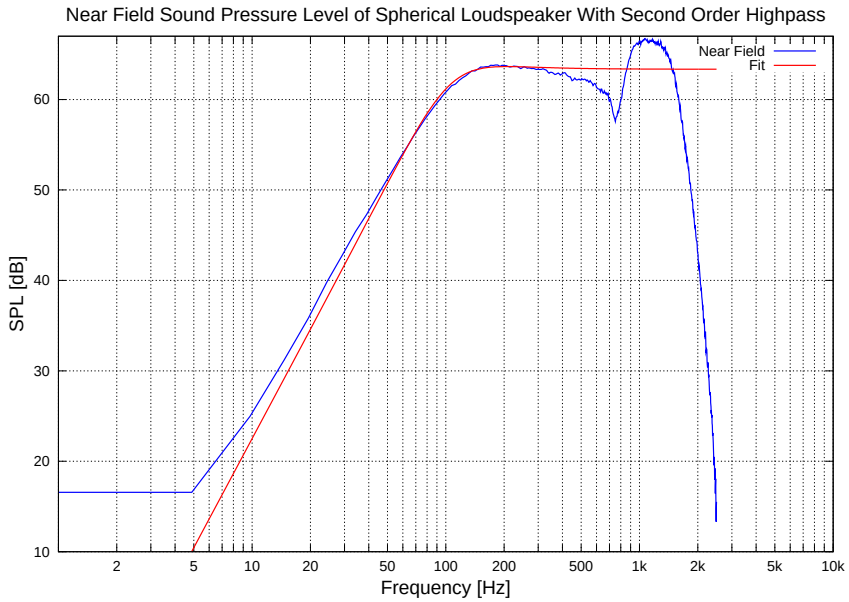

Figure 3.36: Near field response of spherical loudspeaker with fit. We see that the second order filter fits fairly well to the near field response between 50 and 300 Hz. Loudspeaker filter parameters: $A = 1470$, $\omega_o = 660$ rad/s and $Q = 0.82$.

3.5.2 Results

The described method was applied to the measurements from the subtraction technique. After carrying out the algorithm presented in Figure 3.35 we obtain the results shown in Figures 3.37 and 3.38. The wood panelled wall data indicates additional absorption at low frequencies when using the impulse response shortening (f <250 Hz). A 2.5 ms rectangular window was used on this data. We see both the rise and fall in absorption for the office divider when using different window lengths (below 300 Hz). The low-frequency tendency of the absorption curve changes based on the window length due to truncation at low frequencies (the low-frequency wave amplitude could be positive, zero or negative during rectangular truncation) [42]. Both of the results tend to show no or little change above 1 kHz. It is important to note that the original absorption coefficients were computed with different window lengths. For the wood panelled wall, approximately 2.4 ms and for the office divider 5 ms. The impulse response shortening procedure was implemented using 2.5 ms for the wood panelled wall and 2.5, 3, 4 and 5 ms for the office divider. It is not clear which window length would best describe the frequency region below 200 Hz. This method will be revisited in Chapter 4.

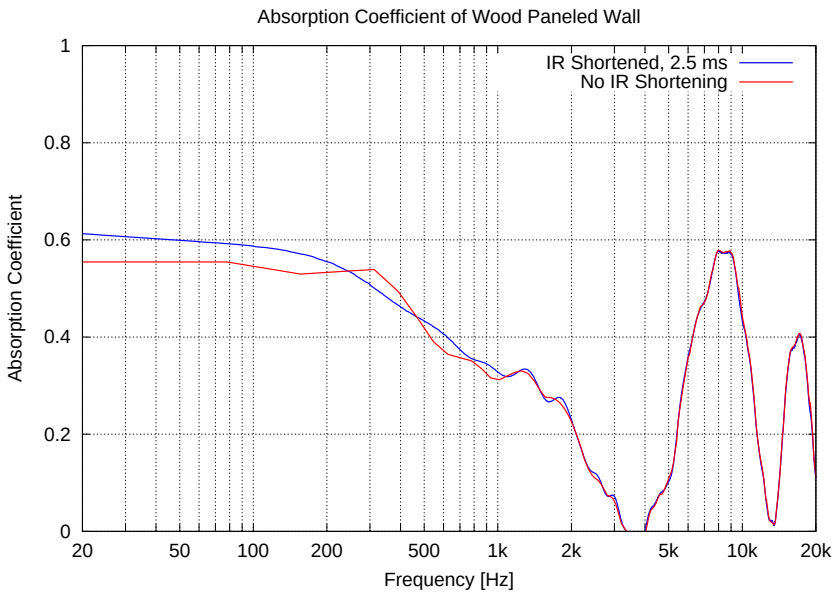

Figure 3.37: Absorption coefficient of wood panelled wall using impulse response shortening. We see that the impulse response shortened data indicates an increase in absorption for frequencies below 250 Hz. In addition, there is little change above 1 kHz.

3.5.3 Discussion

Impulse response shortening was introduced and implemented in order to improve frequency resolution. This procedure has allowed resolution down to low frequencies without the need for a wide time window. In our case, we have used rectangular windows of 2.5, 3, 4 and 5 ms in width. These results were compared with data having no impulse response shortening applied. It is not clear how to interpret the accuracy of this method. Different window lengths cause the frequency response to rise and fall in the low frequency region, depending on where the impulse response is truncated. This indicates that the method is dependent on the window length. On the other hand this method is very interesting. It attempts to solve one of the most serious problems when performing measurements in a room, namely the room itself.

The impulse shortening technique uses the low-frequency character of the loudspeaker in order to flatten the frequency response. However we also have a surface under study which interacts with the sound wave. Should the surface be modelled and used to filter the response as well? In order to properly model the surface it must be measured, our approach then enters a circular loop. A proper study of this problem is required. This will be discussed briefly in the conclusion of this work but not necessarily solved.

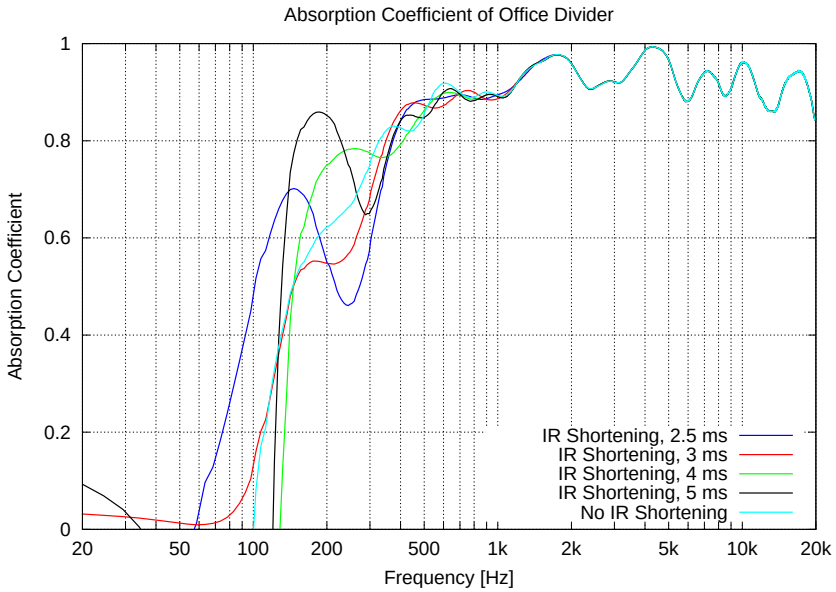

Figure 3.38: Absorption coefficient of office divider using impulse response shortening. We see that the choice of window length results in more or less absorption at low frequencies. In addition, there is little change above 1 kHz.

3.6 Portable Reverberation Chamber

3.6.1 Theory

There are several standard methods used to determine the absorption coefficient of materials. The two most common methods are by use of the impedance tube [15] and the reverberation room [16]. Here we will discuss the *in situ* implementation of a reverberation room.

The Centre for Pavement and Transportation Technology, Department of Civil Engineering at the University of Waterloo has constructed a wooden structure to act as a miniature reverberation room. This is used primarily for the measurement of pavement surfaces, however in principle it may be used on a variety of surfaces. The walls are made of high density fibreboard and have a slight slope. The ceiling of the chamber is flat and houses a loudspeaker and a microphone holder. There is no bottom to the chamber, which allows measurements to be conducted by simply placing the apparatus on the surface under study. This is depicted in Figure 3.39.

One method used to determine the absorption coefficient of the surface under study is by assuming that a diffuse sound field exists in the chamber (more on this assumption later). In this case, the reverberation time may be obtained from the impulse response of a given measurement [34]. The principle of the method lies in Sabine's formula, which relates the reverberation time to the total absorption in the room:

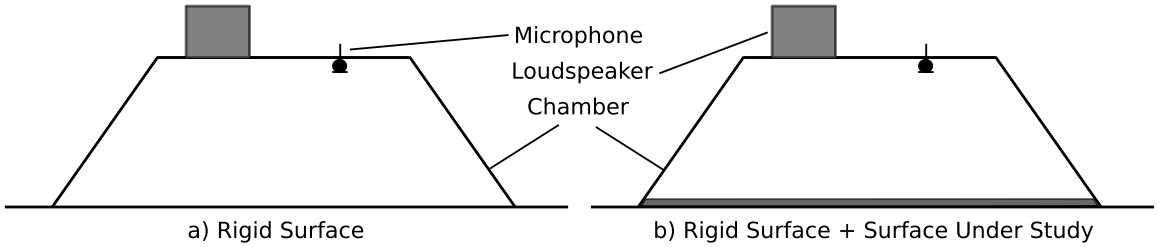

Figure 3.39: *In situ* implementation of a reverberation chamber measurement (side view). a) Reference measurement: reverberation chamber on rigid surface. b) Measurement at the surface under study, the reverberation chamber is simply placed upon the surface.

$$T_{60} = \frac{55.3V}{cA} \tag{3.32}$$

where T_{60} is the time it takes for the sound level in the chamber to decay by 60 dB, called the reverberation time, V is the volume of the room in cubic metres, c the speed of sound and A is the total absorption of the room given by

$$A = \sum_k S_k \alpha_k. \tag{3.33}$$

S_k and α_k are the surface area and absorption coefficient of the different surfaces in the chamber, respectively. Note that the units of A are square metres.

All geometrical factors for the miniature reverberation chamber are known. The unknowns are the absorption coefficients of the wooden walls, however they are all built with the same material and should therefore be the same. We will now show how two measurements may be used to determine the absorption coefficient of a surface under study. First, a reference measurement is made on a rigid surface. Second, a measurement is made on the surface under study in the same fashion (keeping all parameters constant). This method is represented in Figure 3.39. As we can see, the two measurement configurations have five surfaces in common (walls and ceiling). For the reference measurement, the sixth surface is rigid, for the surface measurement, the rigid surface is replaced by the surface under study (or the surface under study is placed on the reference surface).

We will now calculate the total absorption for each case. For the rigid surface, the total absorption is A_R,

$$A_R = S_1\alpha_1 + S_2\alpha_2 + S_3\alpha_3 + S_4\alpha_4 + S_5\alpha_5 + S_R\alpha_R \tag{3.34}$$

here we assume that each of the wood surfaces of the chamber have different absorption coefficients and surface areas (some of the surface areas, and most likely their absorption coefficients, are in common between surfaces). The subscripts 1 to

5 represent the walls and ceiling of the chamber whereas the subscript R represents the rigid surface of a reference sample. The absorption coefficient of the reference surface is zero since it is rigid, leaving

$$A_R = S_1\alpha_1 + S_2\alpha_2 + S_3\alpha_3 + S_4\alpha_4 + S_5\alpha_5 \tag{3.35}$$

which is the absorption of the apparatus itself. For the surface under study, we have

$$A_s = S_1\alpha_1 + S_2\alpha_2 + S_3\alpha_3 + S_4\alpha_4 + S_5\alpha_5 + S_s\alpha_s \tag{3.36}$$

where S_s and α_s are respectively the surface area and absorption coefficient of the surface under study. The absorption coefficient of the surface is obtained by taking the difference between (3.36) and (3.35) and dividing by S_s,

$$\alpha_s = \frac{A_s - A_R}{S_s}. \tag{3.37}$$

This is the result found in the standard for the reverberation room method [16]. The total absorption of the surfaces is also determined from the Sabine formula. By using (3.32) in (3.37), we may express the absorption coefficient as a function of the reverberation times:

$$\alpha_s = \frac{55.3V}{cS_s}\left(\frac{1}{T_{60,s}} - \frac{1}{T_{60,R}}\right) \tag{3.38}$$

where $T_{60,s}$ is the reverberation time with the surface under study in place and $T_{60,R}$ is the reverberation time with the rigid surface in place. Once again we may obtain the reverberation time by use of an impulse response measurement. The impulse responses are therefore the only measures needed to describe the absorption characteristics of the surface. Note that we have omitted the effect of the loudspeaker and microphone. This would simply add two more terms to both the absorption of the rigid surface and the absorption of the surface under study. These terms would be removed when taking the difference between (3.35) and (3.36), once again resulting in (3.37).

3.6.2 Diffuse Sound Field Assumption

It is important to note that the development of the preceding theory is based on the assumption that a diffuse field exists in the enclosure of the measurement apparatus. This is not necessarily true, and therefore merits some investigation. ASTM Standard C 423 - 08 [16] discusses the construction of a typical reverberation chamber. Several important considerations are summarized in the following paragraph.

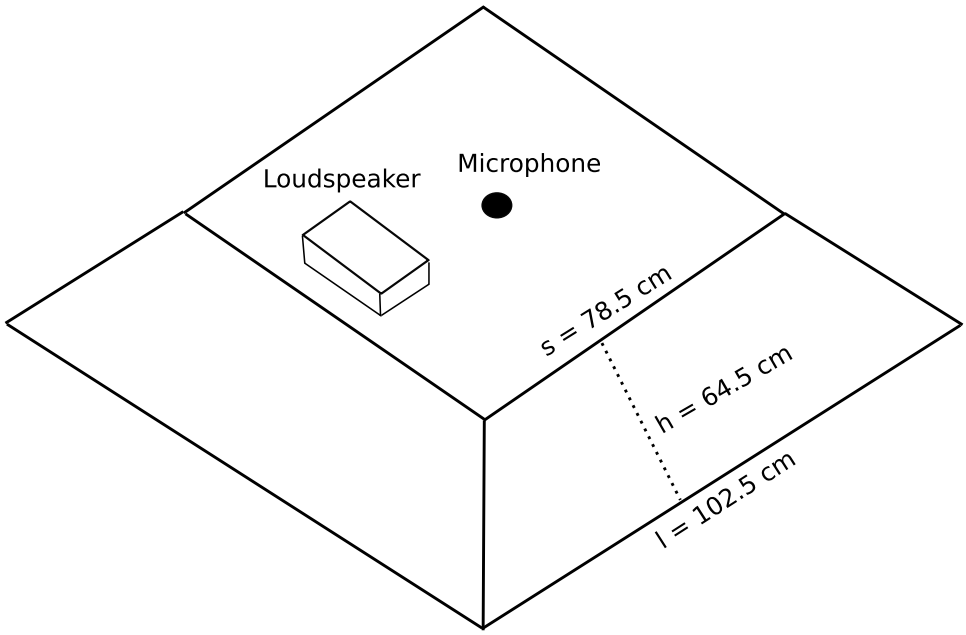

Figure 3.40: Reverberation chamber dimensions. This view shows the angled sides of the chamber and the fact that the ceiling and base are square structures having different side lengths.

It is noted that there may be absorption at lower frequencies by the room boundaries, which is most likely the case for the wooden boundaries of the present chamber. The room absorption, which is the absorption coefficient in Sabines (1 Sabine = 1 m^2) divided by the surface area of the room, is required to be equal to, or below 0.05 for one-third octave bands centred at frequencies between 250 and 2500 Hz. For one-third octave bands centred at frequencies below 250 Hz, or above 2500 Hz, the absorption is required to be equal to or below 0.10.

The limit of background noise during a measurement is specified as *"15 dB below the lowest level used to calculate the decay"*. However, it is evident that this should be kept to a minimum. The biggest issue with the chamber construction is its geometry. The standard requires that the minimum volume of the chamber be 125 m^3. The volume of the chamber is a small 0.53 m^3. This room will therefore have distinct resonances at higher frequencies than a conventional room. The standing wave pattern may be quite complex. In addition none of the dimensions of the room should be equal, which is not the case here (see Figure 3.40).

In general, volume diffusers or reflective panels may be used to diffuse sound in the chamber [6], aiding the requirement that the sound field be diffuse. However there is not much room in the box to do so. On the other hand, the construction features slanted walls which may aid in creating a diffuse sound field. In the following we will assume that the sound field is diffuse in order to apply Sabine's formula and therefore, determine the absorption coefficient of the surface under study.

3.6.3 Results

Fibreglass Panels

Fibreglass panels that are typically used in loudspeaker enclosures were chosen as an absorptive surface. The panel dimensions and measurement configurations are shown in Figure 3.41. The floor of our laboratory was chosen as a rigid reference surface. A measurement was carried out on the floor with and without the fibreglass panels. The sample configurations are shown in Figure 3.41 parts b) through e).

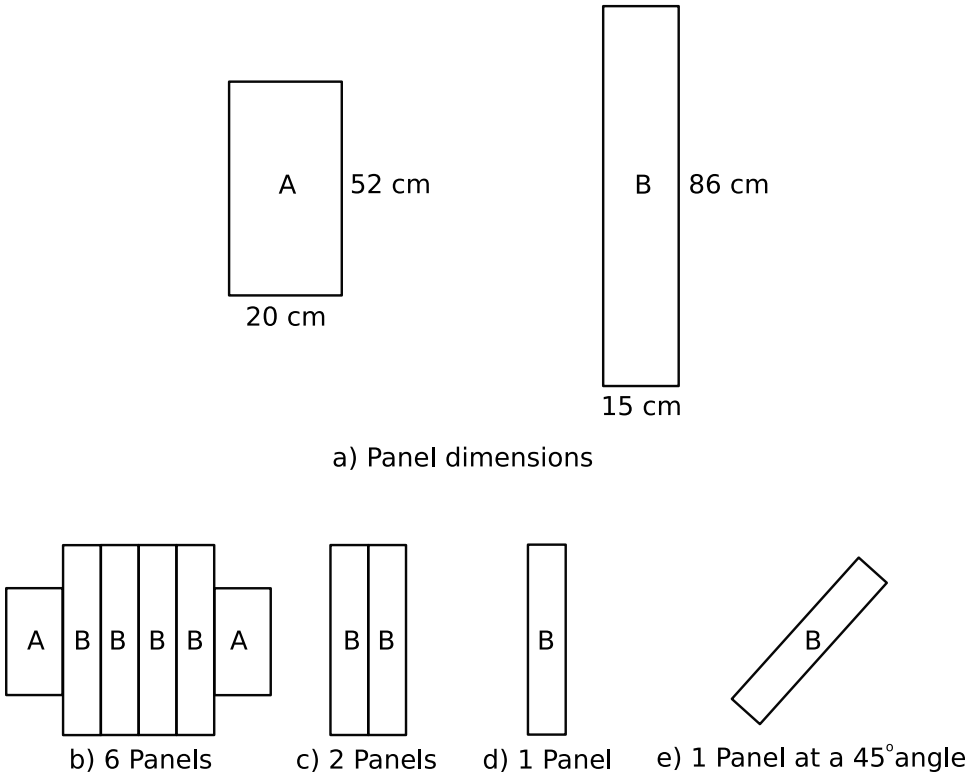

Figure 3.41: a) Fibreglass panel dimensions and b) through e) Measurement configurations.

It is useful to look at the sound pressure levels as a function of frequency for these measurements. Figure 3.42 shows distinct resonances (and anti-resonances) from about 170 Hz to 1.5 kHz. The same measurements, smoothed one octave, are shown in Figure 3.43. The curves follow closely from 130 to 350 Hz where they then begin to separate. As expected, increasing the absorptive material reduces the SPL at the microphone position (at high frequencies).

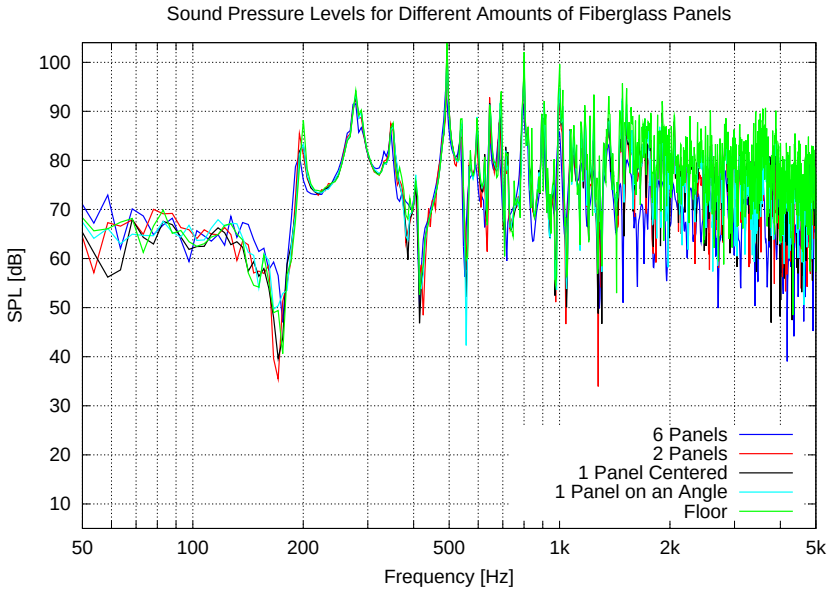

Figure 3.42: SPL of fibreglass panel measurements. Distinct resonances are seen from 170 Hz to 1.5 kHz.

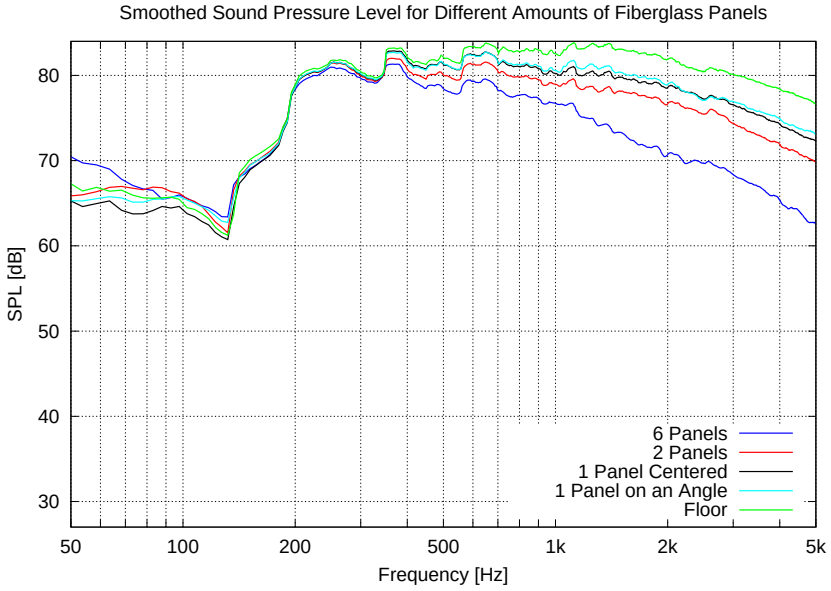

Figure 3.43: 1-Octave smoothed SPL of fibreglass panel measurements. The measurements follow closely from 130 to 350 Hz. Data begins to separate at high frequencies, indicating that the addition of absorptive material is reducing the sound level at the microphone position.

Once the reverberation times were calculated, they were used in (3.38) in order to obtain the absorption coefficient of the surface under study. The results are given in Figure 3.44. There is very little absorption at low frequencies. This is normal since we are using a very thin fibreglass panel (nominally 4 cm thick). Absorption tends to rise at high frequencies. For the 1-panel and 6-panel configurations, it even surpasses one. It is odd that the 2-panel data does not surpass an absorption coefficient of one while a single panel does. Coefficients that rise above one have been attributed to diffraction effects at the edges of samples in the reverberation room method [6]. We may nevertheless conclude that these samples have significant absorption coefficients above 1.5 kHz.

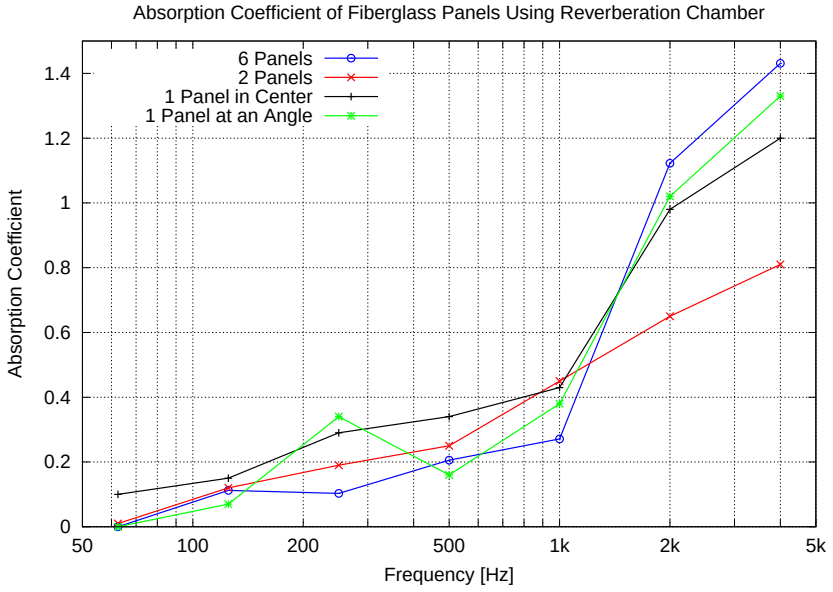

Figure 3.44: Absorption coefficient of fibreglass samples using reverberation chamber. Absorption coefficients rise above unity for frequencies between 1.7 and 4 kHz.

Floor, Carpet and Pavement

The portable reverberation chamber was also used on a rigid laboratory floor, a carpeted surface (without an underlay), another rigid floor and a paved surface. The results for the sound pressure levels (reference pressure is arbitrary) are shown in Figures 3.45 and 3.46. In the case of the carpet, we would expect some absorption at high frequencies and very little at low frequencies. The sound pressure levels show a difference at low frequencies (Figure 3.45). We would expect little absorption in this region and therefore, similar results for both the floor and carpet measurements. Gaps between the bottom of the chamber and the carpet may exist, since the carpet is not a smooth surface. This would allow air to exit the chamber and reduce the sound pressure level at the microphone position. Alternatively, a systematic error

could have resulted in an offset in the spectra (the chamber was moved from one location to another).

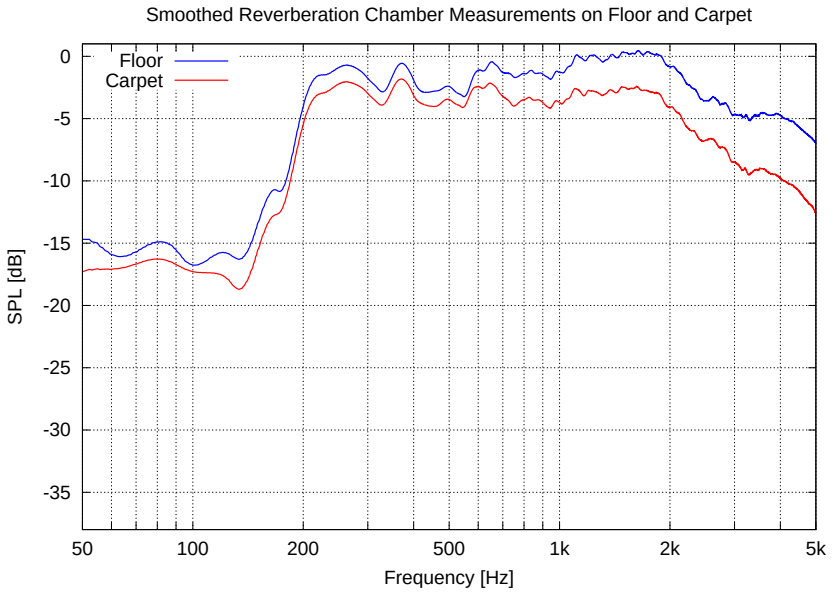

Figure 3.45: 1-Octave smoothed SPL of floor and carpet measurements (reference pressure is arbitrary). At high frequencies the difference between measurements is almost 5 dB, indicating significant absorption, however at low frequencies where little absorption is expected, 1-3 dB differences are seen. Gaps between the carpeted floor and the reverberation chamber may explain this difference.

Measurements were also taken on a smooth rigid floor, a pavement surface and the pavement surface with a 1/16 inch steel sheet (Figure 3.46). Small differences are found between 150 Hz and 1 kHz. At high frequencies the pavement and sheet measurement yield the greatest sound pressure level. At low frequencies the floor measurement has the highest sound pressure level. It is not clear which surface should be taken as our reference here. The floor is rigid and smooth, wereas the pavement is rough but still quite rigid.

The pavement unfortunately had tiny rocks at some locations on its surface (as do most pavement surfaces). This reduced the amount of contact between the sheet and the pavement which may have allowed the sheet to resonate. We may notice that the addition of the sheet has decreased the sound pressure level at low frequencies and increased the sound pressure level at high frequencies. It is not clear what is happening at low frequencies. Note that the pavement+sheet and the floor measurements are nearly identical above 2.5 kHz.

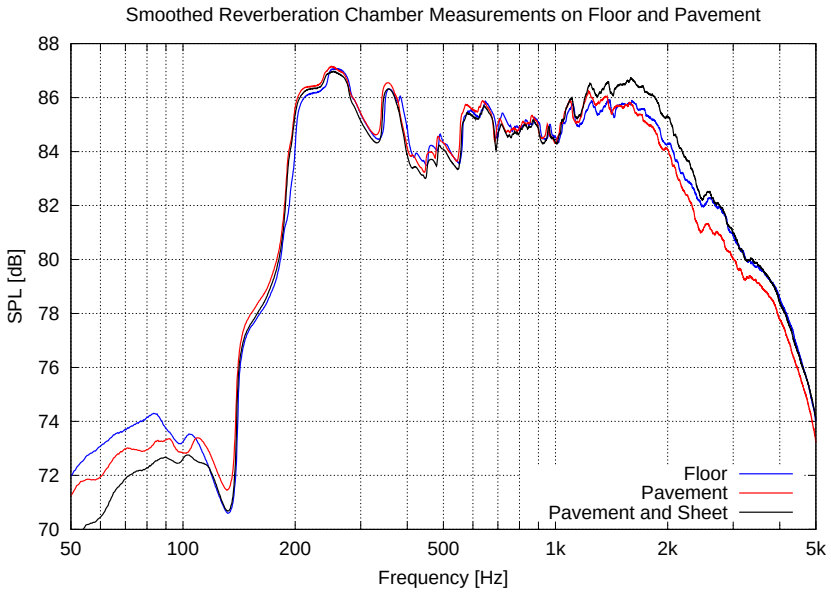

Figure 3.46: 1-Octave smoothed SPL of floor and pavement measurements. Results are similar between 150 Hz and 1 kHz. At high frequencies the pavement and the sheet are the most reflective. At low frequencies the floor seems to be the most reflective.

3.6.4 Discussion

A miniature reverberation chamber has been used to measure the acoustic absorption coefficient. Many resonances are found in the measured spectra with significant energy up to 1.5 kHz. The sound field in the enclosure is not diffuse at low frequencies. This device is however portable and may be placed on a surface under study. It of course could not be used on a non-horizontal surface without some support arrangement and therefore has limited application *in situ*. High-frequency absorption coefficients have surpassed unity using this method, rising as high as 1.4.

The Centre for Pavement and Transportation Technology generally uses this apparatus to measure pavement surfaces. A reference measurement could be taken on a surface that is known to be rigid and then consecutively compared with a measurement at another surface. Relative changes in the pressure spectra or in the absorption coefficient between pavement surfaces may then be measured and compared quantitatively. In this case, the importance is on the consistency of the measurement configuration. Although the resulting absorption coefficient may not represent what we would expect in a room acoustics perspective (due to the lack of diffuseness of the sound waves in the chamber), this instrument may be used to compare the performance of multiple surfaces in a consistent fashion. In particular, Figures 3.45 and 3.46 have shown relative differences in dB between measurements at a rigid floor and other surfaces.

It is interesting to consider another approach to quantify the absorptive characteristics of a surface. We may simply take the ratio of the pressure during the measurement of the surface under study to the pressure at a measurement of the reference surface. This could be considered to represent a measure of reflection characteristics of the surface. We assume that the propagation direction of the sound waves is not significantly changed when the surface under study is placed under the chamber. That is, that the sound propagates in the same fashion and interacts with the same surfaces in both measurements (however the rigid surface becomes the surface under study of course). The result of this ratio is shown in Figure 3.47. These results indicate that there is significant absorption at high frequencies. If both measurements are the same then the pressure ratio is one. If the surface is fully absorbing then the pressure ratio would be very low. It is possible that this could represent the magnitude of the reflection factor if the system was properly calibrated.

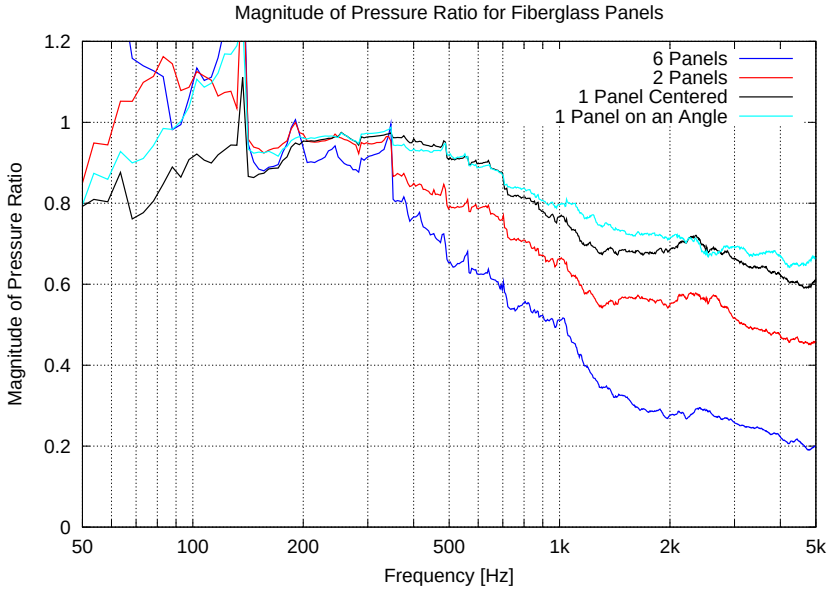

Figure 3.47: Pressure ratio of fibreglass samples using reverberation chamber. This ratio is close to one for low and middle frequencies and decreases at high frequencies. A ratio of one indicates little absorption. A ratio below one indicates that absorption is taking place.

3.7 Surface Pressure Method

3.7.1 Theory

The surface pressure method was first developed by Ingård and Bolt [14]. Two measurements are taken in order to determine the reflection factor. First, the pressure is measured at a hard wall surface. Second, the pressure at the same location is measured with the surface under study substituted for the hard wall. These two pressure measurements are then used to calculate the complex reflection factor of the surface. In Ingård and Bolt's method, a plane wave source is oriented towards a surface in an anechoic chamber. The surface under study had a layer of absorptive material, followed by a partitioned or unpartitioned air space. Behind this airspace was an acoustically hard wall [13]. These surfaces have a frequency dependent absorption coefficient that can be calculated.

We will now show how to calculate the reflection factor from the two measurements. Let p_R be the pressure at the hard wall (R for "rigid") and p_s be the pressure at the surface under study. Then

$$p_R = p_i + r_R p_i = 2p_i \tag{3.39}$$

since the surface has a reflection factor of 1 for all frequencies ($r_R = 1$). For the study surface,

$$p_s = p_i + r p_i. \tag{3.40}$$

The ratio of (3.40) to (3.39) may be re-arranged to yield the reflection factor in magnitude and in phase:

$$r = 2w - 1 \tag{3.41}$$

where $w = p_s/p_R$. This result is not necessarily true in a room where reflections from walls are also captured by the microphone. However, we will assume for the moment that this relationship is true and attempt a measurement on the wood panelled wall of Section 3.3.2 (see Figures 3.6 and 3.7).

3.7.2 Wood Panelled Wall Measurement and Discussion

Experiment

The wood panelled wall introduced in Section 3.3.2 was measured using the method presented in the previous section. Two measurements are taken with the microphone flush with the surface: 1) At the wood panelled wall with a metal sheet and 2) At the wall alone. The sheet is made out of steel, 3/16th of an inch thick (4.8

mm), with sides of 30 and 45 cm. The underlying assumption in this method is that the sheet and the wall together form a rigid surface. The microphone in this arrangement is attached to a loudspeaker as shown in Figure 3.48, giving a 28 cm loudspeaker-microphone distance. This setup is moved up to the surface until the microphone is only a few millimetres away from the surface.

Figure 3.48: Loudspeaker-microphone arrangement for the surface pressure method. A small electret microphone is fixed to the loudspeaker support by a thick, steel support wire. The loudspeaker-microphone distance is then fixed to 28 cm.

Measurements taken at the wall alone, and at the wall with the sheet are shown in Figure 3.49. Both measurements are very close, indicating that the presence of the sheet has not significantly altered the pressure at the wall. A frequency domain representation of these data is shown in Figure 3.50. Looking at the smoothed curves, we notice that the data are very close over the entire frequency range. The factor $w = p_s/p_R$ is then calculated to give the reflection factor (see (3.41)). The magnitude of the reflection factor is presented in Figure 3.51.

This surface was chosen because: 1) It should be highly reflective at high frequencies and 2) It should show a resonance[4]in absorption at low frequencies due to a mass-air-mass resonance (Section 2.3.3). It is clear that the magnitude of the reflection factor is one for frequencies above 500 Hz. From 50-180 Hz, this surface also shows significant reflection, while in the 180-500 Hz range it features a dip in the reflection spectrum. It is possible that this dip is caused by a mass-air-mass resonance. These results are unreliable below 100 Hz.

[4]This resonance causes an increase in absorption and therefore a decrease in the reflection factor.

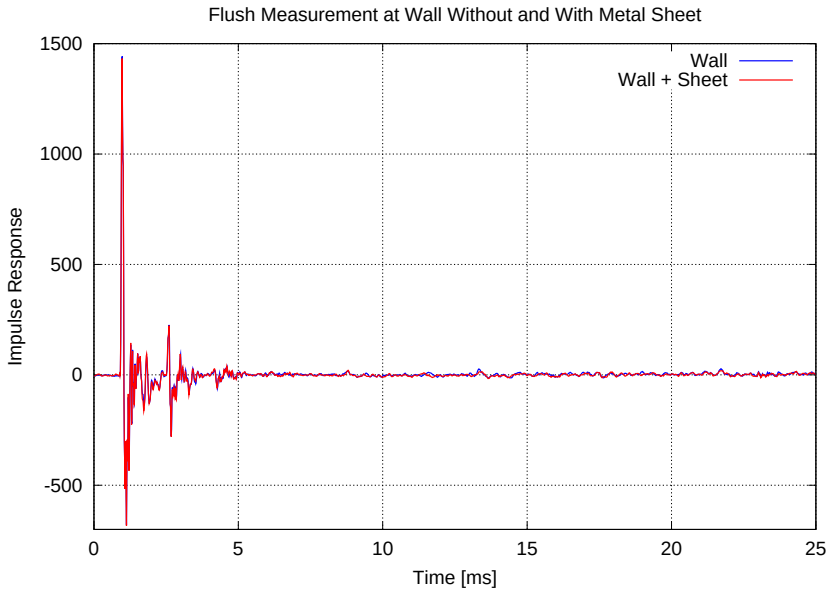

Figure 3.49: Impulse response of wooden wall and metal sheet.

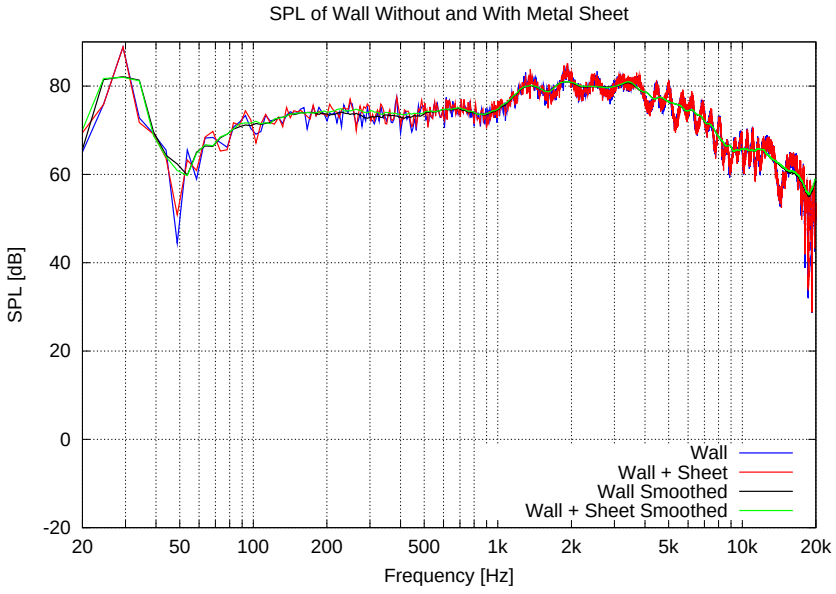

Figure 3.50: SPL of wooden wall and metal sheet.

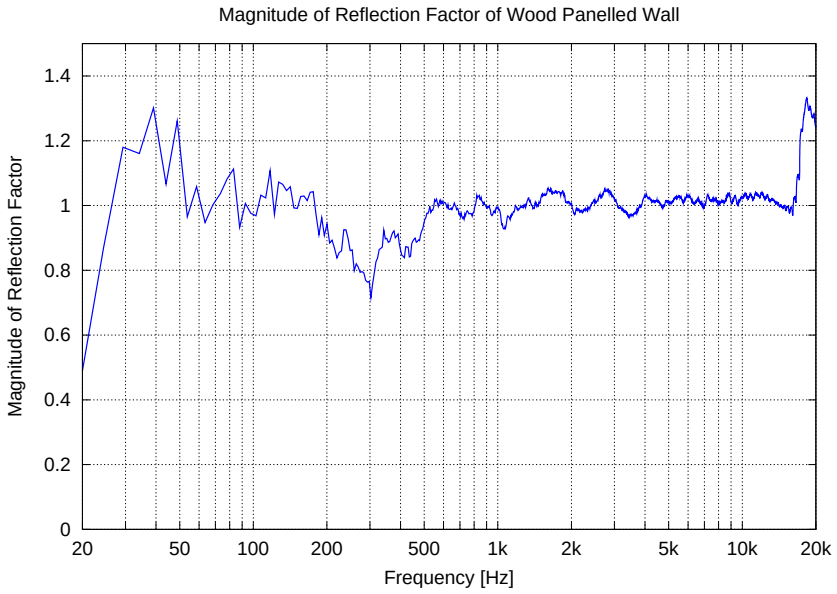

Figure 3.51: Magnitude of reflection factor of wood panelled wall using 1/3 octave smoothed pressures.

Discussion

The present method has been applied in a normal room without consideration of its implementation for a non-anechoic environment. This method has some interesting features and a test measurement has shown characteristics of the surface under study, namely, high reflection with the presence of a resonance at low frequencies. We have other issues to investigate with this setup, and will do so in more detail. Several authors have discussed the requirement for a minimum sample size (or sheet size in our case) in order to make measurements at low frequencies [24, 30] (also see [29] for a strip of absorptive material on a rigid surface). Minimum sample size limitations make it desirable to increase the size of the sheet so that it covers more area on the surface[5]. Our approach to reduce diffraction (edge effects) is to increase the level of the incident signal by placing the source close to the microphone. A consideration of the *in situ* implementation of this method is discussed in Chapter4, covering the effect of room reflections, the sheet material, geometry, and an appropriate mounting structure to hold the sheet against the surface under study.

[5]There will then exist more Fresnel zones on the sheet. A discussion of the relationship between sample size and Fresnel zones is given in [30].

Chapter 4

Surface Pressure Method

4.1 Introduction

The surface pressure method was introduced in Section 3.7. We had applied this method without any consideration of the reflections from the room surfaces or the effect of the loudspeaker itself. A small sheet was mounted flush with the surface under study in order to create a "rigid" surface. The acoustic pressure was measured with and without the sheet in place, resulting in: 1) A rigid surface measurement, p_R and 2) A measurement at the surface under study, p_s.

More consideration is needed of this method. Section 4.2 will therefore present a development of the theory for this configuration, including the sound wave contributions from the loudspeaker (scattering) and the room surfaces. It is difficult to characterize all of these wave components in practice, requiring approximations to the theory in order to calculate the reflection factor of the surface under study. This is discussed in Section 4.2.1.

4.2 Theory for a Normal Room

We would like to apply the methodology of Section 3.7 in a room. However, in this case we are required to include the reflection of sound from the room surfaces, as well as the scattering of sound by the loudspeaker. It will be shown that (3.41) still holds under particular conditions using this approach in a normal room. In the following, we assume spherical waves having a sinusoidal time dependence $e^{j\omega t}$ and phase shift due to propagation e^{-jkq}, q being the propagation distance of the acoustic wave. We must include any reflections from the room boundaries as well as the scattering from the loudspeaker used as an acoustic source. The pressure will be defined regardless of the surface for the moment (surface under study or rigid), it is generally written as

$$p = p_i + p_r + p_{sl} + p_{rsl} + p_{Rm} + p_{rRm} \tag{4.1}$$

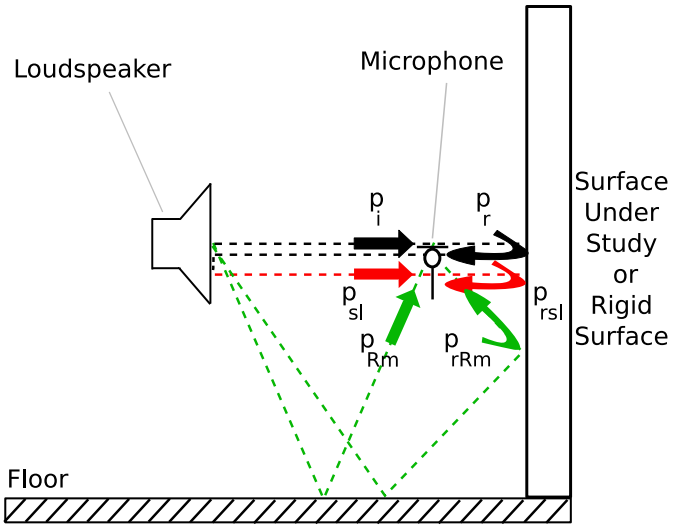

Figure 4.1: Pressure contributions for the surface pressure method. The incident pressure waves are shown as straight arrows. The reflections of these waves off the surface under study (or sheet) are shown as curved arrows.

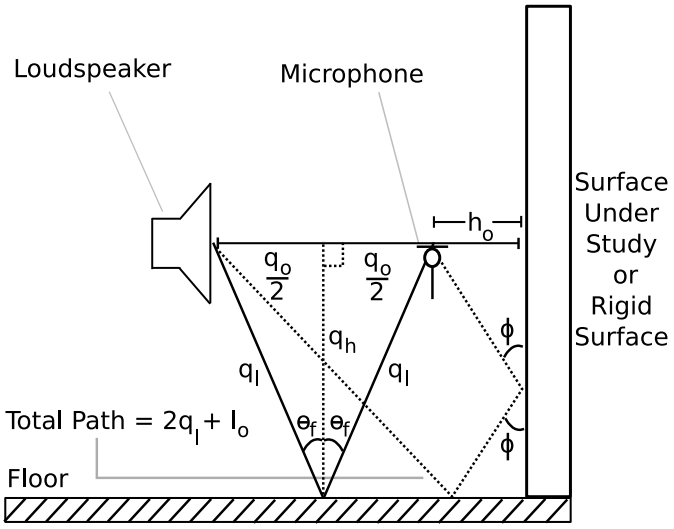

Figure 4.2: Geometry for surface pressure method.

where (see Figure 4.1):

p_i : Incident sound pressure

p_r : Reflected sound pressure from the surface

p_{sl} : Wave scattered by the loudspeaker

p_{rsl} : Reflection of the scattered wave by the surface

p_{Rm} : Room reflections

p_{rRm} : Reflection of room reflections by the surface

These pressure waves are denoted by arrows in Figure 4.1. The room reflections are not completely shown, instead we have shown only the reflection from the floor which is assumed to be the closest room surface besides the surface under study. As time advances, more and more pressure waves reflect around the room and arrive at the microphone position. They come in at all angles of incidence and have been attenuated due to the spreading of the waves and the interaction with the room surfaces. Our first assumption is that only the first reflection from the room, the floor reflection, is important. We will therefore neglect all other room reflections, setting $p_{Rm} = p_f$ and $p_{rRm} = p_{rf}$ (f denotes floor).

These acoustic waves are modelled as spherical waves (omitting the $e^{j\omega t}$ time dependence which is common to all waves), using the distances in Figure 4.2:

$$p_i = \frac{q_{ref}}{q_o} p_o e^{-jkq_o} \tag{4.2}$$

$$p_r = r\frac{q_{ref}}{q_o + 2h_o} p_o e^{-jk(q_o+2h_o)}. \tag{4.3}$$

We use a scattering amplitude approach for the scattered wave from the loudspeaker. A spherical wave is incident on the loudspeaker and then scattered, forming another spherical wave

$$p_{sl} = \left[r\frac{q_{ref}}{2q_o + 2h_o} p_o e^{-jk(2q_o+2h_o)} \right] \frac{q_s}{q_o} e^{-jkq_o} = \frac{r q_{ref} q_s p_o}{q_o(2q_o + 2h_o)} e^{-jk(3q_o+2h_o)}. \tag{4.4}$$

Note that we have simply multiplied the wave incident on the loudspeaker by a distance factor q_s, the scattering amplitude, which has both an angular and frequency dependence [29] (the proper distance factors have been written as well). We are assuming that the scattering results in a spherical wave with a modified amplitude and phase, thus q_s is complex. This wave is then reflected from the surface (surface under study or rigid)

$$p_{rsl} = \frac{r^2 q_{ref} q_s p_o}{(q_o + 2h_o)(2q_o + 2h_o)} e^{-jk(3q_o+4h_o)}. \tag{4.5}$$

The acoustic waves reflecting from the floor are also modelled as spherical waves,

$$p_f = \frac{q_{ref}}{2l} p_o e^{-jk2l} \tag{4.6}$$

$$p_{rf} = r_\phi \frac{q_{ref}}{2l + l_o} p_o e^{-jk(2l+l_o)} \tag{4.7}$$

where l_o represents the extra distance the surface reflected floor wave has travelled relative to the original floor wave (see Figures 4.1 and 4.2). The angle of incidence of this wave, ϕ would have to be known in order to specify l_o. In addition, the reflection factor of the surface may have a dependence on the angle of incidence and is therefore denoted as, r_ϕ (whereas r is for normal incidence). Now that the form of the pressure waves have been determined, we may write the pressure at the surface (surface under study or rigid) as

$$\begin{aligned} p = {} & \frac{q_{ref}}{q_o} p_o e^{-jkq_o} + r \frac{q_{ref}}{q_o + 2h_o} p_o e^{-jk(q_o+2h_o)} \\ & + r \frac{q_{ref} q_s}{q_o(2q_o + 2h_o)} p_o e^{-jk(3q_o+2h_o)} + r^2 \frac{q_{ref} q_s}{(q_o + 2h_o)(2q_o + 2h_o)} p_o e^{-jk(3q_o+4h_o)} \\ & + \frac{q_{ref}}{2l} p_o e^{-jk2l} + r_\phi \frac{q_{ref}}{2l + l_o} p_o e^{-jk(2l+l_o)}. \end{aligned} \tag{4.8}$$

The first line in (4.8) is the incident wave and its reflection from the surface. The second line is the scattered wave from the loudspeaker and its reflection from the surface. Finally, the third line is the floor contribution and its reflection from the surface. In practice, the distance $h_o = 0$ since the microphone is placed flush with the surface (a few milimetres). This results in

$$\begin{aligned} p = {} & \frac{q_{ref}}{q_o} p_o e^{-jkq_o} + r \frac{q_{ref}}{q_o} p_o e^{-jkq_o} \\ & + r \frac{q_{ref} q_s}{2q_o^2} p_o e^{-jk3q_o} + r^2 \frac{q_{ref} q_s}{2q_o^2} p_o e^{-jk3q_o} \\ & + \frac{q_{ref}}{2l} p_o e^{-jk2l} + r_\phi \frac{q_{ref}}{2l} p_o e^{-jk2l} \end{aligned} \tag{4.9}$$

which may be simplified to

$$p = p_s = (1 + r) \left(\frac{q_{ref}}{q_o} p_o e^{-jkq_o} + r \frac{q_{ref} q_s}{2q_o^2} p_o e^{-jk3q_o} \right) + q_{ref} p_o e^{-jk2l} \left(\frac{1}{2l} + \frac{r_\phi}{2l} \right). \tag{4.10}$$

This is the expression for the pressure at the surface under study, whereas at the rigid surface it is ($r = r_\phi = 1$)

$$p_R = 2\left(\frac{q_{ref}}{q_o}p_o e^{-jkq_o} + \frac{q_{ref}q_s}{2q_o^2}p_o e^{-jk3q_o}\right) + \frac{q_{ref}}{l}p_o e^{-jk2l}. \tag{4.11}$$

We now have two equations: (4.10) and (4.11), and four unknown quantities: q_s, ϕ (which would give us l_o), r_ϕ and r. The pressure amplitude p_o is common to every factor and will not be present in the expression for r. Approximations are required in order to isolate the reflection factor from these equations. This will be discussed in Section 4.2.1.

4.2.1 Approximations Used to Determine the Reflection Factor

The given measurement configuration and approach has brought us two equations relating the reflection factor; however, there are four unknowns: r, r_ϕ, q_s, and ϕ. Our goal is to determine r. Information is therefore required for the floor reflections in the room, ϕ and the scattering characteristics of the loudspeaker, q_s. In addition, we now have a factor of r_ϕ to consider. Several approximations must be made in order to simplify the present analysis.

First we will consider the reflection of sound pressure from the floor. These contributions would not be present in an entirely anechoic environment. Alternatively, the impulse response could be gated in order to remove the floor reflection from a measurement. However, as we discussed in Section 3.3, this may only preserve the high-frequency data and falsify the information at low frequencies depending on the chosen window length.

The general motivation behind our analysis is that reflections from the room surfaces degrade a measurement. If we were able to neglect these reflections, then we would simply consider the signal at the microphone to be composed of the incident and reflected contributions from the loudspeaker and the surface under study. How may this difference in level be achieved? In the simplest fashion, reduce the loudspeaker-microphone distance and consequently, the microphone-surface under study distance. This is the strategy used in making near-field loudspeaker measurements. We will therefore keep a short distance between the loudspeaker and microphone in the measurements.

Consider the configuration shown in Figure 4.2. If the signal level of the incident pressure wave is much higher than the level of the floor reflection, the floor reflections may safely be neglected. Notice that

$$p_i \propto \frac{1}{q_o} \tag{4.12}$$

and

$$p_f \propto \frac{1}{2q_l} = \frac{1}{2\sqrt{q_h^2 + q_o^2/4}}. \tag{4.13}$$

The difference in signal levels may be demonstrated by substituting typical distances for q_o and q_h in (4.12) and (4.13). Let $q_o = 28$ cm and $q_h = 150$ cm, then: $p_i \propto 3.6$ and $p_f \propto 0.63$, the ratio of these indicates that p_i is almost six times the amplitude of p_f. This shows that the incident level p_i is 15 dB above the strongest reflection in the room and therefore, indicates that neglecting the room reflections will result in some error. The expressions in (4.10) and (4.11) may now be written without the floor contributions, as

$$p_s = (1+r)\left(\frac{q_{ref}}{q_o}p_o e^{-jkq_o} + r\frac{q_{ref}q_s}{2q_o^2}p_o e^{-jk3q_o}\right) \tag{4.14}$$

and for the rigid surface,

$$p_R = 2\left(\frac{q_{ref}}{q_o}p_o e^{-jkq_o} + \frac{q_{ref}q_s}{2q_o^2}p_o e^{-jk3q_o}\right). \tag{4.15}$$

It is now time to combine these two equations in order to isolate the reflection factor; we begin by multiplying p_s by two and subtracting p_R

$$\begin{aligned} 2p_s - p_R &= 2(1+r)\left(\frac{q_{ref}}{q_o}p_o e^{-jkq_o} + r\frac{q_{ref}q_s}{2q_o^2}p_o e^{-jk3q_o}\right) \\ &- \quad 2 \quad \left(\frac{q_{ref}}{q_o}p_o e^{-jkq_o} + \frac{q_{ref}q_s}{2q_o^2}p_o e^{-jk3q_o}\right) \\ &= 2r\left(\frac{q_{ref}}{q_o}p_o e^{-jkq_o} + \frac{q_{ref}q_s}{2q_o^2}p_o e^{-jk3q_o}\right) + (r^2-1)\frac{2q_{ref}q_s}{2q_o^2}p_o e^{-jk3q_o}. \end{aligned} \tag{4.16}$$

Notice that the first term in brackets is the pressure at the rigid surface multiplied by r, rp_R. Let us divide (4.16) by p_R, and use $w = p_s/p_R$ (this is not to be confused with the angular frequency ω)

$$2\frac{p_s}{p_R} - 1 = 2w - 1 = r + (r^2-1)\frac{2q_{ref}q_s p_o e^{-jk3q_o}/2q_o^2}{2\left(q_{ref}p_o e^{-jkq_o}/q_o + q_{ref}q_s p_o e^{-jk3q_o}/2q_o^2\right)} \tag{4.17}$$

which may be simplified to

$$2w - 1 = r + (r^2-1)Q_s \tag{4.18}$$

where

$$Q_s = \frac{q_s}{2q_o e^{jk2q_o} + q_s}. \tag{4.19}$$

The factor Q_s represents the contribution of the scattered wave from the loudspeaker, which is a function of q_s, q_o and k. When $Q_s \neq 0$, (4.18) can be solved for r. To simplify the notation, let $W = 2w - 1$, and let us calculate the roots (r's) of

$$r^2 + \frac{r}{Q_s} - \left(1 + \frac{W}{Q_s}\right) = 0 \tag{4.20}$$

The roots are

$$r = -\frac{1}{2Q_s} \pm \sqrt{\frac{1}{4Q_s^2} + \frac{W}{Q_s} + 1}. \tag{4.21}$$

Note that there are two roots with opposite signs. The scattering from the loudspeaker is therefore needed in order to calculate the reflection factor of the surface. In principle, this could be found by taking a reference measurement at a surface with a known reflection factor and isolating Q_s in (4.18):

$$Q_s = \frac{W - r}{r^2 - 1} = \frac{2w - 1 - r}{r^2 - 1} = \frac{2p_s/p_R - 1 - r}{r^2 - 1}. \tag{4.22}$$

Care must be taken not to use a surface having a reflection factor of unity. If the reflection factor of the reference surface is unity[1], then Q_s has a pole and rises to infinity. On the other hand if the surface had a reflection factor of zero then no wave would be reflected from the surface, resulting in no scattered wave from the loudspeaker. In this case, $w = p_s/p_R = 1/2$, since the surface under study is perfectly absorbing and the rigid surface is perfectly reflective, resulting in $Q_s = 0$, as required.

Let us now consider what will happen if Q_s is zero. Intuition tells us that there would be no scattered wave, and therefore we would only be considering the incident and reflected sound waves at the surface under study. If we substitute $Q_s = 0$ in (4.18), we obtain the relationship $r = 2w - 1$, as in an anechoic environment. The factor Q_s can then be seen as a correction which must be applied to our calculations when the scattering of the reflected wave by the loudspeaker is significant. This factor is proportional to q_s, indicating that $Q_s \to 0$ as $q_s \to 0$.

[1]If the reflection factor were -1, this would be a "pressure release" boundary, which would also result in a pole in Q_s.

4.3 Experimental Setup of the Surface Pressure Method

We will now consider how to implement this type of measurement *in situ*. The basis of this method is that we have a reference surface that is rigid, which may be placed in the position of the surface we are measuring. Since we would like to use a non-invasive technique, we may not place the rigid surface in the location of the surface under study, however we may place it in front of this surface.

The noise in the room is different from position to position, due to resonances and differences in noise source locations. This means that our rigid surface measurement should be taken at the same location as the measurement of the surface under study, or very close. This requires a very thin, rigid, surface. These two requirements are contradictory. Both the bending stiffness (A.2) and the mass increase with the thickness of the sheet. The greater these values, the more rigid the surface. In addition, for this method to be applicable *in situ*, it is necessary that the equipment be easily transportable. This requires the sheet and support structure to have a low mass. Once again we arrive at another contradiction, this time between the rigidity of our sheet and transportability. Finally, the setup should allow measurements to low frequencies, down to 50 Hz or less for example. This final necessity implies that the surface of the sheet should be large, so that the sound waves interact with the sheet and not a combination of the sheet and the surface under study. We may summarize the requirements of the rigid surface as follows:

1. The sheet must be as rigid as possible
2. The sheet must be as thin as possible
3. The sheet must be as light as possible
4. The sheet must be as large as possible

In more rigorous terms, we may relate the above statements to the properties of materials:

1. The sheet must have a high Young's modulus E, a high density ρ_m, and a considerable thickness h
2. The sheet must have a small thickness h
3. The sheet must have a low density ρ_m
4. The sheet must have a large area

We see that these requirements contradict one another, and therefore, a compromise must be made. A high Young's modulus, density and considerable sheet thickness will decrease the transmission coefficient of this surface (2.3). The bending stiffness is proportional to the Young's modulus of a material. The greater the bending stiffness, the greater the reflection coefficient ($\rho = 1 - \tau$) in the stiffness controlled region. This is also true for the mass controlled region: The higher the mass of the sheet, the greater the reflection coefficient.

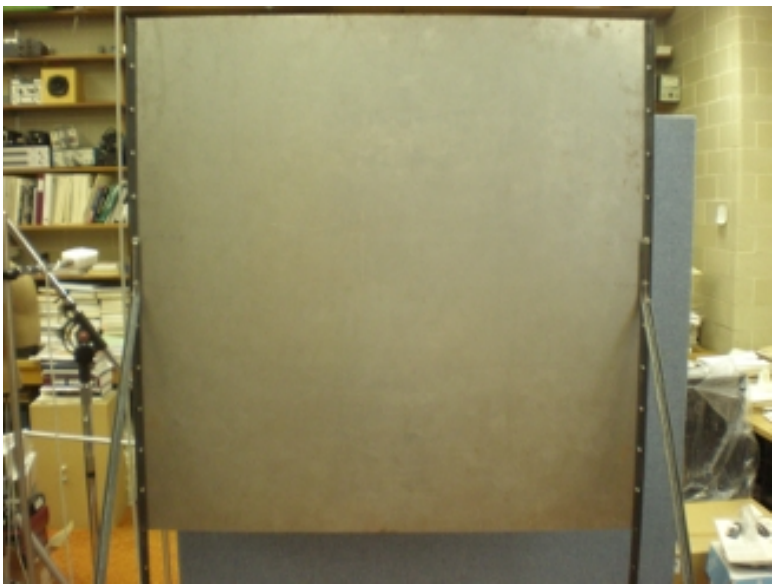

Figure 4.3: Front view of steel sheet setup. This photograph shows the sheet and support system, which is constructed of angled steel bars.

Figure 4.4: Angled view of steel sheet setup. This photograph shows the complete construction of the setup. Vertical supports hold the sheet at a particular height. Angled bars go from the middle of the sheet to the floor for increased support.

Preliminary measurements were carried out with a small 30 cm by 45 cm steel sheet having a mass of approximately 1/2 kg. However this would not satisfy all of the requirements that we have stated due to low mass and small dimensions. We therefore chose to use a larger steel sheet. Steel has a high Young's modulus ($E = 200$ GPa) and density ($\rho = 7700$ kg/m^3). A thickness h of 1/16 of an inch was chosen, or $h \simeq 1.6$ mm. The length and width of the steel sheet are approximately 1.2 m, yielding an area of 1.44 m^2 and a mass of 17.7 kg. This sheet is shown with its support structure in Figures 4.3 (front view) and 4.4 (angled view).

A compromise between size and weight is made for this method. A support system is also needed to hold the steel sheet against the surface under study. We would again require that the supports be rigid (massive and high Young's modulus) and transportable. The supports were chosen to be constructed of 1.9 cm (3/4 inch) angled steel bars shown in Figure 4.5.

Figure 4.5: Side view of steel sheet setup. This photograph shows an angled support going from the middle of the sheet to the ground. The height of the sheet and all supports are adjustable.

Periodic holes where made at a 10 cm spacing in both the supports and the steel sheet to allow height adjustments. Ideally it would be possible to place the sheet flush with the surface under study. The supports are therefore placed on the front of the sheet with bolts going through the back into countersunk holes, allowing the bolt heads to be flush with the back of the steel sheet. This allows the sheet to be placed very close to a wall. A countersunk fastening is shown in Figure 4.6.

The base of the horizontal support is slotted in order to increase the contact between the sheet and the surface under study (see Figure 4.8). A quick adjustment

Figure 4.6: A view of the back of the steel sheet showing countersunk fastening. This allows bolts to be inserted flush with sheet surface and therefore, does not reduce the amount of contact between the sheet and the surface under study.

is possible by sliding the angled support bar forward in the slot, applying more pressure to the sheet and therefore increasing the contact between the two surfaces (see Figures 4.7 and 4.8). This configuration takes 15 minutes to assemble and the supports may be folded to allow for ease of transportation. In general, one individual will not be able to carry all of the equipment mentioned above. Two or three trips must then be taken to relocate the sheet and supports.

A spherical loudspeaker is used in this setup. The microphone is attached to the loudspeaker, maintaining a loudspeaker-microphone distance of 28 cm (see Figure 3.48). A measurement is taken with the microphone flush with the sheet (which is at the surface under study). The sheet structure must then be moved in order to take a measurement at the surface under study. The loudspeaker and sheet support positions are marked using masking tape, the loudspeaker arrangement is moved, and the steel structure is taken down. The supports are then returned to their position at the surface. This ensures that any diffraction from the supports is present for both measurements (however diffraction will depend on the surface under study as well). Finally the loudspeaker is returned to its original position and a measurement is made with the microphone at the surface under study.

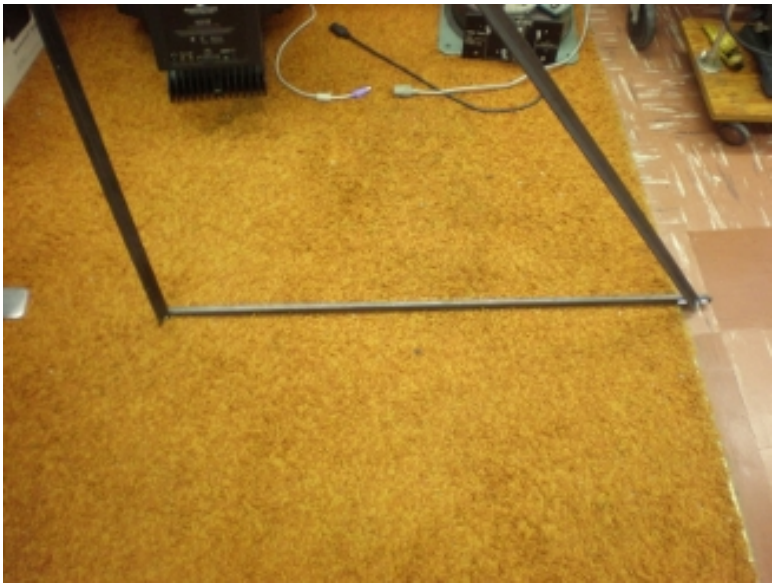

Figure 4.7: This angled bar applies pressure to the steel sheet allowing it to increase or decrease the contact between the sheet and the surface under study.

Figure 4.8: The slot in the base of this floor support is attached to the bottom of the angled bar. This may be adjusted so that the bottom of the angled bar is closer to the sheet, increasing the contact between the sheet and surface.

4.4 Results

We will now compare the results of this method on three types of surfaces:

- A rigid surface
- An absorptive surface
- A resonant surface

This will illustrate the performance of the surface pressure method for the entire range of reflection/absorption coefficients.

4.4.1 Rigid Surface: Glazed Block Wall

The rigid surface that we had chosen is found at multiple locations in the Physics building at the University of Waterloo. Glazed blocks form this surface which are shown in Figure 4.9. Several measurements of this surface will be compared in different locations of the building. It is expected that measurements will show low absorption coefficients.

Figure 4.9: Rigid surface to be measured. A wall consisting of glazed blocks.

We would expect the sound pressure levels at both the sheet with the wall, and the wall alone, to be essentially the same. This is a consequence of the surface

being rigid: adding a sheet to the wall will not significantly change the impedance of the surface.

Three measurement locations were used in the Physics building, all in stairwells: 1. Back door of the 2nd floor (BD2) 2. Front door of the 2nd floor (FD2) and 3. Back door of the 3rd floor (BD3). A total of six measurements were performed: one at BD2, one at FD2 and four at BD3. The geometry of each room is given in Appendix B. It is important to note that each measurement setup will occur in different environments on essentially the same surface. It will be useful to compare the results from each measurement.

First, measurements were carried out on the glazed block wall at location BD2. The steel sheet was configured as shown in Figures 4.3 to 4.8. A loudspeaker-microphone distance of 28 cm was used. The impulse response at the sheet is shown using different tapered window lengths in Figure 4.10. We may notice that small window lengths remove the low frequency oscillations from the impulse response. This is also shown in Figure 4.11 where all windowed sound pressure levels converge for frequencies above 1 kHz. However, below this we see differences due to truncation of the impulse response.

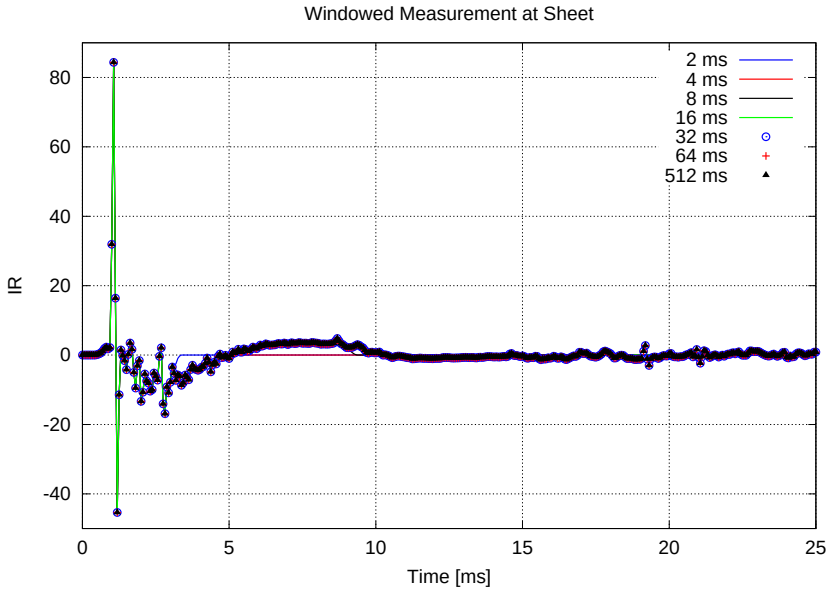

Figure 4.10: Impulse response of sheet at glazed block wall for different window lengths. It is apparent that small window lengths remove low-frequency oscillations from the impulse response.

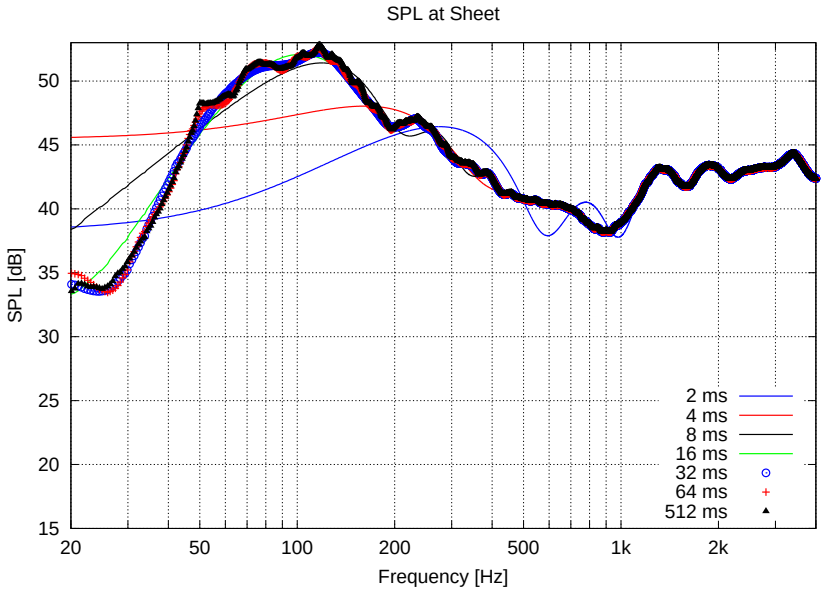

Figure 4.11: Sound pressure level at sheet and glazed block wall for different window lengths. Differences in sound pressure level are caused by the truncation of the impulse response, altering low-frequency data.

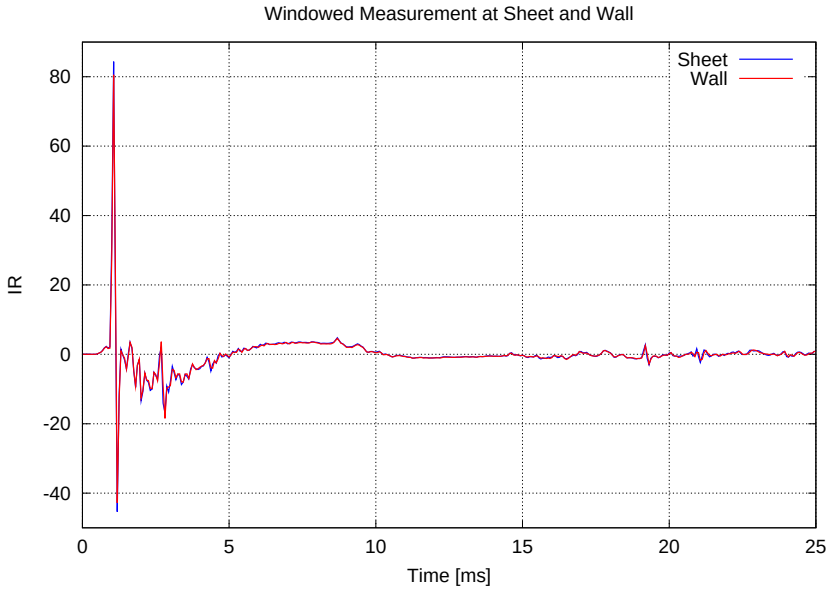

Figure 4.12: Impulse response at sheet and at glazed block wall. Both measurements follow very well implying that the sheet does not significantly change the sound field at the surface.

A time window of 64 ms would allow a frequency resolution of about 15 Hz, which is sufficient for our purposes. Using this time window, the impulse responses and sound pressure levels of the sheet+wall and wall measurements are shown in Figures 4.12 and 4.13. It is apparent that there is very little difference between the two measurements.

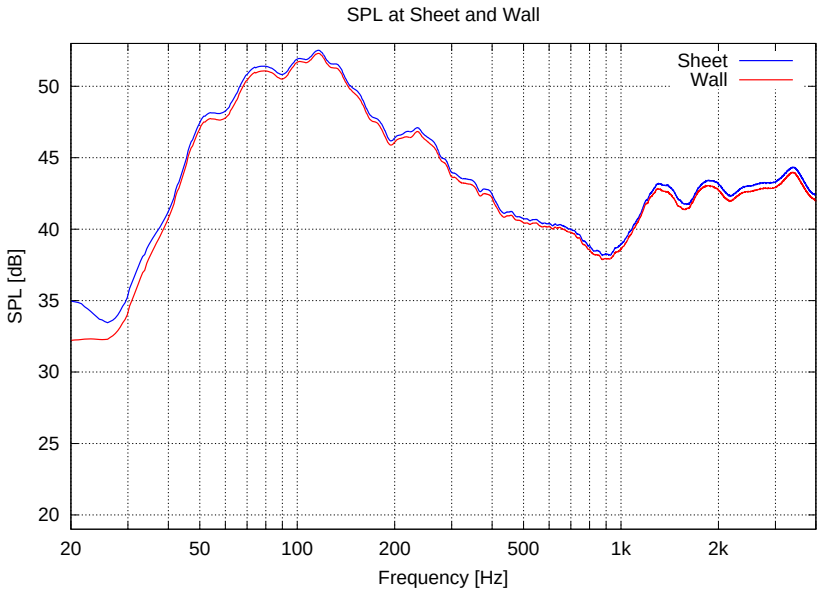

Figure 4.13: Sound pressure level at sheet and at glazed block wall. Both measurements follow very well implying that the sheet does not significantly change the sound field at the surface.

The reflection factor and absorption coefficient may now be calculated from the frequency responses of the surface under study and the rigid surface measurements. The magnitude of the reflection factor is shown in Figure 4.14 for multiple window lengths. We are only concerned with measurements down to 50 Hz. We see that the 16, 8, 4 and 2 ms data rise and drop at the low frequencies due to impulse response truncation. This surface has a reflection factor of magnitude 0.9-0.95 over most of the frequency range.

This reflection factor translates to an absorption coefficient of 0.1-0.2 over most of the frequency range, as seen in Figure 4.15. Note that the absorption coefficient is denoted by "A" on the vertical axis. We may also look at the results obtained using different amounts of smoothing (see Figure 4.16). Additional smoothing reduces the oscillations in the absorption coefficient. For the remainder of the presented results, if not specified otherwise, 1/3-octave smoothing and a 64 ms tapered window are used.

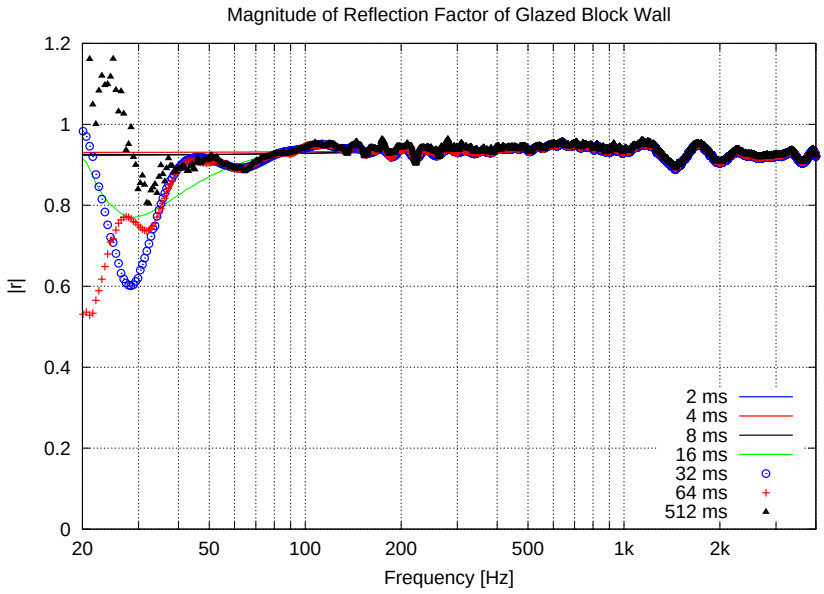

Figure 4.14: Magnitude of reflection factor of glazed block wall for different window lengths. The surface under study has a magnitude of the reflection factor of 0.9-0.95 over most of the frequency range

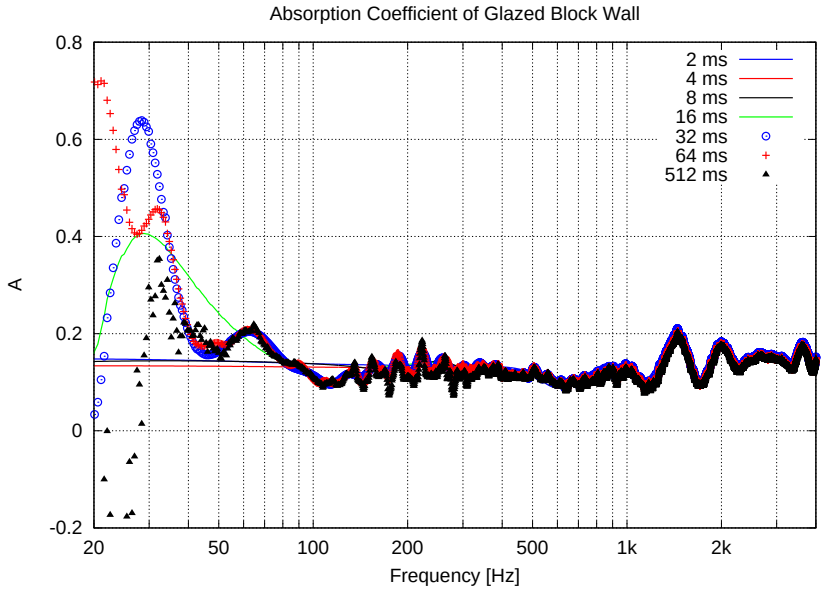

Figure 4.15: Absorption coefficient of glazed block wall for different window lengths.

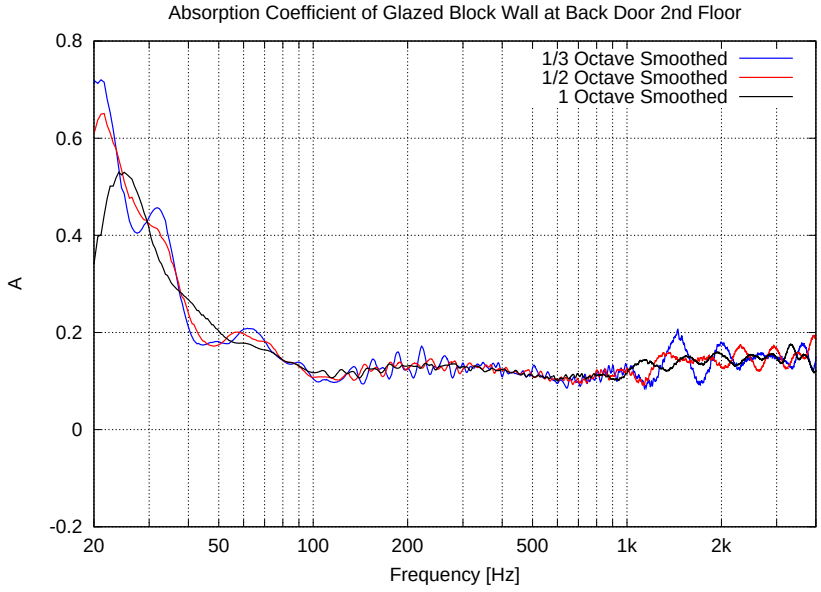

Figure 4.16: Absorption coefficients of glazed block wall for different octave width smoothing. The window length is 64 ms and the absorption ranges between 0.1 and 0.2 over most of the frequency spectrum.

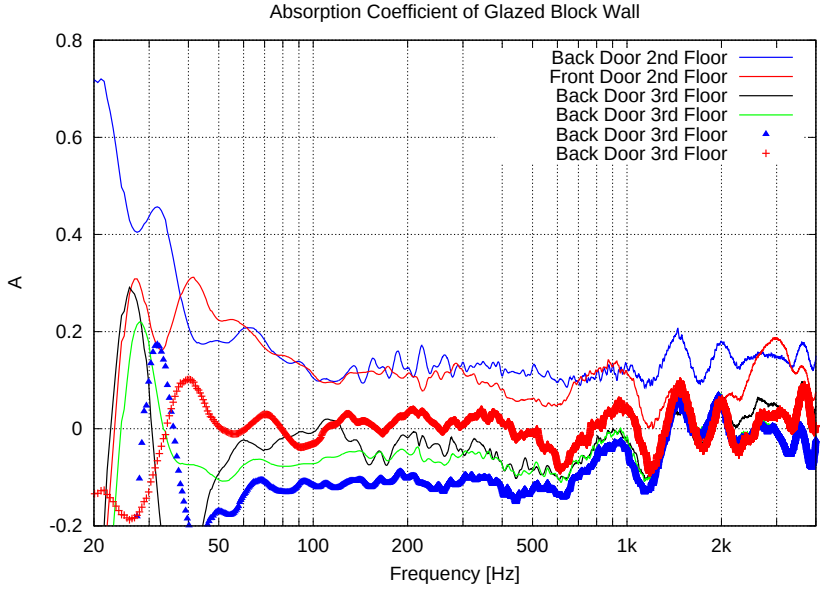

Figure 4.17: Absorption coefficient of multiple glazed block walls at different locations. Notice the consistency between the 2nd floor measurements and the 3rd floor measurements. There seems to be a frequency independent offset between measurements.

Figure 4.17 displays the results for all six measurements at the three locations. The absorption coefficients of these walls vary by approximately ± 0.1 over the most reliable frequency range (50 Hz to 4 kHz). Of course we should not be obtaining negative absorption coefficients. Mounting conditions are suspected to contribute to the variation in absorption coefficient between measurements, which will be shown later. However we see that the data follow reasonably well for the 2nd floor locations and for the 3rd floor locations (maximum variation of 0.2 at the 3rd floor location). The discrepancies seen here may also be due to the microphone being placed at a slightly different location after the sheet structure was taken down. Extreme caution was taken not to move the microphone connected to the loudspeaker, but a small variation is always possible. In addition, the microphone is placed at a single point at the surface under study. Measurements at BD3 were generally performed on separate days, in some cases up to a month apart. The exact location of wall was not measured for each case.

This difference in absorption is troubling. These walls were expected to have similar absorption coefficients. We may certainly conclude that the glazed block walls are highly reflective over the entire frequency range of interest. Potential causes of variation in absorption will have to be investigated. In fact, the solid green and the blue triangle measurement curves were taken at the same location of the wall in Figure 4.17. The sheet and support assembly was taken down after the first measurement and reassembled. Another measurement was then taken. We see that this has resulted in a difference of as much as 0.1 in absorption. This suggests that systematic errors exist when mounting the sheet structure. The effect of mounting conditions will be investigated in Section 4.4.4.

4.4.2 Absorptive Surface: Office Divider

One common absorptive surface in use in many buildings is office dividers. Due to their availability and large surface area, this was chosen as an absorptive test surface. The office divider is shown in Figure 4.18. It is expected that the office divider will absorb most of the incident acoustic pressure at high frequencies, with a reduction in absorption at low frequencies. In terms of sound pressure level, we would assume that the difference between the two measurements, sheet+office divider and office divider alone, should fall between 0 ($p_r = p_i$) and 6 dB ($p_r = 0$).

The impulse response at the sheet and office divider is shown in Figure 4.19. We see that the measurement at the divider peaks at about half of the maximum value of the sheet measurement. In addition, we see that the low-frequency character of the impulse response is preserved in the office divider data. The sound pressure levels at the surface under study and the sheet are shown in Figure 4.20. Differences of 0 to 6 dB are seen in the data, with the greatest difference at high frequencies, even rising to a difference of 10 dB near 2 kHz. The office divider is seen to reflect very little sound above 1 or 2 kHz in Figure 4.21.

Figure 4.18: Absorptive surface to be measured, an office divider.

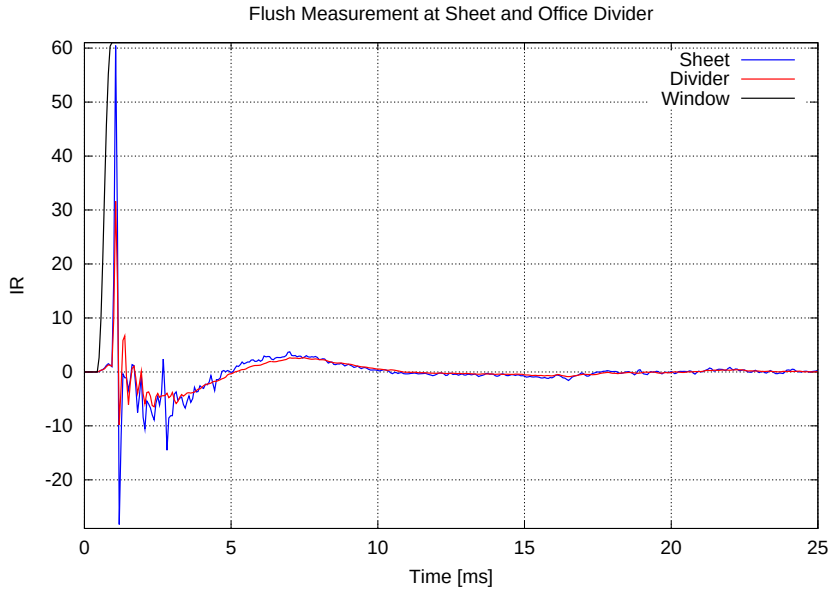

Figure 4.19: Impulse response at sheet and an office divider. Note that the maximum of the office divider's data is about half that of the sheet data. In addition, the low-frequency character of the impulse response is still visible in the office divider data.

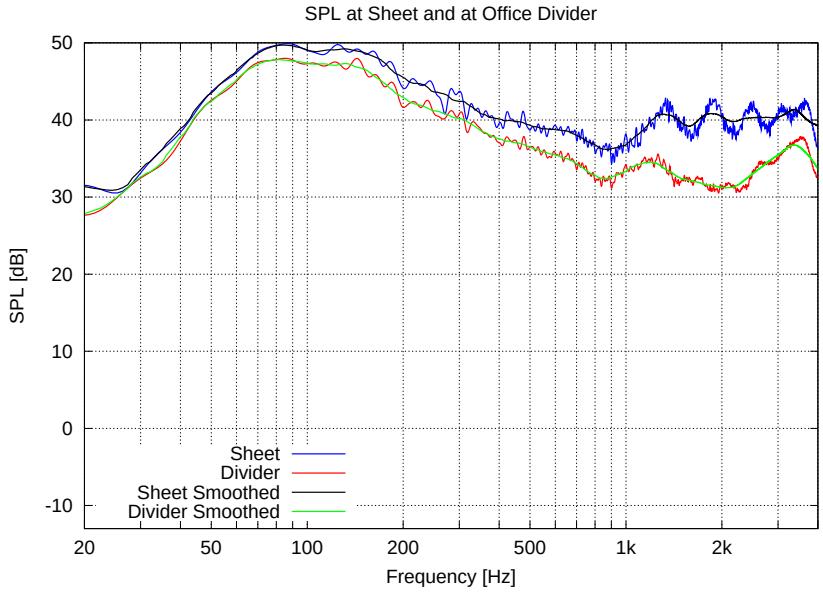

Figure 4.20: Sound pressure level at sheet and an office divider. The difference between the sheet and divider measurements varies generally between 0 and 6 dB. At 2 kHz, the difference is as much as 10 dB. Notice that there are oscillations in the sheet measurement that are not present in the office divider measurement above 1 kHz. This is due to the scattered wave from the loudspeaker.

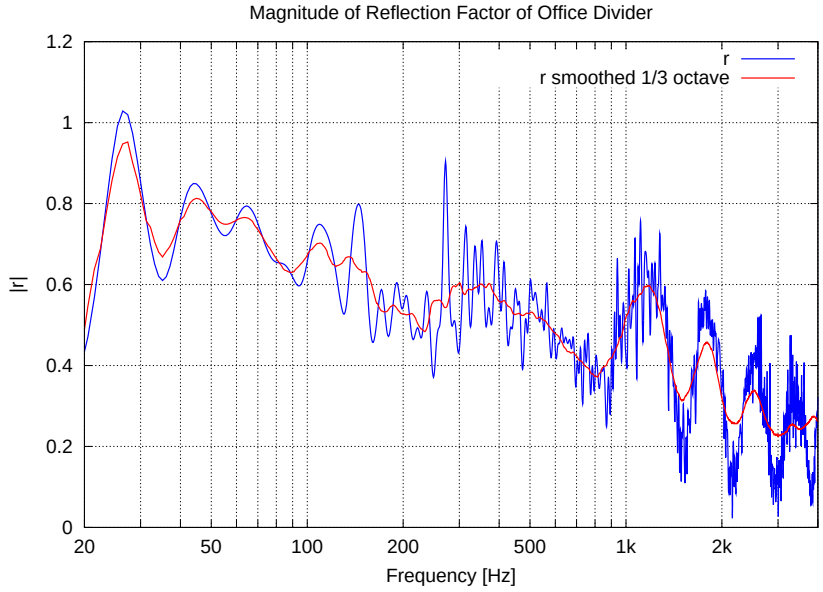

Figure 4.21: Magnitude of reflection factor for an office divider. This surface is reflective at low frequencies and absorptive at high frequencies. The scattering of sound from the loudspeaker causes fluctuations in absorption above 1 kHz.

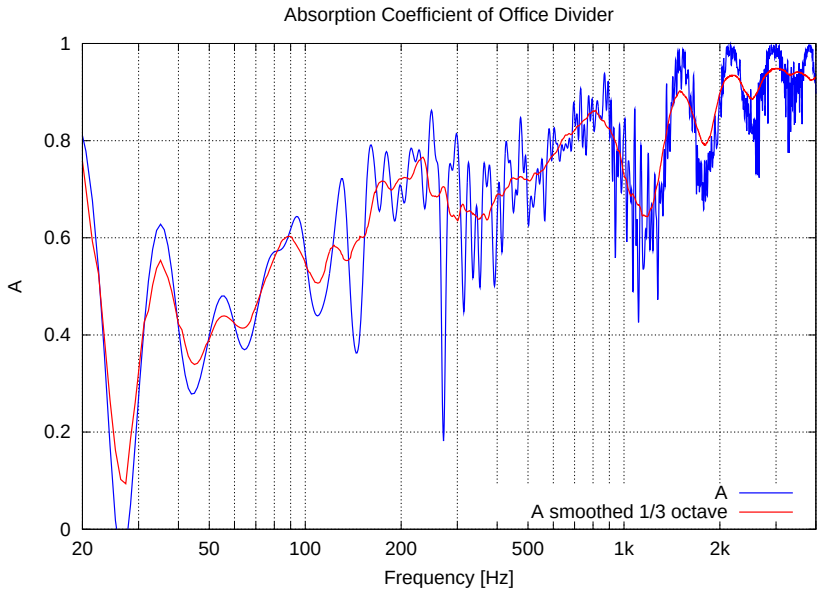

Figure 4.22: Absorption coefficient of an office divider. This surface is reflective at low frequencies and absorptive at high frequencies. The scattering of sound from the loudspeaker causes fluctuations in absorption above 1 kHz.

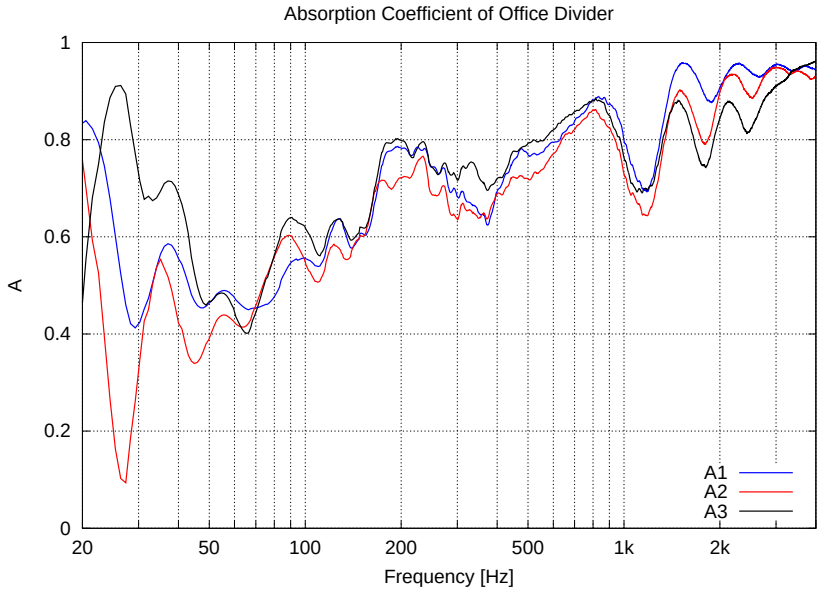

Figure 4.23: Multiple measurements of absorption coefficient for an office divider. The variation in absorption coefficient (± 0.05) is not as significant as that for the glazed block surface. The scattering of sound from the loudspeaker causes fluctuations in absorption above 1 kHz.

In terms of absorbed sound intensity, the absorption coefficient of the office divider is shown in Figure 4.22. We see that this device absorbs sound intensity very well above 500 Hz. We also notice the gentle decrease in absorption with reducing frequency which is typical for absorptive devices of this kind[2]. The fluctuations in absorption above 1 kHz are caused by the scattered wave from the loudspeaker, which is only present in the sheet measurement. Smoothing will slightly reduce the amplitude of these oscillations. Figure 4.23 displays the results for three separate measurements performed on the office divider. We may note that the variation in absorption (± 0.05) is less than that for the glazed block surface. One factor contributing to this difference is the mounting of the steel sheet which will be discussed in Section 4.4.4. Another contribution may be the slight displacement of the loudspeaker as it is moved and placed back in its original position at the surface between measurements (in order to remove the steel sheet and support structure). The microphone position may not be the same in both cases but this error should not be more than a centimetre. Diffraction from the edges of the steel sheet will cause fluctuations in the absorption spectrum. The scattering of sound from the loudspeaker is the primary cause for the oscillations in absorption at high frequencies.

4.4.3 Surface Having Resonance: Wood Panelled Wall

The third surface is a wall consisting of regularly spaced wooden panels backed by an airspace and a rigid wall (such as the glazed block surface). Approximate values of the airspace depth, the stud spacing and the densities of the walls may be used with (2.46) to calculate the resonance in this system. This composite wall should have a fairly broad mass-air-mass resonance where maximum absorption will occur. For all other frequencies, this surface is expected to be reflective. The mass-air-mass resonance was calculated to be approximately 150 Hz in Section 2.3.3.

The impulse responses of the measurements are shown in Figure 4.24, which follow each other closely, indicating that there is little absorption. Figure 4.25 supports this fact; however there is some difference in sound pressure level from 80 to 300 Hz. As a result, high reflection is seen over most of the frequency range, however there is a dip in reflection from 80 to 300 Hz (Figure 4.26), which indicates a resonance in absorption (Figure 4.27). This resonance is the mass-air-mass resonance, which seems to peak at 135 Hz. This is very close to the prediction given in Section 2.3.3 using approximate values for the mass of the panels, airspace and the mass of the wall behind the airspace.

[2]We generally need very thick fibreglass or foam absorbers to absorb acoustic waves at low frequencies.

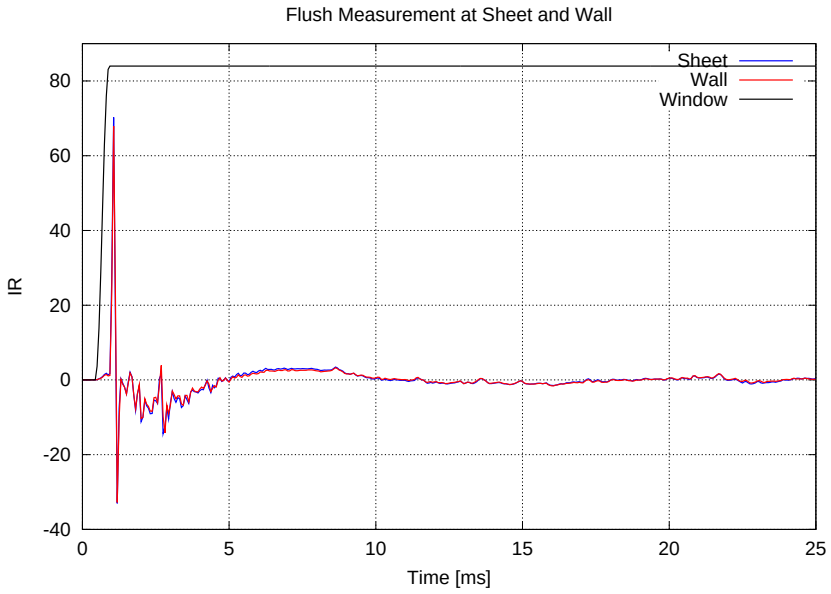

Figure 4.24: Impulse response at sheet and wood panelled wall.

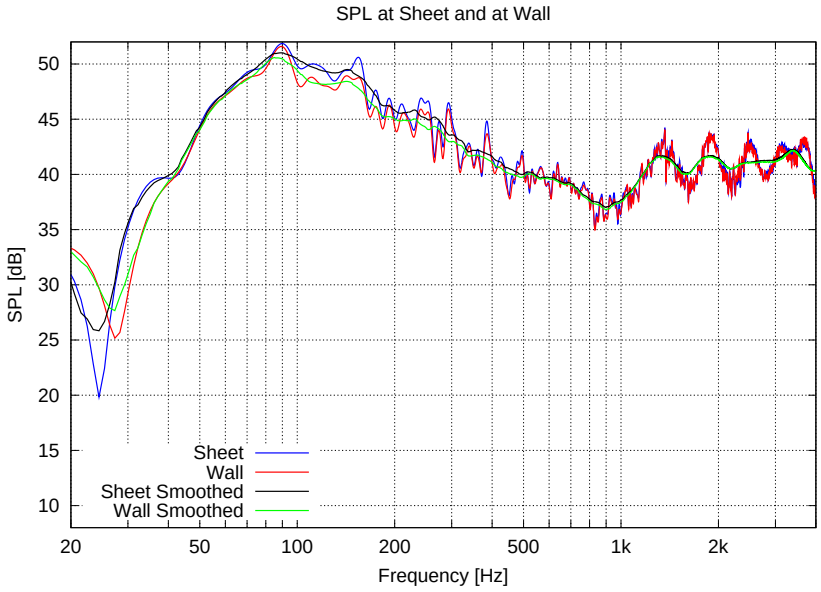

Figure 4.25: Sound pressure level at sheet and wood panelled wall.

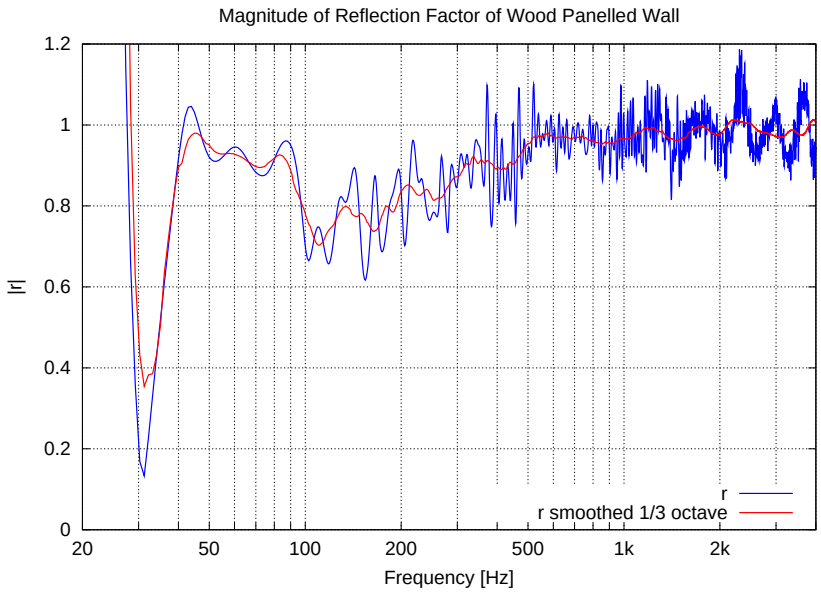

Figure 4.26: Magnitude of reflection factor for a wood panelled wall.

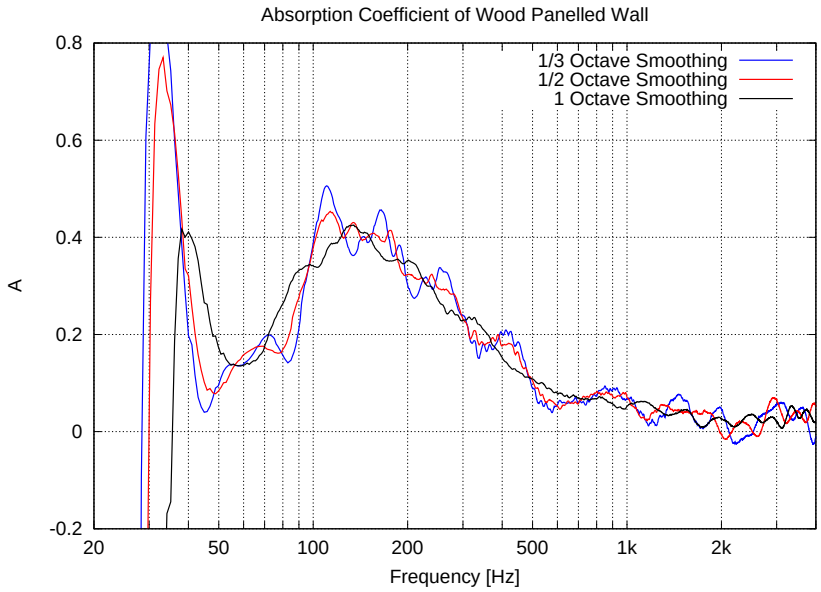

Figure 4.27: Absorption coefficient of a wood panelled wall using different octave smoothing widths. The mass-air-mass resonance frequency centre is at 135 Hz.

4.4.4 Effect of Mounting

The discrepancies between measurements suggest that the experimental procedure may suffer from error. This could be caused by controllable factors such as the mounting of the steel sheet or the difference in microphone positions between measurements. Another possible source of error could be attributed to diffraction from the steel sheet itself and its supporting structure. The effect of mounting will now be investigated.

In principle we would like this sheet to be as close as possible to the surface under study. More or less contact between the sheet and the surface is obtained by adjusting the angled support via a slot at the base. This was varied in the following measurements. Two extreme positions were considered: 1. The sheet is flush with the surface under study and 2. The sheet is no longer in contact with the surface under study (there is a 1-2 cm gap between the surface and sheet). In both cases the microphone is millimetres away from the sheet, meaning that the loudspeaker-microphone assembly is not at the same position for both of these measurements. These conditions are used to place an upper bound on the error that may be created from the improper mounting of the sheet and support equipment. Measurements were performed at the sheet and then at the wall with the above conditions.

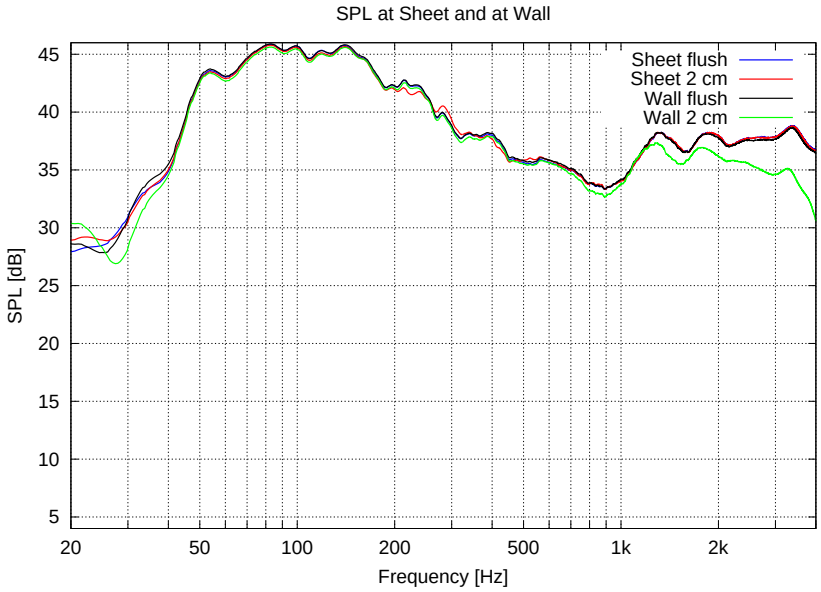

Figure 4.28: Sound pressure level of glazed block measurements wall for different mounting conditions.

The sound pressure levels obtained for each configuration are shown in Figure 4.28. It is seen that the flush sound pressure levels and the measurement of the sheet for the 2 cm position are quite similar. In fact this indicates that the sheet is fairly rigid, even moving the sheet (and loudspeaker-microphone) 2 cm from the wall did not change the measurement. We do see however that the 2 cm wall

data drops in level at high frequencies. The measurement is unchanged in the low frequency region since the wavelength is much larger than the 2 cm spacing. The absorption coefficient (Figure 4.29) is close to zero for the flush measurements. The 2 cm wall data results in an absorption coefficient oscillating above and below zero for frequencies above 150 Hz. The maximum amplitude of these oscillations is approximately 0.3, which is significant.

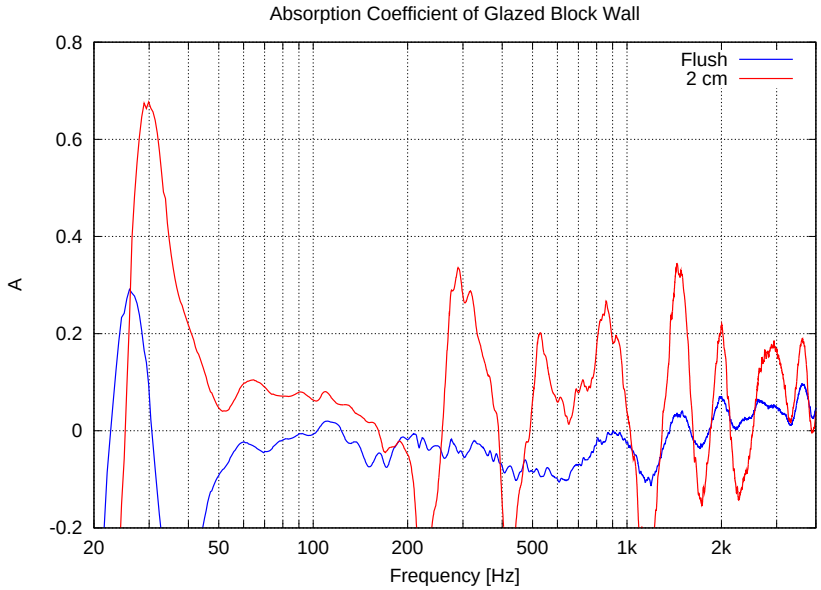

Figure 4.29: Absorption coefficient of glazed block wall for different mounting conditions.

In the case of the office divider, three positions were measured: 1. Sheet flush with the surface under study 2. Sheet 1/2 cm away from the surface and 3. Sheet 2 cm away from the surface. The sound pressure levels are found in Figure 4.30. These results are fairly interesting. The first three data curves (top blue, red and black) are the sheet measurements, which are nearly identical. This is because the microphone is always very close to the sheet even though from one mounting condition to the other the distance between the sheet and the office divider is changing. The green curve and the data represented by triangles represent the divider measurements which show some differences. The 2 cm and 1/2 cm positions are very close over the entire frequency range. These measurements do not follow the flush sound pressure level at high frequencies however.

Calculated absorption coefficients are shown in Figure 4.31. A difference of ± 0.1 in absorption is found (less than the case for the glazed block wall). A common trend is also clear from this data, all the peaks and dips line up nicely apart from the data at frequencies near 2 kHz.

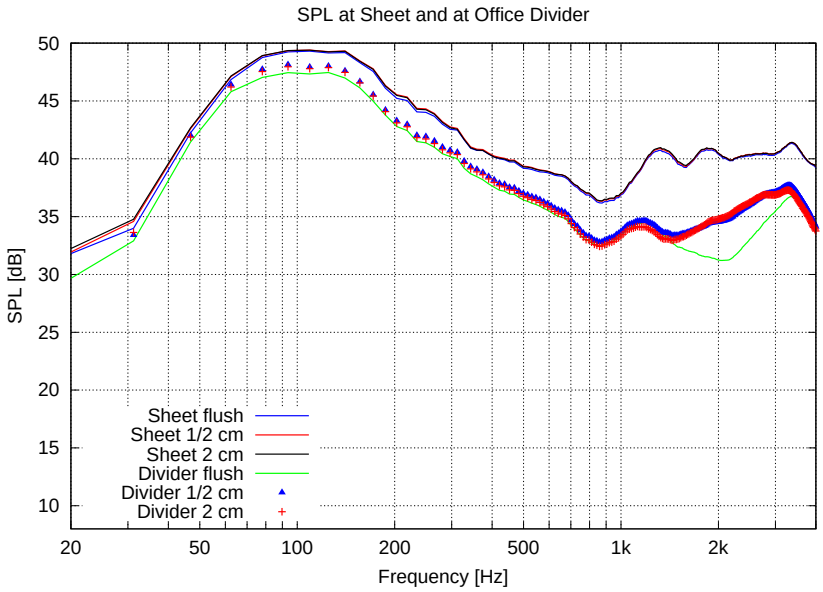

Figure 4.30: Sound pressure level of office divider measurements for different mounting conditions. The sheet measurements are nearly identical (blue, red and black solid lines). The office divider measurements differ slightly, more so at higher frequencies.

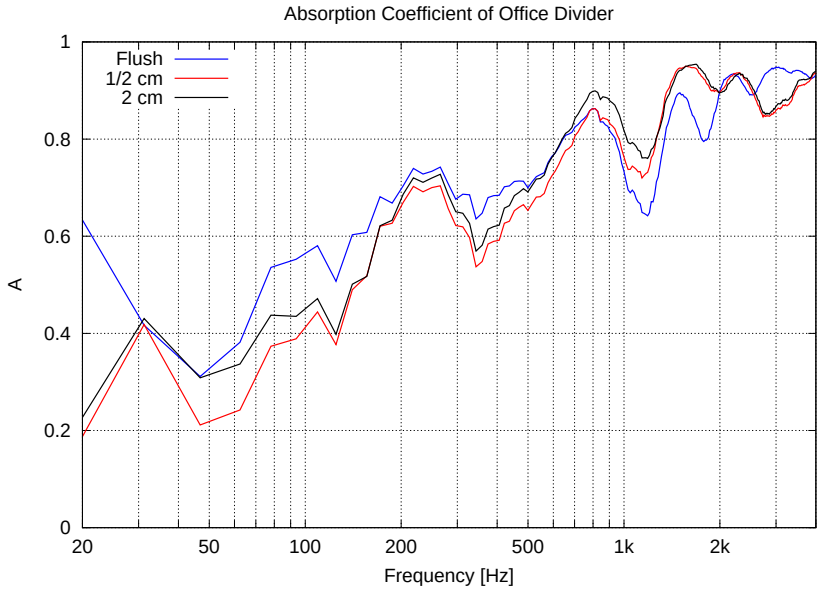

Figure 4.31: Absorption coefficient of office divider for different mounting conditions. A variation of ± 0.1 in absorption is seen.

4.4.5 Effect of Loudspeaker-Microphone distance

It has been assumed up to this point that the current loudspeaker-microphone distance does not pose a problem during measurements. We are not certain if this is the optimal distance for our present measurement setup. Four measurements were carried out for different loudspeaker-microphone positions at the office divider: 77 cm, 28 cm, 10 cm and 1 cm. Note that these distances correspond to the distance between the loudspeaker and microphone, the microphone is always a few millimetres from the sheet or the surface under study. The results of these measurements are shown in Figure 4.32. In principle all of these measurements should be identical.

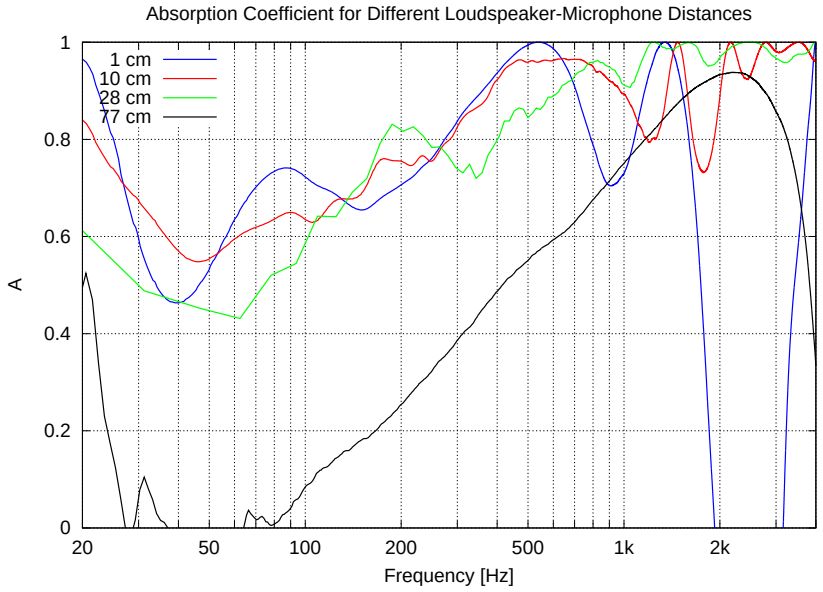

Figure 4.32: Absorption coefficient of office divider for different loudspeaker-microphone distances. The 77 cm data is not trustworthy due to the possible movement of the microphone position. A significant dip is found in the 1 cm data spectrum at 2.5 kHz.

Let us first consider the 77 cm data. Remember that the microphone is attached to the loudspeaker. At 3/4 of a meter loudspeaker-microphone distance, this attachment features significant bending. It is therefore possible that the microphone position had moved between measurements (sheet measurement and surface under study measurement). This distance is clearly inappropriate for the given configuration unless a stronger loudspeaker-microphone attachment is used.

The 1 cm, 10 cm and 28 cm data are similar over most of the frequency range. A sharp dip is found in the absorption for the 1 cm data. There may be several reasons for this. First, we are neglecting the scattering of sound by the loudspeaker itself which should not be done in a situation where the loudspeaker is so close to the sheet/surface under study. Second, interference is possible between the incident

and reflected waves from the sheet, however this would not be present at the office divider since this surface absorbs almost all the incident pressure above 1 kHz. Additionally, we should mention that a near-field measurement such as this will show an important variation in level when displaced a small distance.

It would be advantageous to use near-field measurements of this type to characterize a surface since this effectively removes the room from the measurement. The signal level at the microphone would be dominated by the incident, reflected and loudspeaker scattered waves while the room reflections could safely be neglected. We have not accounted for the scattering of sound from the loudspeaker in our absorption coefficient calculations. A loudspeaker-microphone distance of 28 cm was therefore used. Smaller distances than this will increase the level of the scattered wave and increase measurement error.

4.4.6 Diffraction From Sheet and Mounting Structure

Diffraction effects could also contribute to measurement errors. Both the sheet and the mounting supports can diffract sound waves. The edges of the steel sheet will cause more diffraction than the supports, since the sheet covers a larger area of the surface under study. The supports have always been present during measurements, both with and without the sheet at the surface under study. Two measurements were taken at the glazed block wall with and without the supports in order to determine if any differences in sound pressure level occur. The results are shown in Figure 4.33, which indicate that diffraction effects from the sheet supports are negligible in this instance. This seems to be the case for the edges of the sheet as well, since the sound pressure levels also follow closely (Figure 4.13). Maximum diffraction will occur when there is a large variation in impedance between the sheet and the surface under study. This is the case for measurements on the office divider, which is fairly absorptive. Notice that the strongest oscillations in absorption are seen for the office divider (Figure 4.23), which was originally believed to be diffraction. Closer inspection shows that it is due to the scattered wave from the loudspeaker.

4.4.7 Impulse Shortening

Impulse response shortening was used to determine if the absorption coefficient could be determined using the method described in Section 3.5. The result is shown in Figure 4.34 for the wood panelled wall and four rectangular window lengths: 2.5 ms, 5 ms, 10 ms and 64 ms. It is clear that the resonance peak shifts based on the window width that is used. The differences seen here by the 2.5, 5 and 10 ms data compared to the 64 ms data are similar to the differences between multiple measurements (approximately 0.2). Once again we see that the low-frequency absorption rises and falls based on the chosen window length.

Figure 4.33: Sound pressure levels with and without sheet supports. Both sound pressure levels are nearly identical over the whole frequency range.

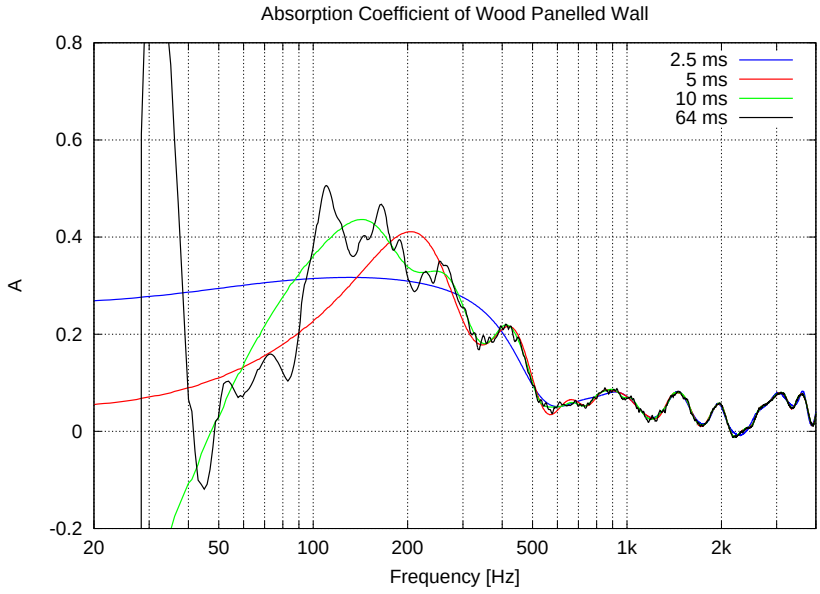

Figure 4.34: Absorption coefficient of wood panelled wall using impulse response shortening. It is seen that a longer window length shifts the resonance peak to lower frequencies.

4.5 Discussion

In this chapter we have covered the theory and implementation of the surface pressure method *in situ*. This method was originally used in an anechoic chamber with a large surface under study backed by a rigid wall. It has been shown that approximations are required in order to obtain the *in situ* reflection factor of a surface. The first approximation required that the room reflections be negligible compared to the incident and reflected waves. Second, the scattering of sound pressure by the loudspeaker was neglected. As the loudspeaker becomes closer to the surface, the incident and reflected waves increase in level. However, so does the scattered wave from the loudspeaker, a compromise must therefore be made.

Experiments confirmed characteristics of a rigid surface, an absorptive surface and a resonant surface. The absorption coefficient of the rigid surface was found to be ± 0.1 over most of the frequency range. It was shown that the configuration of the mounting system could contribute an error of ± 0.3 in extreme cases. This value is an upper bound of the mounting error, and in practice this error may be ± 0.1 or $\pm\ 0.2$ since the sheet is always in contact with the surface under study. Three mounting conditions were tested on the office divider. A variation of ± 0.1 is found which could account for the difference of ± 0.05 between absorption coefficient measurements.

The wood panelled wall was measured and clearly shows a resonance in absorption at 135 Hz. Using approximate values for the panel mass, airspace depth and the rigid wall mass behind the airspace, we calculated a resonance frequency of 150 Hz. Impulse-shortened data show similar results for large time window widths. The smaller the window width, the higher the resonance peak shifts in frequency.

Diffraction from the edges of the sheet and mounting structure will occur. Most of the diffraction will come from the edges of the steel sheet and will be significant if the sheet and surface under study differ greatly in impedance. Measurements from Section 4.4.6 have indicated that there is little diffraction when measuring a rigid wall. The results from the office divider will have more diffraction. This cannot be seen due to fluctuations in the absorption spectrum which are caused by the scattered wave from the loudspeaker. Note that diffraction is important at both low and high frequencies. This requires further investigation.

The effect of the loudspeaker microphone distance was discussed and shown to cause problems when performing near-field measurements (loudspeaker-microphone distance of 1 cm) or distant measurements (loudspeaker-microphone distance of 77 cm). Near-field measurements have a significant scattered wave from the loudspeaker and distant measurements require a strong microphone support. The effect of the loudspeaker scattering could be taken into consideration if this system was properly calibrated. A measurement could be performed at a surface of known acoustic impedance. The factor Q_s (and thus q_s) could then be determined and near-field measurements could subsequently be used. Small differences in microphone position for near-field measurements will result in grave errors. This approach

should be given more thought in the future.

The surface pressure method has been shown to be applicable *in situ*. Measurements are possible in the entire frequency range of interest, 50 Hz to 4 kHz. Low-frequency constraints are possible due to ambient noise, which is significant at very low frequencies. Several improvements should be investigated for this method. The mounting of the sheet has been shown to be subject to error. An improved mounting system could therefore fix this problem. The inclusion of the scattering effects could possibly reduce experimental error, as well as allow the use of near field measurements. Consistency in measurement positioning would be even more important if near-field measurements were used; however the room reflections could safely be neglected in this case.

Chapter 5

Summary and Conclusions

5.1 *In Situ* Measurements

We have demonstrated and discussed the difficulties relating to *in situ* measurements. Problems primarily occur at low frequencies, which have not decayed prior to the truncation of the impulse response. Noise is also always present and noise spectra usually show more energy as frequency decreases, making it difficult to achieve the same signal-to-noise levels at low frequencies. Reflections and scattering from the room and furniture will contribute to the sound pressure measured at the microphone position. These have to be reduced as much as possible during measurements, which is usually done by changing the location of equipment or by truncating the impulse response using a window. This generally increases the frequency spacing in the frequency domain. In addition, low frequency results will vary with the truncation location of the impulse response. A large frequency spacing (poor frequency resolution) results in the smoothing of data at low frequencies. If the surface under study is very active in this region, the truncation of the impulse response could result in the smearing of meaningful information.

Results have shown that the absorption characteristics of the surfaces measured in this study vary depending on the measurement method that was employed. Limitations have therefore been discussed for these methods. In most of the cases, one element that is left out of the theory for *in situ* measurements is the effect of the loudspeaker itself, which may reflect, scatter and diffract sound waves. This is apparent when comparing the results from the wood panelled wall using the tube loudspeaker and the KEF (Figures 3.27 and 3.22). At high frequencies, the tube loudspeaker data shows an absorption coefficient of $\pm$ 0.1. The results with the KEF oscillate between $\pm$ 0.2 which may be caused by diffraction from its cabinet.

In addition, we have discussed the use of impulse shortening and gating in order to improve the resolution of results at low frequencies. We suspect that the presented approach was not complete. A low frequency model of the loudspeaker was used, however none was used for the surface under study. This procedure may

shorten the impulse response of the loudspeaker although this does not necessarily shorten the reflected response from the surface under study. A low frequency model of the surface under study may be required to properly implement this shortening procedure. We do not know this information prior to a measurement, this is what we are trying to measure. Mommertz [27] [28] pre-emphasized his MLS signals so that the impulse response of the loudspeaker was very narrow. He does not mention how he accounts for the impulse response of the surface under study, which may not be narrow. This would require more study.

The *in situ* implementation of a reverberation chamber was presented. A diffuse sound field was assumed in order to determine the absorption coefficient of a surface under study. This is a useful device for measuring horizontal surfaces that are relatively flat. There are many distinct resonances in this box up to several kHz, indicating that the sound field inside the chamber is not diffuse. This method utilizes a rigid reference surface to determine the absorption coefficient. It is important that the reference surface is as rigid as possible and non-porous. In addition, the chamber should not have similar contact between the rigid surface and the surface under study.

5.2 Surface Pressure Method

The surface pressure method has been applied *in situ*. This was done by approximating a rigid surface by the use of a thin steel sheet. This sheet is not entirely rigid, however; a compromise must be made between sheet size/mass and its portability. Originally, the authors of this method [14] had replaced the study surface by a rigid surface of similar dimensions. It is clear that this could not be implemented in the same fashion *in situ*, therefore the steel sheet is quite thin, allowing the microphone position to be virtually unchanged between both measurements. In this case, the approximation that the same noise and reverberation is incident on the surface (sheet or study surface), is more justified.

Interestingly, this method compares the study surface with a rigid surface. The measurement at the rigid surface should give the maximum level of sound pressure measurable in this configuration. We have also discussed the subtraction technique, which relies on the comparison of a perfectly absorbing surface (air) with the surface under study. The measurement in air will give the minimum level of sound pressure measurable in this configuration. We have seen that rigid surface measurements using the subtraction technique have shown unexpected results. On the other hand, the surface pressure method has been applied to surfaces covering the full range of absorption characteristics.

The supporting structure for the steel sheet was designed such that the sheet could be mounted at different heights with variable contact between the surface and the sheet. Errors in mounting have been discussed, and shown to be as large as $\pm$ 0.1 for a perfectly reflective surface and slightly less for an absorptive surface. The

microphone loudspeaker distance was also shown to yield variable results at large and small distances. At large distances this was caused by the instability of the microphone support, which would bend under its own weight. At small distances the interaction between the loudspeaker and the sound field is significant, which was previously neglected in the theory.

This method has shown the characteristics of three surfaces covering the entire range of absorption: a rigid surface, a resonant surface and an absorptive surface. Measurements were taken down to 50 Hz, having a resolution which other methods failed to achieve. The mass-air-mass resonance peak was clearly identified in the absorption spectrum for the resonant surface. Restrictions on the frequency resolution are based on the size of the surface under study and the steel sheet, which would merit more attention if this method is to be improved. This is related to diffraction effects which were neglected in this study.

The mass of this measurement configuration is considerable. The mounting structure (steel sheet and supports) has to be assembled and dis-assembled in order to measure the absorption characteristics of a surface. This is a disadvantage of this method.

Near-field measurements were suggested in order to increase the sound level of the incident and reflected waves compared to the room reflections and diffraction. This would then allow these contributions to be safely neglected. On the other hand, this will also increase the sound level of the scattered wave from the loudspeaker. A compromise is made between the strength of the diffracted waves and the strength of the scattered wave. We have previously shown that the scattering can be incorporated in the theory for the reflection factor. If near-field measurements are used, then the scattering of the loudspeaker would have to be known. This approach may be impractical if the scattering cannot be measured accurately. In addition, small variations in loudspeaker-microphone positioning between measurements could cause significant errors. The construction of the mounting structure may benefit from an alternative design which would eliminate mounting error and maintain accurate positioning of the loudspeaker and microphone.

5.3 Recommendations for Future Work

Several problems should be further investigated in order to improve the accuracy of the surface pressure method. First, it would be important to eliminate or reduce the error caused by the mounting of the steel sheet. An apparatus could also be used to fix the loudspeaker and microphone position relative to the support structure. In addition, a calibration measurement could be used on a rigid surface, open air, or a surface of known acoustic impedance in order to improve the accuracy of the method. All measurements were performed at normal incidence, therefore measurements for other angles of incidence should be attempted.

The diffraction of sound by the sheet and support structure should be further

investigated. If the diffraction were calculated for the current setup, this could be removed in the post-processing of the measurement data. Alternatively, a calibration measurement may compensate, or normalize the effects of diffraction. If an alternative design and proper calibration were made, near-field measurements would perhaps be possible. The scattering from the loudspeaker would have to be known in this case, and as mentioned previously, this may be difficult to measure/calculate.

The impulse response shortening and gating method works in conjunction with the other proposed methods. This is a valuable approach since it reduces the amount of time-data necessary to obtain sufficient frequency resolution at low frequencies. In particular, the reflection method and the subtraction technique could benefit significantly from this approach. Simple windowing has resulted in the smoothing of the absorption coefficient at low frequencies with these methods. More study may be required in order to verify the applicability of this method. Low-frequency data recovery is based on the modelling of the loudspeaker. We speculate that the surface under study should be modelled as well. If this were the case, then assumptions of the surface would have to be made, which may cause problems.

Two additional measurement approaches were considered by the author but time constraints did not allow their investigation. The use of a combined pressure-velocity measurement device, termed a "microflown" would allow the specific acoustic impedance to be calculated at the study surface. However, calibration difficulties exist due to amplitude and phase mismatch [22] between pressure and velocity sensors. Second, a similar concept may be implemented using a microphone and an accelerometer. The response of the accelerometer would require time integration in order to yield velocity data. In the frequency domain, this is simply done by dividing the frequency response by $j\omega$. Once again, this would result in the specific acoustic impedance of the surface and may be used to determine the reflection factor and absorption coefficient. Calibration would have to be performed such that the ratio of pressure to velocity would truly represent the specific acoustic impedance of the study surface.

5.4 Conclusions

In situ measurements have proved to be difficult. Different results are obtained using different measurement methods. In general the measurement environment is not controllable and therefore noise and room reflections have to be tolerated or removed. We have seen that the removal of room reflections will affect the resulting frequency resolution. For these reasons it is expected that *in situ* measurements will not achieve the same accuracy as in a laboratory. On the other hand, the reverberation chamber and the impedance tube methods, which are known as standard methods used to characterize materials are also subject to measurement errors[1].

The surface pressure method was the preferred method for conducting *in situ* measurements of acoustic absorption. The surface under study was compared with a rigid surface at the same location in a room, resulting in similar noise and reverberation for both measurements. Absorption coefficients were obtained from 50 Hz to 4 kHz, showing the characteristics of a rigid surface, a resonant surface and an absorptive surface. Once again, the accuracy of these results is not yet clear. Improvements to this method are possible and have been discussed in Section 5.2. In particular the measurement of a surface of known acoustic impedance, and the calibration of this system would be beneficial.

A simple and effective *in situ* measurement of the acoustic properties of a surface is still sought after. The methods proposed in this study may achieve the desired accuracy with some more development. It is the author's hope that this work may serve as a stepping stone to further develop the methods presented herein.

[1]Round robin tests of one sample in various reverberation chambers has shown differences of 0.1-0.2 in the absorption coefficient [16]. Dutilleux has also shown that the incorrect mounting of a sample in an impedance tube can result in significant errors [8].

Appendix A

Transmission of Sound for Panels and Plates

A.1 Flexural Vibrations of Finite Elastic Plates

Sheets and plates do not only vibrate due to external forces, but also once set in motion, have restoring forces analogous to a spring. The effect of this property is given by a few parameters, the elastic modulus E, Poisson's ratio s, as well as the mass per unit area σ and thickness h of a plate. In the following it is assumed that the plate is thin. More specifically, this requires that the wavelength of a bending wave on the plate is larger than six times the plate thickness [43].

In order to discuss the effects due to the elastic properties of a plate, we must first define the relevant parameters. The elastic modulus is related to the change in length of a material under stress, which is mathematically represented by Hooke's law [26]

$$S = E\epsilon \tag{A.1}$$

where S is the longitudinal stress (applied pressure) and ϵ is the longitudinal strain: the elongation of a material divided by its original length. Here we consider that the plate has a restoring force, given by its bending modulus B [31] (bending stiffness),

$$B = \frac{Eh^3}{12(1-s^2)}. \tag{A.2}$$

Particular modes of vibration will exist if the plate is finite, which is the topic of the present section. The following development highlights the results found in Junger and Feit [18]. The boundary conditions at the edges of the plate are complicated. Here we consider a plate of length l_x and l_y that is simply supported (hinged) at it's extremities in the xy plane. The displacement of the plate, $\xi = \xi(x, y)$, is related to the bending moments, M_x and M_y by

$$M_x = -B\left(\frac{\partial^2 \xi}{\partial x^2} + s\frac{\partial^2 \xi}{\partial y^2}\right) \tag{A.3}$$

and

$$M_y = -B\left(\frac{\partial^2 \xi}{\partial y^2} + s\frac{\partial^2 \xi}{\partial x^2}\right). \tag{A.4}$$

The boundary conditions are specified by the support on the plate. In the case of a simply supported plate, the displacement ξ and the bending moments, are zero along the plate edges:

$$\xi(x, y) = 0, \qquad x = 0, l_x \text{ or } y = 0, l_y \tag{A.5}$$

$$\frac{\partial^2 \xi(x, y)}{\partial x^2} = 0, \qquad x = 0, l_x \tag{A.6}$$

$$\frac{\partial^2 \xi(x, y)}{\partial y^2} = 0, \qquad y = 0, l_y. \tag{A.7}$$

The unforced equation of motion of the plate is

$$B\left(\frac{\partial^4 \xi}{\partial x^4} + 2\frac{\partial^4 \xi}{\partial x^2 \partial y^2} + \frac{\partial^4 \xi}{\partial y^4}\right) - \rho_s h \omega^2 \xi = 0 \tag{A.8}$$

which is satisfied for a particular form of ξ and particular angular frequencies. These are the normal modes of vibration of the plate, described by [18]

$$\omega_{mn} = \pi^2 \sqrt{\frac{B}{\rho_s h}} \left[\left(\frac{m}{l_x}\right)^2 + \left(\frac{n}{l_y}\right)^2\right]. \tag{A.9}$$

When a force is applied at the position (x_o,y_o), the equation of motion of the plate becomes

$$B\left(\frac{\partial^4 \xi}{\partial x^4} + 2\frac{\partial^4 \xi}{\partial x^2 \partial y^2} + \frac{\partial^4 \xi}{\partial y^4}\right) - \sigma \omega^2 \xi = F\delta(x - x_o)\delta(y - y_o) \tag{A.10}$$

where δ is the Dirac delta, that is to say that the force F is present at $x = x_o$ and $y = y_o$ and zero elsewhere. The solution to this differential equation is of the form

$$\xi(x, y) = -\frac{4F}{\sigma l_x l_y} \sum_{m=1}^{\infty} \sum_{n=1}^{\infty} \frac{\sin(\frac{m\pi x_o}{l_x}) \sin(\frac{m\pi x}{l_x}) \sin(\frac{n\pi y_o}{l_y}) \sin(\frac{n\pi y}{l_y})}{\omega^2 - \omega_{mn}^2} \tag{A.11}$$

where $\sigma l_x l_y$ is the mass of the plate. Analogous to the case for acoustics, we are seeking the mechanical impedance of the plate, Z_m, which is given by the quotient of the force F, to the velocity of the plate multiplied by the inward normal ($\vec{n_{in}}$), $-j\omega\xi(x,y)$ [18],

$$Z_m(x,y) = \frac{F}{-j\omega\xi(x,y)} = -\frac{jM}{4\omega}\sum_{m=1}^{\infty}\sum_{n=1}^{\infty}\frac{\omega^2-\omega_{mn}^2}{\sin(\frac{m\pi x_o}{l_x})\sin(\frac{m\pi x}{l_x})\sin(\frac{n\pi y_o}{l_y})\sin(\frac{n\pi y}{l_y})}. \tag{A.12}$$

The numerator of Z_m indicates that the mechanical impedance has zeros at $\omega = \omega_{mn}$, the plate's normal modes of vibration. In other words, it would only require a slight force on the plate in order to set it in motion at these frequencies.

The previous results thus indicate that the physical properties of a plate, such as dimension, density and elastic characteristics, result in resonant behaviour. This will selectively reflect or transmit sound energy at particular frequencies. It is also important to note that no loss factor has been included in the previous analysis. The damping coefficient for a material, η, sometimes accompanies the previously mentioned physical parameters.

As in the previous section, we will present an example of an aluminium and a steel plate. Table A.1 summarizes the material properties of given dimensions l_x and l_y, density, thickness, Young's modulus and Poisson ratio. The first 25 resonance frequencies of both plates are given in (A.13) and (A.14) by use of $\omega = 2\pi f$ in (A.9).

Material	l_x [m]	l_y [m]	h [10^-3·m]	ρ [10^3·m^3/s]	E [10^{10}·N/m^2]	s
Aluminium	1.2		1.6	2.8	7.4	0.33
Steel				7.8	20	0.28

Table A.1: Material properties of Steel and Aluminium, see Pierce [31] for more details.

$$f_{amn} = \begin{pmatrix} 5.3 & 13.2 & 26.4 & 44.8 & 68.6 \\ 13.2 & 21.1 & 34.3 & 52.7 & 76.5 \\ 26.4 & 34.3 & 47.5 & 65.9 & 89.7 \\ 44.8 & 52.7 & 65.9 & 84.4 & 108.1 \\ 68.6 & 76.5 & 89.7 & 108.1 & 131.8 \end{pmatrix} \text{ Hz} \tag{A.13}$$

$$f_{smn} = \begin{pmatrix} 5.4 & 13.6 & 27.2 & 46.3 & 70.8 \\ 13.6 & 21.8 & 35.4 & 54.4 & 79.0 \\ 27.2 & 35.4 & 49.0 & 68.1 & 92.6 \\ 46.3 & 54.4 & 68.1 & 87.1 & 111.6 \\ 70.8 & 79.0 & 92.6 & 111.6 & 136.1 \end{pmatrix} \text{ Hz} \tag{A.14}$$

where f_{amn} is for aluminium and f_{smn} is for steel. We see that the results are very similar. This is due to the fact that the ratio of bending stiffness to mass per unit area for each sheet ($B/\rho_s h$) is very close: 6.2 $\mathrm{m}^4/\mathrm{s}^2$ for aluminium and 5.8 $\mathrm{m}^4/\mathrm{s}^2$ for steel (see (A.9)). We see that more than half of the resonance frequencies are above or equal to 50 Hz. This indicates that such a sheet would have resonances in our region of interest. Section 2.3 discusses other effects that may dominate the motion of the plate in the frequency region of interest. In the next section, we discuss the coincidence/damping controlled region. This was above the frequency range of interest in this thesis.

A.2 Coincidence/Damping Controlled Region

The coincidence/damping controlled region begins at the critical frequency given by (2.45). This is when the sound wave and the movement of the panel are in phase, see Figure A.1. The coincidence effect only happens when [44]

$$\sin\theta^* = \frac{\lambda}{\lambda_p} \tag{A.15}$$

where $\theta = \theta^*$ is the incident angle at coincidence, λ the wavelength of the acoustic wave and λ_p the wavelength of the vibrations in the panel. This may be rearranged in order to determine the coincidence angle,

$$\theta^* = \sin^{-1}\left(\frac{\lambda}{\lambda_p}\right). \tag{A.16}$$

At normal incidence, $\theta = \theta^* = 0$ and we have

$$\frac{\lambda}{\lambda_p} = 0 \tag{A.17}$$

requiring that $\lambda \ll \lambda_p$ since $\lambda = 0$ corresponds to an infinite frequency. In fact, this effect is important when the incident wave is not at normal incidence. The first coincidence frequency is at glancing angle incidence ($\theta^* = \pi/2$). For more information on this effect, see [44].

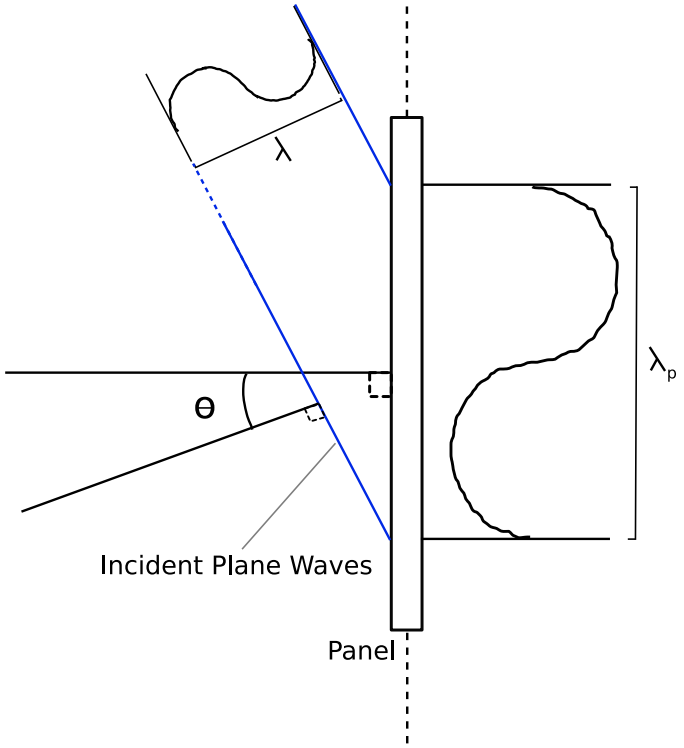

Figure A.1: Bending waves on a panel. An acoustic wave is incident at an angle $\theta = \theta^*$ on a panel having bending waves. Coincidence occurs when the ratio of the incident pressure wave wavelength to bending wave wavelength is equal to $\sin\theta^*$. Figure has been reproduced from [18].

Appendix B

Geometry of Sound Pressure Method Measurement Locations

B.1 Front Door 2nd Floor

Figure B.1: Photograph of the FD2 location. The wall to the right of the picture was measured. Notice the section of wall extending into the measurement area.

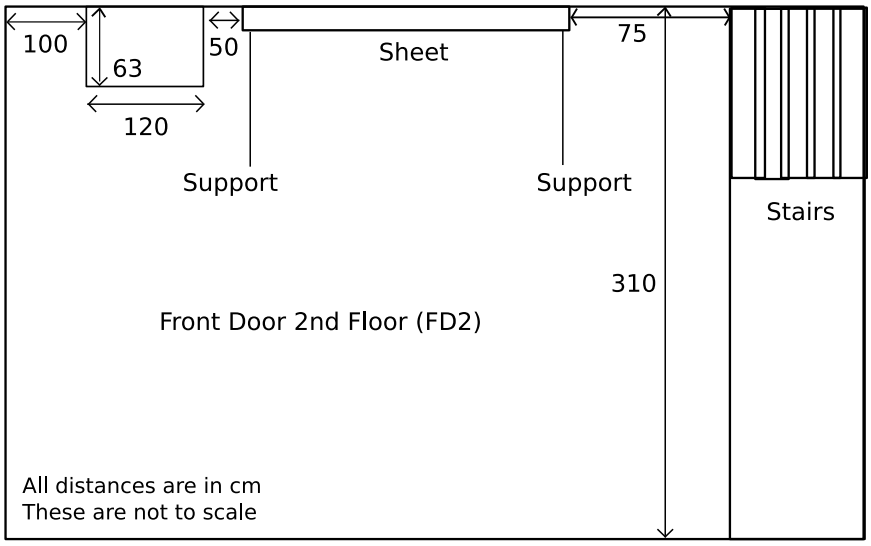

Figure B.2: Geometry of room and measurement configuration in FD2. A section of wall was protruding into the room in the left top corner.

B.2 Back Door 2nd Floor

Figure B.3: Photograph of the BD2 location. The wall to the right of the picture was measured.

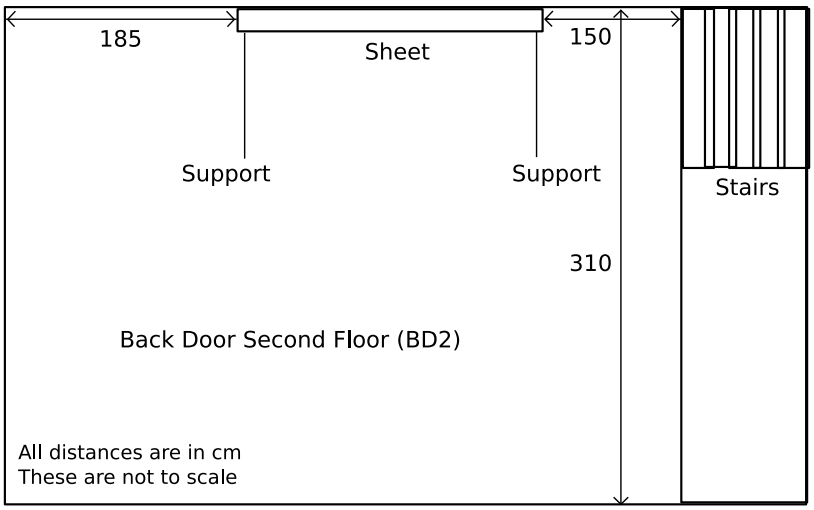

Figure B.4: Geometry of room and measurement configuration in BD2.

B.3 Back Door 3rd Floor

Figure B.5: Photograph of the BD3 location. The wall to the left of the picture was measured.

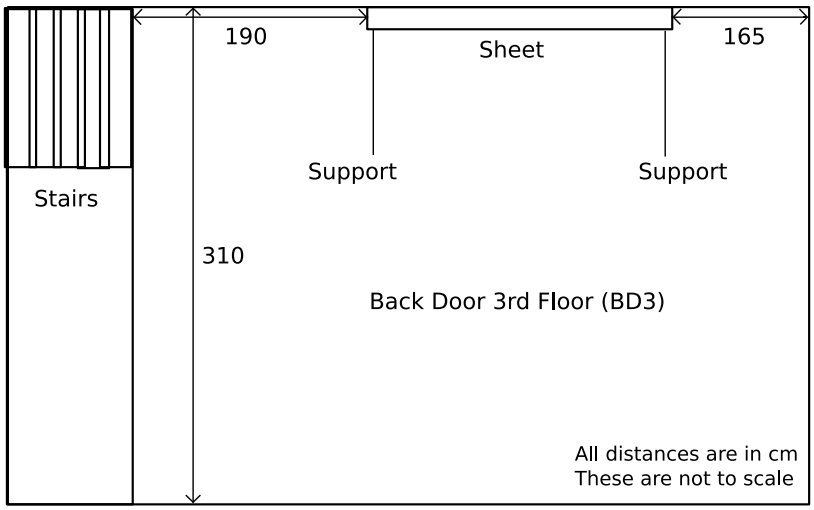

Figure B.6: Geometry of room and measurement configuration in BD3.

References

[1] BS CEN/TS 1793-5:2003. *Road Traffic Noise Reducing Devices – Test Method for Determining the Acoustic Performance – Part 5: Intrinsic Characteristics – In Situ Values of Sound Reflection and Airborne Sound Insulation.* 4

[2] F. Anfosso, M. Garai, and J.-P. Clairbois. Adrienne: Une méthode européenne pour la qualification sur site des ecrans antibruit. *Bullettin de Liason des Ponts et Chausées*, 225, 2000. 4

[3] J. Backman. Low-frequency extension of gated loudspeaker measurements. *Audio Engineering Society 124^{th} Convention*, May 2008, paper 7353. 55

[4] R. F. Barron. *Industrial Noise Control and Acoustics*, pages 108–117. Marcel Dekker, Inc., 2003. 18, 19, 20, 21

[5] L. Beranek. *Acoustics*, pages 11, 35–36. Acoustical Society of America, 1993. 11

[6] T. J. Cox and P. D'Antonio. *Acoustic Absorbers and Diffusers: Theory, Design and Application*, pages 1–5, 43–44, 68–70. Spon Press (Taylor & Francis Group), 2004. 1, 62, 65

[7] J. Ducourneau, V. Planeau, J. Chatillon, and A. Nejade. Measurement of sound absorption coefficients of flat surfaces in a workshop. *Applied Acoustics*, pages 710–721. 4

[8] G. Dutilleux. *Mésure In Situ de l'Absorption Acoustique des Matériaux Dans le Batiment.* PhD thesis, L'Institut National des Sciences Appliquees de Lyon, 1999. 2, 3, 5, 110

[9] G. Dutilleux, T. E. Vigran, and U. R. Kristiansen. An in situ transfer function technique for the assessment of the acoustic absorption of materials in buildings. *Applied Acoustics*, 62:555–572, 2001. 4

[10] L. Fincham. Refinements in the impulse testing of loudspeakers. *Journal of the Audio Engineering Society*, vol. 33:133–140, 1985. 5, 7, 55

[11] M. Garai, M. Brengier, P. Guidorzi, and Ph. L'Hermite. Procedure for measuring the sound absorption of road surfaces in situ. In *Euro Noise 98 Conference*, 1998. 3

[12] D. E. Hall. *Basic Acoustics*, pages 142–143. Harper & Row Publishers, Inc., 1987. 9

[13] U. Ingård and R. H. Bolt. Absorption characteristics of acoustic material with perforated facings. *Journal of the Acoustical Society of America*, 23(5):533–540, 1951. 69

[14] U. Ingård and R. H. Bolt. A free field method of measuring the absorption coefficient of acoustic materials. *Journal of the Acoustical Society of America*, 23(5):509–516, 1951. 5, 7, 69, 107

[15] ASTM International. *Annual Book of ASTM Standards: C 384 - 04 Standard Test Method for Impedance and Absorption of Acoustical Materials by Impedance Tube Method*, volume 04.06. 2008. 3, 59

[16] ASTM International. *Annual Book of ASTM Standards: C 423 - 08 Standard Test Method for Sound Absorption and Sound Absorption Coefficients by the Reverberation Room Method*, volume 04.06. 2008. 3, 5, 7, 59, 61, 110

[17] ASTM International. *Annual Book of ASTM Standards: E 996 - 04 Standard Guide for Field Measurements of Airborne Sound Insulation of Building Facades and Faade Elements*, volume 04.06. 2008. 6

[18] M. C. Junger and D. Feit. *Sound, Structures, and Their Interaction*, pages 213–214. Acoustical Society of America Through the American Society of Physics, 1993. 111, 112, 113, 115

[19] K. Kimura and K. Yamamoto. The required sample size in measuring oblique incidence absorption coefficient experimental study. *Applied Acoustics*, 63:567–578, 2002. 5

[20] H. Kuttruff. *Room Acoustics*, pages 248–254. Elsevier Sience Publishers LTD, 1991. 3

[21] J.-F. Li and M. Hodgson. Use of pseudo-random sequences and a single microphone to measure surface impedance at oblique incidence. *Journal of the Acoustical Society of America*, 102(4):2200–2210, 1997. 4, 26

[22] Y. Liu and F. Jacobsen. Measurement of absorption with a p-u sound intensity probe in an impedance tube (l). *Journal of the Acoustical Society of America*, 118(4):2117–2120, 2005. 109

[23] N. Londhe, M. D. Rao, and J. R. Blough. Application of the iso 13472-1 in situ technique for measuring the acoustic absorption coefficient of grass and artificial turf surfaces. *Applied Acoustics*, 70:129–141, 2009. 4

[24] M. Garai. Measurement of the sound-absorption coefficient in situ: The reflection method using periodic pseudo-random sequences of maximum length. *Applied Acoustics*, 39:119–139, 1993. 3, 7, 26, 72

[25] S. Mallais. In situ determination of acoustic absorption coefficients. *Presented at the 125th Convention of the Audio Engineering Society, San Francisco, CA, USA*, October 2–5 2008, paper 7549. 4

[26] D. B. Marghitu. *Mechanical Engineer's Handbook*, pages 126–127. Academic Press, 2001. 111

[27] E. Mommertz. Angle-dependent in-situ measurements of reflection coefficients using a subtraction method. *Applied Acoustics*, 46:251–263, 1995. 4, 5, 7, 48, 49, 52, 54, 107

[28] E. Mommertz and S. Müller. Measuring impulse responses with digitally pre-emphasized pseudorandom noise derived from maximum *Applied Acoustics*, 44:195–214, 1995. 5, 107

[29] P. M. Morse and K. U. Ingård. *Theoretical Acoustics*, pages 259–262, 309–311, 411, 458–463. Princeton University Press, 1986. 11, 26, 72, 75

[30] C. Nocke. In-situ acoustic impedance measurement using a free-field transfer function method. *Applied Acoustics*, 59:253–264, 2000. 4, 72

[31] A. Pierce. *Acoustics: An Introduction to it's Physical Principles and Applications*, pages 110, 132, 144–147. Acoustical Society of America, 1989. 11, 111, 113

[32] D. Raichel. *The Science and Application of Acoustics*, pages 283–284, 289–291. Springer Science+Business Media, Inc., 2006. 16, 18, 21

[33] D. Rife and J. Vanderkooy. Transfer-function measurementwith maximum-length sequences. *Journal of the Audio Engineering Society*, 27(6):419–444, 1989. 24

[34] M. R. Shroeder. Integrated-impulse method measuring sound decay without using impulses. *Journal of the Acoustical Society of America*, 66(2):497–500, 1979. 3, 59

[35] R. Stevens. Improving impedance tube measurements using maximum length sequences. Master's thesis, University of Waterloo, 2003. 2, 3

[36] R. Stevens. A novel method to measure the absorption coefficient of outdoor plane surfaces using sound pressure levels at two positions. *Spring Noise Conference, Banff, BC, Canada*, 2007. 6

[37] Y. Takahashi, T. Otsuru, and R. Tomiku. In situ measurements of surface impedance and absorption coefficients of porous materials using two microphones and ambient noise. *Applied Acoustics*, 66:845–865, 2005. 4

[38] J. Vanderkooy. Simple theory cabinet edge diffraction. *Journal of the Audio Engineering Society*, 39(12):923–933, 1991. 5, 29

[39] J. Vanderkooy. Polar plots at low frequencies: The acoustic centre. *Presented at the 120th Convention of the Audio Engineering Society, Paris, France*, May 20–23 2006, paper 6784. 28

[40] J. Vanderkooy. Applications of the acoustic centre. *Presented at the 122nd Convention of the Audio Engineering Society, San Francisco, CA, USA*, May 5–8 2007, paper 7102. 29

[41] J. Vanderkooy. The acoustic center: A new concept for loudspeakers at low frequencies. *Presented at the 121st Convention of the Audio Engineering Society, San Francisco, CA, USA*, October 5–8 2006, paper 6912. 47

[42] J. Vanderkooy and S. Lipshitz. Can one perform quasi-anechoic loudspeaker measurements in normal rooms? *Audio Engineering Society 125th Convention*, paper 7525, October 2008. 5, 7, 55, 56, 57

[43] T. E. Vigrain. *Building Acoustics*, pages 89–99. Taylor & Francis, 2008. 111

[44] C. E. Wilson. *Noise Control - Measurement, Analysis, and Control of Sound and Vibration*, pages 244–246. Krieger Publishing Company, 1994. 114

[45] R. E. Ziemer, W. H. Tranter, and D. R. Fannin. *Signals and Systems: Countinuous and Discrete*, pages 48–68, 152–153. Maxwell MacMillan Canada, 1993. 24